National University of Ireland

Maynooth

Department of Biology

2013

The Interactions for the RBP Receptor, Stimulated by Retinoic Acid Gene 6

Kate Mc Quaid

NUI MAYNOOTH

Ollscoil na hÉireann Má Nuad

A Thesis submitted to the

National University of Ireland

for the degree of

Doctor of Philosophy

October 2013

Supervisor
Prof. John Findlay
Department of Biology
National University of Ireland
Maynooth
Co. Kildare

Head of Department
Prof. Paul Moynagh
Department of Biology
National University of Ireland
Maynooth
Co. Kildare

Table of Contents

Declaration of Authorship

This thesis has not previously been submitted in part to this or any other university and is the sole work of the author.

_____

Kate Mc Quaid B.Sc

Acknowledgements

Firstly I wish to express a sincere thank you to Prof. John Findlay for giving me the opportunity to conduct research in his lab. I will always be extremely grateful for the advice and support that he has given to me over the years that I have been in NUI Maynooth. I would also like to thank Science Foundation Ireland for funding my research.

To all the members of the Membrane Protein Lab past and present a big thank you for sharing all their expertise over the past four years. I would like to personally thank Akos, Gemma, Conor and Darren for all their help and guidance.

Thank you to all my friends who have been a great support during the last four years especially Natasha, Siobhan, Adam, Ashling, Helen, Susan and Therese. I also must say a massive thank you to David for always being so understanding and supportive and for cheering me up on the tougher days.

I owe an enormous debt of gratitude to my family, Ari, Ann and Max. Thank you for all your support and always believing in me. I would never of made it to where I am today without their help and to them I dedicate this thesis.

Abstract

Vitamin A, or retinol, is a fat-soluble vitamin, essential for many important processes including proliferation, reproduction, vision and immunocompetence. Retinol binding protein (RBP) is the principal carrier of retinol in the blood from its storage site, the liver, to retinol dependant tissues. The long sought RBP receptor was recently identified as stimulated by retinoic acid gene 6 (STRA6), a 74 kDa multitransmembrane protein with no similarity to any other protein receptor. At present, receptor function, architecture and structure-function relationships remain relatively unexplored. Identification of any protein(s) that interact with STRA6 is imperative in identifying any other role STRA6 may play in the body.

The membrane yeast two hybrid (MYTH) represents a powerful tool to facilitate the characterisation of membrane protein interactions and was utilized to detect proteins that interact with full-length STRA6. A human kidney and a human brain library were screened. The human kidney screen was repeated in the presence of RBP-ROH to identify any protein interactions dependent on the presence of holo-RBP. The MYTH screens resulted in 11 unique protein interactions for STRA6. These interactions could not be verified using pull-down experiments despite numerous attempts.

In the hope of gaining insights into STRA6's architecture and function, the predicted large third intracellular loop (ICL3) of STRA6 was extracted from the full length protein, introduced into a carrier protein, Im7, and characterised. STRA6-ICL3 was found to form a tetramer. The native Im7 is monomeric; therefore, the domain conferred tetrameric behaviour. These data suggest that native STRA6 is likely to occur as a tetramer and that at least some of the oligomerization sites are located on this large intracellular loop. By determining the circular dichroism spectra for STRA6-ICL3,

the first structural data for STRA6 was collected. These data revealed that STRA6-ICL3 was mostly composed of β-sheet and random coil. Crystallization trials were also attempted and a crystal is eagerly awaited.

List of Figures

Chapter 1 Introduction

Chapter 3 Membrane Yeast Two Hybrid

Chapter 4 Hit Verification

Chapter 5 Third Intracellular Loop of STRA6

Abbreviations

3-AT	3-amino-1 2 3-triazole
ApoE	Apolipoprotein E
ATP	Adenosine 5'-triphosphate
ATRA	All-*trans*-Retinoic Acid
BCMO1	β-Carotene-15,15′-Monooxygenase
BCMO2	β-Carotene-9′,10′-Monooxygenase
BLAST	Basic Local Alignment Search Tool
BSA	Bovine Serum Albumin
CAPS	*N*-cyclohexyl-3-aminopropanesulfonic acid
CCL2	C-C Motif Chemokine 2
CD	Circular Dichroism
CHAPS	3-[(3-Cholamidopropyl) dimethylammonio]-1-propanesulfonate
CRBP	Cellular Retinol-Binding Protein
CRBPII	Cellular Retinol Binding Protein II
CREBBP	CREB-Binding Protein
Cub	C-Terminal (amino acids 34-76) of Yeast Ubiquitin
DBD	DNA Binding Domains

DDM	N-Dodecyl-β-D-Maltoside
DDK-tag	8 Amino Acid Affinity Tag, Sequence DYKDDDDK
DGAT1	Acyl-CoA:Retinol Acyltransferase
DMEM	Dulbecco's Modified Eagle's Medium
DMPC	1, 2-dimyristoyl-*sn*-glycero-3-phosphocholine
DTBP	Dimethyl 3, 3′ -Dithiobispropionimidate
DTT	Dithiothreitol
ECL	Enhanced Chemiluminescent
EDTA	Ethylenediaminetetraacetic Acid
ER	Endoplasmic Reticulum
ERABP	Epididymal Retinoic Acid Binding Protein
FCS	Foetal Calf Serum
FLAG®-tag	(registered trademark of Sigma Aldrich, see DDK- tag)
GLUT4	Glucose Transporter Type 4
GM-CSF	Granulocyte-Macrophage Colony Stimulating Factor
Grb2	Growth Factor Receptor-Bound Protein 2
GST	Glutathione-S-Transferase
HA-tag	9 Amino Acid Affinity Tag, Sequence YPYDVPDYA
HAT	Histone Acetyltransferase
HDACs	Histone Deacetylases

HEK293T	Human Embryonic Kidney 293T Cells
His-tag	6 Amino Acid Affinity Tag, Sequence HHHHHH
HRP	Horseradish Peroxidase
HSCs	Hepatic Stellate Cells
ICL3	Third Intracellular Loop of Human STRA6
IFITM1	Interferon-Induced Transmembrane Protein 1
IFITM3	Interferon-Induced Transmembrane Protein 3
IL-2	Interleukin-2
Im7	ColE7 Immunity Protein from *Escherichia coli*
IMAC	Immobilised Metal Ion Affinity Chromatography
IPTG	Isopropyl β-D-1-thiogalactopyranoside
IR	Insulin Receptor
JNK	C-Jun N-Terminal Protein Kinase
LB	Luria-Bertani Medium
LBD	Ligand Binding Domains
LDAO	N,N-Dimethyldodecylamine N-oxide
LiOAc	Lithium Acetate
LpL	Lipoprotein Lipase
LRAT	Lecithin:retinol acyltransferase
MAP	Mitogen-Activated Protein

MCP-1	Monocytes Chemoattractant Protein-1
MEDs	Mediator Complexes
MIF	Macrophage Migration Inhibitory Factor
MW	Molecular Weight
Myc-tag	10 Amino Acid Affinity Tag, Sequence EQKLISEEDL
MYTH	Membrane Yeast Two Hybrid
N-CoR	Nuclear Receptor Corepressor
NFDM	Non-Fat Dry Milk
Ni-NTA	Nickel-Nitrilotriacetic Acid
NubG	N-Terminal (Amino Acids 1-38) of Yeast Ubiquitin with Isoleucine 13 to Glycine Mutation
NubI	Wild Type N-Terminal (Amino Acids 1-38) of Yeast Ubiquitin
OCIAD2	Ovarian Cancer Immuno Reactive Antigen Domain Containing Protein 2 (OCIAD2)
PBS	Phosphate Buffered Saline
PBS-t	Phosphate Buffered Saline (0.05 % (v/v) Tween-20)
PDB	Protein Data Bank
PDK1	Phosphoinositide-Dependent Kinase 1
PDZK1-IP1	PDZK1-Interacting Protein 1
PEG	Polyethylene Glycol

PEPCK	Phosphoenolpyruvate Carboxykinase
PI3K	Phosphoinositide 3-Kinase
PMSF	Phenylmethylsulfonyl Fluoride
PLP2	Proteolipid Protein 2
PLRP2	Pancreatic Lipase Related Protein 2
PPARs	Peroxisome Proliferator-Activated Receptors
PPIs	Protein-Protein Interactions
PTL	Pancreatic Triglyceride Lipase
PTM	Post-Translational Modification
PVDF	Polvinylidene Fluoride
RA	Retinoic Acid
RAR	Retinoic Acid Receptor
RARE	RA-Responsive Elements
RBP	Retinol-Binding Protein
REH	Retinyl Ester Hydrolase
RPE	Retinal Pigment Epithelial
RXR	Retinoid X Receptor
SB	Super LB Broth
SDS	Sodium Dodecyl Sulphate

SDS-PAGE	Sodium Dodecyl Sulphate Polyacrylamide Gel Electrophoresis
SEC	Size-Exclusion Chromatography
SERP1	**S**tress-associated Endoplasmic Reticulum (ER) protein 1
SMRT	Silencing Mediator for Retinoid and Thyroid Hormone Receptors
SNP	Single Nucleotide Polymorphism
SOB	Super Optimal Broth
SOC	Super Optimal Broth with Catabolite Repression
SOCS-3	Suppressor of Cytokine Signalling-3
Sos	Son of Sevenless
SR-B1	Scavenger Receptor Class B, Type I
STRA6	Stimulated by Retinoic Acid Gene 6
STRA6-CT	Third Intracellular Loop of STRA6 (P^{224}-L^{298})
STRA6-ICL3	STRA6 C-Terminus (L^{535}-P^{667})
StrepII-tag	8 Amino Acid Affinity Tag, Sequence WSHPQFEK
T2D	Type-II Diabetes
TAE	Tris-Acetate-EDTA
TAFs	TBP-Associated Factors
TB	Terrific Broth
TBP	TATA-Binding Protein

TCEP	Tris (2-carboxyethyl) phosphine hydrochloride
TE	Tris EDTA
TERMs	Tetraspanin-Enriched Microdomains
TLR4	Toll-Like Receptor 4
TNF-α	Tumor Necrosis Factor Alpha
TTR	Transthyretin
UBPs	Ubiquitin Binding Proteases
X-gal	Bromo-Chloro-Indolyl-Galactopyranoside
VDR	Vitamin D Receptor
VDREs	VD_3 Response Elements
YPG	Yeast Extract Peptone Dextrose
YPM	Yeast Extract Peptone Methanol
YTH	Yeast Two Hybrid

Amino Acid Abbreviations

Amino Acid	3 Letter Abbreviation	1 Letter Code
Alanine	Ala	A
Arginine	Arg	R
Asparagine	Asn	N
Aspartic Acid	Asp	D
Cysteine	Cys	C
Glutamic Acid	Glu	E
Glutamine	Gln	Q
Glycine	Gly	G
Histidine	His	H
Isoleucine	Ile	I
Leucine	Leu	L
Lysine	Lys	K
Methionine	Met	M
Phenylalanine	Phe	F
Proline	Pro	P
Serine	Ser	S
Tryptophan	Trp	W
Threonine	Thr	T
Tyrosine	Tyr	Y
Valine	Val	V

Chapter 1

Introduction

1.1 Retinol

Vitamin A, or retinol, is a fat-soluble vitamin, essential for many important processes including proliferation, differentiation, reproduction, vision and immunocompetence (Blomhoff and Blomhoff, 2006). Retinol is obtained from the diet and is stored as retinyl esters in hepatic stellate cells, white adipose tissue and the lung (Lobo et al., 2013). Once retinol reaches the target tissues, it is usually converted into retinoic acid (RA) (Desvergne, 2007). RA regulates the expression of hundreds of genes, encoding a wide range of proteins including transcription factors, enzymes, structural proteins, cell-surface receptors and growth factors (Albalat, 2009) by directly activating its nuclear hormone receptors, retinoic acid receptors (RARs), γ, α, and β2. RARs associate with a partner, retinoid X receptors (RXR), γ, α2, and β (McKenna, 2012). RARs bind the abundant form of RA, all-trans RA and 9-cis-RA, as illustrated in Figure 1.1, whereas RXRs bind 9-cis-RA only. RAR/RXR heterodimers and RAR homodimers bind RA-responsive elements (RARE) in the regulatory regions of direct target genes (Duester, 2008). These cognate binding sites correspond to a 5 bp-spaced direct repeat of polymorphic arrangements of the canonical motif 5'-PuG(G/T)TCA (Gudas and Wagner, 2011).

RARs and RXRs are members of the nuclear receptor (NR) superfamily. NRs are modular proteins, with evolutionarily conserved DNA binding domains (DBD) and ligand binding domains (LBD). The DBD confers sequence specific DNA recognition. The LBD is a highly structured domain comprising a ligand dependent activation function, as well as being required for nuclear localization and homo- and/or heterodimerization. In the absence of a ligand (e.g. all-trans RA), RAR–RXR heterodimers (apo-heterodimers) are believed to be bound to RAREs of target genes together with transcriptional co-repressors, nuclear receptor corepressor (N-CoR) or silencing mediator for retinoid and thyroid hormone receptors (SMRT), which then recruit histone deacetylases (HDACs). This results in local chromatin condensation and gene silencing. Binding of the ligand leads to co-repressor dissociation and results in the recruitment of histone acetyltransferase (HAT) co-activators, such

as CREB-binding protein (CREBBP) and p160, relieving the chromatin mediated silencing induced by HDACs. Recruitment of ATP-dependent chromatin remodelling machineries, such as SWItch/Sucrose NonFermentable (SWI–SNF), prepares the template for the action of the basal transcriptional machinery, consisting of the RNA polymerase II holoenzyme, together with the TATA-binding protein (TBP) and TBP-associated factors (TAFs), and mediator complexes (MEDs) (Wurtz et al., 1996). After ligand addition, many genes that do not possess RAREs are transcriptionally regulated indirectly. This indirect regulation occurs because the direct target genes of RA include many different transcription factor genes, these transcription factors then transcriptionally activate their target genes to generate secondary responses (Gudas and Wagner, 2011).

RXRs also form heterodimers with several metabolic regulators, including peroxisome proliferator-activated receptors (PPARs) (Desvergne, 2007), thyroid hormone receptors (TRs) and vitamin D receptor (VDR) (Bugge et al., 1992). In vision, the RA precursor, 11-cis-retinal acts as the chromophore for the visual pigment rhodopsin (Zhong et al., 2012). Photon absorption isomerizes the chromophore to all-trans, leading to the generation of an active intermediate, metarhodopsin II, that initiates a cascade of reactions resulting in a change in membrane potential and hence the conversion of light to an electrical signal (Blakeley et al., 2011).

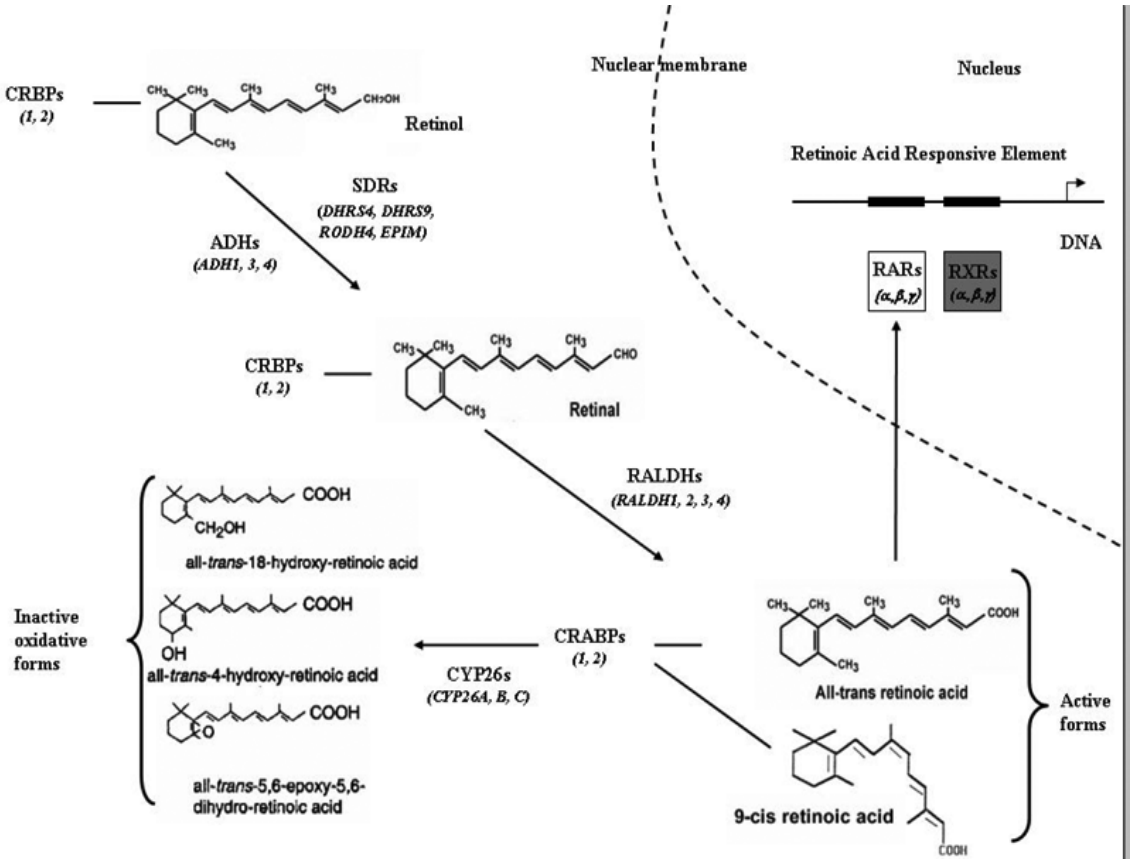

Figure 1.1: Intracellular Retinoid Signalling Pathway. Taken from (Marceau et al., 2006)

Retinol is converted into retinal and retinoic acids, before either it acts through nuclear retinoid receptors or is inactivated by hydroxylation (Marceau et al., 2006).

1.1.1 Retinol Metabolism

Retinoids describes the family of molecules comprising both natural and synthetic analogues of retinol and includes retinol, retinal and retinoic acid (Sporn and Roberts, 1983). Retinoid is obtained from the diet as preformed retinol (primarily as retinol and retinyl ester) from the likes of red meat (Frey and Vogel, 2011) or as proretinol carotenoid (usually as α-carotene, β-carotene or β-cryptoxanthin) from plant sources e.g. carrots and red peppers (Desvergne, 2007). Dietary retinol is taken up directly from the intestinal lumen into the enterocyte. Dietary retinyl esters must first undergo enzymatic hydrolysis within the intestinal lumen, by pancreatic triglyceride lipase (PTL) or pancreatic lipase related protein 2 (PLRP2) or at the enterocyte brush border, to allow for uptake of the hydrolysis product retinol. Dietary proretinoid cartenoids are taken up intact in the enterocyte, scavenger receptor class B, type I (SR-B1) has been identified as a key mediator for uptake of β-carotene from the intestinal lumen into the enterocyte. Once inside the enterocyte, they can undergo conversion to retinoid or are packaged unmodified into chylomicrons. Two structurally related proteins, β-carotene-15,15′-monooxygenase (BCMO1), encoded by *Bcmo1*, and β-carotene-9′,10′-monooxygenase (BCMO2), encoded by *Bcmo2*, are the sole mammalian enzymes known to cleave carotenoids (D'Ambrosio et al., 2011).

Inside the enterocyte, retinol is bound to cellular retinol binding protein II (CRBPII). In the adult, CRBPII is reported to be expressed solely in the intestinal mucosa and is proposed to facilitate optimal retinol absorption from the diet. Re-estherication of newly absorbed dietary retinol to retinyl esters is performed by lecithin:retinol acyltransferase (LRAT) and acyl-CoA:retinol acyltransferase (DGAT1), as illustrated in Figure 1.2. LRAT catalyses the transesterification of retinol and DGAT1 catalyses the fatty acyl-CoA-dependent esterification of retinol. Together with phospholipids, cholesterol and triglycerides, the retinyl esters are packed into chylomicrons and released into the lymph (Ong, 1994). Dietary carotenoid that has not undergone conversion to retinoid is also incorporated into the nascent chylomicrons. After entering the general circulation, the nascent chylomicrons

undergo a process of remodelling that involves primarily the hydrolysis of triglyceride by lipoprotein lipase (LpL) and the acquisition of apolipoprotein E (apoE) from the circulation, resulting in the formation of chylomicron remnants. The majority of dietary retinoid (chylomicron and chylomicron remnant retinoid) is taken up by the liver where it is stored in hepatic stellate cells (HSCs), with the remainder being cleared by peripheral tissues (D'Ambrosio et al., 2011).

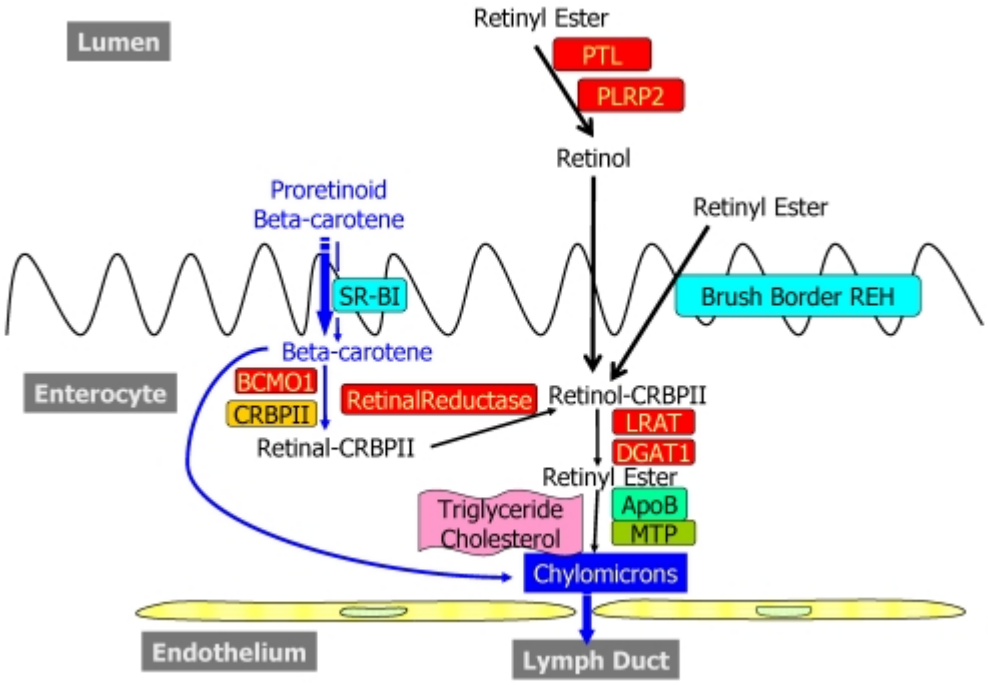

Figure 1.2: Uptake and Metabolism of Dietary Retinoids and Proretinoid Carotenoids within the Intestine. Taken from (D'Ambrosio et al., 2011).

Dietary proretinoid carotenoids, like β-carotene, are taken up into the enterocyte through a process that involves SR-B1. Once inside the enterocyte, β-carotene can be converted to retinal or can be incorporated intact and unmodified along with dietary fat and cholesterol into nascent chylomicrons. Dietary retinyl ester is either hydrolysed in the lumen of the intestine or undergoes hydrolysis at the intestinal brush border catalysed by a brush border retinyl ester hydrolase (REH). Retinol taken into the enterocyte binds to CRBPII and is esterified to retinyl ester. LRAT will catalyse approximately 90% of retinyl ester formation, while the intestinal DGAT1 catalyses the remainder of retinyl ester formation. The resulting retinyl ester is then packed along with dietary fat and cholesterol into nascent chylomicrons, which are secreted into the lymphatic system (D'Ambrosio et al., 2011).

1.1.2 Retinol in Health and Disease

Retinol has numerous important functions and in humans; when retinol intake is not sufficient to meet the body's needs, retinol deficiency occurs. Such deficiency is strongly associated with suppressed immune function and higher morbidity and mortality (Azaïs-Braesco and Pascal, 2000). Retinol deficiency is one of the most prevalent deficiencies of public health importance in developing countries (Radhika et al., 2002), the most common clinical symptom of which is night blindness (Christian et al., 1998). The prevalence of night blindness, in some developing countries, has been found to be as high as 12 % (Radhika et al., 2002). Xerophthalmia designates the group of ocular signs and symptoms related to this deficiency. As already mentioned, 11-cis-retinal acts as a chromophore for the visual pigment rhodopsin. Night blindness is the first symptom of xerophthalmia as rhodopsin requires high concentrations of 11-cis-retinal to create a highly sensitive visual film (Diniz and Santos, 2000). Retinol can potentially induce and modulate epithelial growth and differentiation. Its deficiency causes epithelial alterations such as loss of mucous secreting cells and squamous metaplasia, thereby causing corneal epithelial keratinization and desquamation of surface epithelium (Hayashi et al., 1989). In addition, retinol deficiency causes the disorganization of rod photoreceptor outer segments, degeneration of cone photoreceptor cells, and the loss of LRAT expression in the retinol pigment epithelial (Zhong et al., 2012).

Retinol supplements have been shown to reduce mortality by up to 80 % in South Africa, in patients suffering from acute complicated measles by reducing complications such as diarrhoea (Klein and Hussey, 1990). The underlying basis for the use of retinol supplementation to reduce infectious disease morbidity and mortality is its role in enhancing immunity. Retinoids influence many aspects of immunity, including mucin and keratin expression, haematopoiesis, apoptosis, the growth, differentiation and function of neutrophils, natural killer cells, monocytes/macrophages, Langerhans cells, T and B lymphocytes. Retinoids also influences balance between T helper type 1-like and T helper type 2-like immune

responses, immunoglobulin production and expression of cytokines, such as tumor necrosis factor alpha (TNF-α) and adhesion molecules (Semba, 1998).

Interestingly, the suppression of immunity seen in retinol deficiency may be connected to the vitamin D bioactive metabolite, 1α25-dihydroxyvitamin D3 ($1\alpha,25(OH)_2VD_3$). $1\alpha,25(OH)_2VD_3$ complexes with the nuclear vitamin D receptor (VDR). VDR heterodimerizes with RXR receptors and binds to VD_3 response elements (VDREs) in the promoters of VD_3-responsive genes to exert an inhibitory effect on adaptive immune cells. RA enhances cytotoxicity and T-cell proliferation in the adaptive immune system. By heterodimerizing with RXR receptors, $1\alpha,25(OH)_2VD_3$ competes for the same nuclear partner as RA. In retinol deficient mice, RA does not compete with $1\alpha,25(OH)_2VD_3$ for their common nuclear binding partners and, therefore, the inhibitory effects of $1\alpha,25(OH)_2VD_3$ on adaptive immune cells are not offset by RA (Mora et al., 2008).

Retinol deficiency also causes an increase in the incidence of respiratory tract disease, in accordance with its role in immunity as well as its role in the lung, to ensure the regulation of the cellular differentiation of the respiratory epithelium and lung epithelium (Biesalski, 2003). Furthermore, retinol deficiency compromises mucosal immunity by altering the integrity of mucosal epithelia, including those of the respiratory tract. Retinol deficiency in rats and hamsters leads to loss of ciliated epithelial cells and mucus in the tracheobronchial tree and replacement by stratified, keratinized epithelium. These pathologic alterations of the respiratory epithelium cause an increased risk of developing respiratory disease (Semba, 1998). Retinol supplements have been shown to decrease repeated infections (Biesalski, 2003). Retinol is essential in pregnancy for the developing embryo and deficiency results in severe abnormalities (Zile, 2001). Retinol deficiency can lead to resorption of the foetus (Sivaprasadarao and Findlay, 1988b). It is believed that improving retinol levels of all deficient individuals could save over a million lives annually (Sommer, 1996).

Conversely, retinol intake at marginally above the recommended dietary intake is connected too with risk and is associated with embryonic malformations in pregnancy (Rothman et al., 1995), reduced bone mineral density and increased risk for hip fracture (Melhus et al., 1998). An excess of retinol suppresses osteoblast activity and promotes osteoclast formation thereby stimulating bone resorption and inhibiting bone formation. Excess retinol also dampens the effects of vitamin D, which plays a critical role in bone metabolism by competing for the same nuclear receptors, RXRs (Mata-Granados et al., 2013). Excessive intake, during pregnancy, can cause teratogenic changes, especially during the critical periods of organ and limb development (Sivaprasadarao and Findlay, 1988b). Retinol excess is associated with malformations of the nervous system, ocular malformations, malformations of the ear, craniofacial malformations, cleft palate, defects of the circulatory system, defects of the respiratory systems, defects of the digestive tract, urogenital defects, skeletal malformations, and abnormal postnatal development (Geelen, 1979). Due to the importance of retinol, at the correct concentration, a tightly regulated mechanism for the delivery of retinol to target cells has evolved.

1.2 Retinol Binding Protein

Retinoids are very insoluble in water and consequently within the aqueous environment of the body are usually found bound to specific retinoid-binding proteins (D'Ambrosio et al., 2011). Plasma retinol binding protein (RBP; also known as RBP4) is the principal carrier of retinol in the blood from its storage site, the liver, to retinol dependant tissues (Kanai et al., 1968). RBP circulates in the plasma associated with a second protein, the homotetramer transthyretin (TTR, 54 kDa) which is believed to stabilise the protein and prevent the glomerular filtration and excretion of the relatively small (21 kDa) RBP molecule through renal filtration (van Bennekum AM et al., 2001). Transthyretin has been recognized as one of the most interesting proteins identified to date, because of its multifunctionality. Besides distributing thyroid hormones (THs) in the blood, it indirectly transports retinol

bound to RBP. The first transthyretin to have its 3D structure revealed was from human plasma. Approximately 60 of 127 amino acid residues in the transthyretin monomer are arranged into eight β-strands (named A through H) that are connected by loops to form a sandwich of two β-sheets. Only 5 % of the residues in the monomer, which corresponds to nine amino acid residues, are in a short α-helix. Dimers of transthyretin are composed of a pair of twisted eight stranded β-sheets. The association of two dimers results in a tetrameric structure with two pairs of eight-stranded β-sheets, as illustrated in Figure 1.3. The dimer–dimer contacts predominantly involve hydrophobic interactions of residues in two loops (i.e. A–B and G–H loops) at the edge of the sheets (Prapunpoj and Leelawatwattana, 2009).

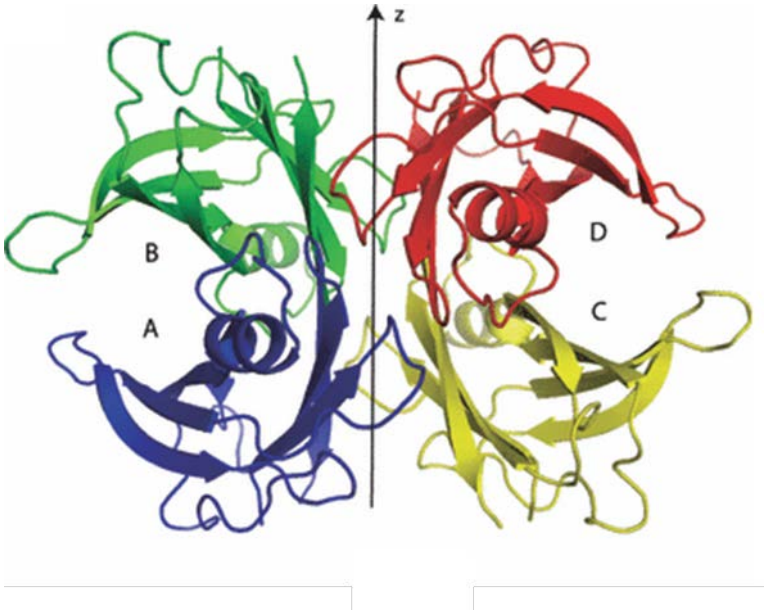

Figure 1.3: The 3D Structures of Human Transthyretin. Taken from (Prapunpoj and Leelawatwattana, 2009)

Ribbon diagrams of transthyretin tetramer. The four identical monomers (A, B, C and D) form a tetramer (shown in colour ramping from blue to red) with a central channel (along the z axis) where two binding sites for THs exist (Prapunpoj and Leelawatwattana, 2009).

RBP belongs to the lipocalin family, a group of widely distributed, mostly extracellular proteins occurring in animals, plants and bacteria (Grzyb et al., 2006). The term 'lipocalin' is derived from the Latin '*lipos*', meaning fats, and '*calyx*', meaning drinking vessel, referring to the binding of lipophilic molecules inside a cup-shaped pocket (Pervaiz and Brew, 1987). RBP is the first member of the lipocalin superfamily for which the X-ray structure was determined (Newcomer et al., 1984). Lipocalins share a highly conserved 3 dimensional structure, an eight stranded β-barrel (Grzyb et al., 2006). The sequence conservation between different members of the lipocalin protein family is low, and alignment is only possible within particular region sequences, illustrated in Figure 1.4. Lipocalins are classified as kernel or outlier lipocalins. The 'kernel' lipocalins are characterized by three common conserved stretches of residues, while 'outlier' lipocalins match no more than two of these three diagnostic motifs (Dittrich et al., 2013).

Lipocalins were first identified for their ability to transport small hydrophobic molecules and are now known to have an important role in the regulation of immunological and developmental processes as well as enzymatic activities, metabolic homeostasis and are involved in the reactions of organisms to various stress factors and in the pathways of signal transduction (Ramana and Gupta, 2009).

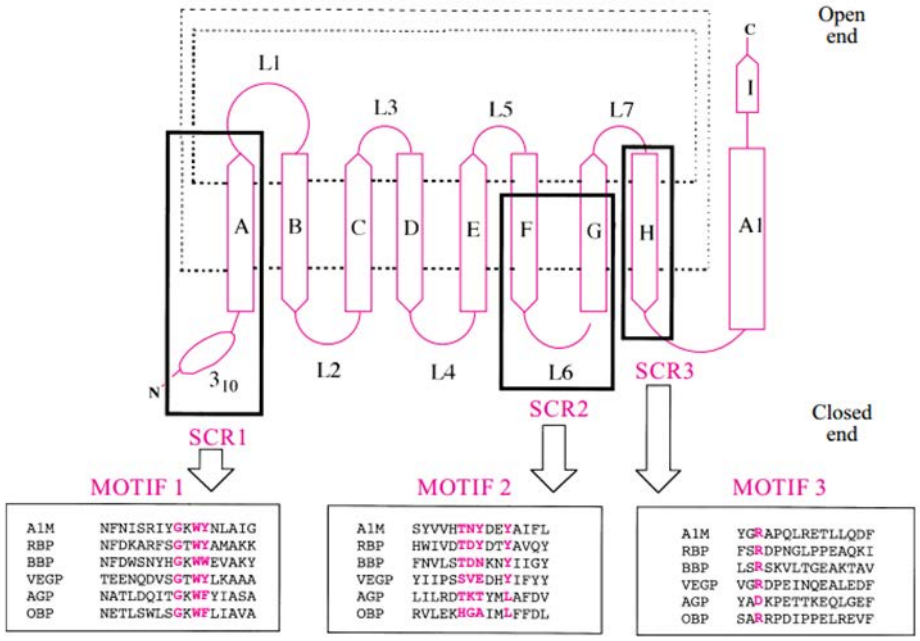

Figure 1.4: Structure of the Lipocalin Fold. Taken from (Flower, 1996)

The nine β-strands of the antiparallel β-sheet are shown as arrows and labelled A-I. The N-terminal 3_{10}-like helix and C-terminal α-helix (labelled A1) are also marked. The hydrogen-bonded connection of two strands is indicated by a pair of dotted lines between them. Connecting loops are shown as solid lines and labelled L1-L7. Those parts which form the three main structurally conserved regions (SCRs) of the fold, SCR1, SCR2 and SCR3, are marked as boxes. Three sequence motifs which correspond to these SCRs are shown (MOTIF 1, MOTIF 2 and MOTIF 3). The first three sequences are from kernel lipocalins and include RBP. The second three from outlier lipocalins (Flower, 1996).

1.2.1 RBP Regulation

Although adequate amounts of retinol are essential to the well-being and survival of the individual, excess intake can be toxic, even to the extent of fatality (Duerbeck and Dowling, 2012). Therefore, the availability and use of retinol has to be under tight control. One molecule of RBP is consumed for the delivery of one molecule of retinol – a remarkably expensive process which attests to the tight control applied to the utilisation of this vitamin. Consistent with this, the turnover of RBP is very high (half-life is hours compared to 2 days for TTR) (Smith et al., 1973), (Ando and Jono, 2008). RBP is synthesised mainly in the liver, with some from the kidney, testis, eye, brain and adipocytes (Redondo et al., 2008). RBP secretion is retinol-dependent (Shirakami et al., 2012). Binding of retinol to RBP is believed to initiate the translocation of holo-RBP (retinol bound) from the endoplasmic reticulum to the golgi complex followed by secretion of holo-RBP into plasma (Blomhoff and Blomhoff, 2006). Retinol deficiency inhibits RBP secretion, leading to protein accumulation in the endoplasmic reticulum of hepatic parenchymal cells (Bushue and Wan, 2010).

It is now long established that retinol is absorbed in the small intestine, stored in the liver, and secreted into circulation bound to RBP (Kanai et al., 1968). However, how retinol enters the cell has been the topic of much debate. Due to the hydrophobic nature of retinol, cellular membranes do not constitute a barrier and retinol can spontaneously cross the membrane. It was shown that binding to RBP is not required for movement of retinol into or out of cells. It was thus proposed that cellular uptake of retinol from RBP in blood occurs spontaneously and simply follows the concentration gradients of free retinol (Noy, 2000). However, although free retinol can also diffuse through membranes, it seldom exists in its free form. Furthermore, direct binding of RBP to a plasma membrane receptor has been demonstrated in pigment epithelial cells (Heller, 1975) and human placental membrane vesicles. It was further shown that free, rather than TTR-associated, RBP bound to the receptor and subsequent receptor mediated retinol uptake occurred. On the release of retinol to the receptor, RBP assumes a low-affinity conformation for both the receptor and

TTR and now, being uncomplexed, is excreted via the kidney (Sivaprasadarao and Findlay, 1988a, Sivaprasadarao and Findlay, 1988b).

It was not until recently that the long sought RBP receptor was finally identified as stimulated by retinoic acid gene 6 (STRA6), in bovine retinal pigment epithelial cells (Kawaguchi *et al.*, 2007). Described as a 74 KDa multi-transmembrane domain protein, STRA6 was shown to satisfy all three criteria expected of the RBP receptor, that is; (i) conferring high affinity RBP binding to cells transfected with bovine STRA6 cDNA; (ii) mediating retinol uptake; and (iii) showing localisation consistent with its function as the RBP receptor (Kawaguchi et al., 2007). Particularly strong expression of STRA6 occurs in cells that compose human blood-organ barriers e.g. the adult brain (Bouillet et al., 1997), the placenta and testis (Quadro et al., 2005, Sivaprasadarao and Findlay, 1988a), the spleen and thymus (Sommer, 1997) as well as in the retinal pigment epithelial (RPE) in the adult eye (Kawaguchi et al., 2007).

1.2.2 Structure and Ligand Binding

RBP binds specifically to TTR, as illustrated in Figure 1.5, and the RBP receptor, STRA6 (Sivaprasadarao et al., 1998). The protein is folded into an orthogonal β-barrel. This barrel is made up of eight anti-parallel β-strands and is open at one end and closed at the other. The retinol binding site is located at the interior of the barrel and is lined largely by hydrophobic amino acid side-chains. The open end of the barrel is lined by loops of structure which connect the β strands, A+B, C+D, and E+F, which form the entrance/exit site for retinol, and G-H. These are known as the AB loop, CD loop, EF loop and GH loop respectively. Structure-function studies, using mutants of RBP and the placental receptor, as well as X-ray diffraction, show that the AB, CD and EF loops bind with TTR; however the EF loop binds with the highest affinity (Sivaprasadarao and Findlay, 1994). Deletion of the EF loop results in much reduced affinity of RBP for TTR (Redondo et al., 2006). The CD and EF loop bind the receptor, the CD loop being the major site. Mutations in the CD loop

resulted in loss of the ability of RBP to bind STRA6. The movement of retinol in and out of the binding pocket is facilitated by the AB loop by switching between the closed and open conformation states. It is believed that binding of the EF loop and TTR stabilizes the closed conformation and that the binding of the CD loop to the receptor stabilizes the open conformation, through a conformational switch of the AB loop (Sivaprasadarao and Findlay, 1994). Another study explored if the binding properties of RBP can be transferred to epididymal retinoic acid binding protein (ERABP). These two proteins display only minor differences with respect to their ligand-binding specificities: whereas RBP binds all the three physiologically relevant retinoids, including retinol, retinaldehyde and retinoic acid, the specificity of ERABP is restricted to retinoic acid. The results demonstrated that substitution of the EF loop alone was sufficient to confer the TTR-binding properties on to ERABP and that RBP binds to the receptor via its loops at the entrance/exit site of the retinol-binding pocket (Sundaram et al., 2002).

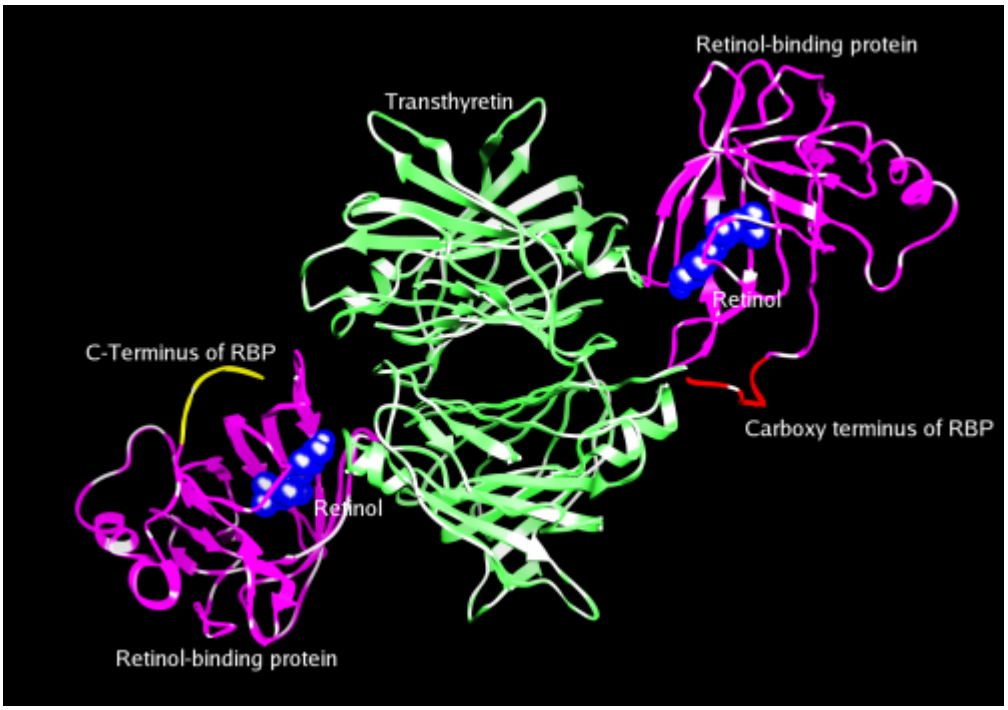

Figure 1.5: Holo-RBP in Complex with TTR. Taken from (Naylor and Newcomer, 1999).

Three-dimensional structure of holo-RBP and TTR complex; TTR (shown in green) can bind two molecules of RBP (shown in purple) *in vitro*, as illustrated. Due to a limiting plasma concentration of RBP, however, a 1:1 stoichiometry is observed *in vivo*. (PDB entry 1qab) (Naylor and Newcomer, 1999).

1.2.3 RBP in Health and Disease

To date, only two human RBP mutations have been identified (Quadro et al., 2002). RBP deficient patients display only a mild clinical phenotype that includes night blindness and modest retinal dystrophy (Biesalski et al., 1999). RBP knock-out mice, totally lacking RBP, have reduced levels of plasma retinol, abnormal vision at birth, which could be corrected with a retinol adequate diet by 5 months of age, and an inability to mobilize retinol from hepatic stores. This suggests that RBP is only essential in times of insufficient retinol intake and for normal vision in young animals (Quadro et al., 1999).

It has been suggested that RBP, from adipose tissue, may have a role in insulin resistance, obesity and ultimately type-II diabetes (T2D). RBP levels are elevated in these states and its normalisation enhances insulin sensitivity (Graham et al., 2006). This will be covered in more detail hereafter, given its pertinence to this thesis.

1.3 Insulin & Diabetes

Insulin (Latin *insula*, meaning "island") is a hormone produced in β-cells in islets of Langerhans in the pancreas. Insulin regulates energy metabolism by initiating several signalling cascades that control cell growth and survival, as well as protein, glycogen and lipid uptake, synthesis and hydrolysis. Where low insulin levels arise glycogen is converted to glucose. After a meal, increased nutrients in the blood cause the secretion of insulin. Insulin prevents gluconeogenesis in the liver and promotes glucose uptake into muscle and adipose tissue through regulated trafficking of glucose transporter type 4 (GLUT4) from intracellular stores to the plasma membrane. GLUT4 is predominantly expressed in muscle cells and adipocytes and mediates insulin-stimulated glucose transport in fat and muscle (Leto and Saltiel, 2012).

Type 1 diabetes is an autoimmune disease whereby T-cell mediated attack of β-cells occur, resulting typically in a dramatic loss of β-cells before type 1 diabetes is diagnosed. In Type-II diabetes, insulin-sensitive tissue loses response to insulin, resulting from an inhibition of insulin signalling. Insulin resistance leads to hyperinsulinemia as β-cells try to control blood glucose levels. Eventually pancreatic β-cells can no longer compensate for insulin resistance causing high blood and urine glucose levels due to impaired cellular uptake (Alberti and Zimmet, 1998). GLUT4 expression is reduced in insulin-resistant states, causing a reduction in insulin-stimulated glucose transport. Glucose intolerance then occurs (Graham et al., 2006). The World Health Organization has estimated that the number of adults with diabetes will more than double from an estimated 143 million in 1997 to 300 million by 2025 (Kumanyika et al., 2002).

1.3.1 Insulin Signalling

Binding of insulin to its receptor, the insulin receptor (IR), triggers the phosphorylation and activation of the IR tyrosine kinase, as illustrated in Figure 1.6. Recruitment and tyrosine phosphorylation of the insulin receptor substrates (IRSs), a family of adapter proteins, including IRS-1, IRS-2, IRS-3, IRS-4, Gab1, and Shc ensues followed by subsequent activation of the phosphoinositide 3-kinase (PI3K) pathway (Leto and Saltiel, 2012, Yadav et al., 2012). Tyrosine phosphorylated IRS proteins serve as docking sites for the SH2 domain of the p85 regulatory subunit of class I PI3K, and the interaction of IRS proteins and PI3K results in PI3K activation and the subsequent synthesis of phosphatidylinositol-3,4,5-trisphosphate [PtdIns(3,4,5)P_3] from PtdIns(4,5)P_2 at the plasma membrane. PtdIns(3,4,5)P_3 in turn serves as a docking site for several PH domain-containing Ser/Thr kinases that are implicated in glucose uptake, including phosphoinositide-dependent kinase 1 (PDK1) and AKT. PDK1 and mTORC2 activate AKT through dual Ser/Thr phosphorylation. AKT then phosphorylates numerous substrates, resulting in GLUT4 translocation to the membrane (Leto and Saltiel, 2012, Saltiel and Kahn,

2001). Insulin produces most of its metabolic actions through the PI3K pathway. Another pathway proceeds through growth factor receptor-bound protein 2 (Grb2)/ Son of Sevenless (Sos) and ras, leading to activation of the mitogen-activated protein kinase 1 (MAP kinase) isoforms ERK1 and ERK2 (Cusi et al., 2000).

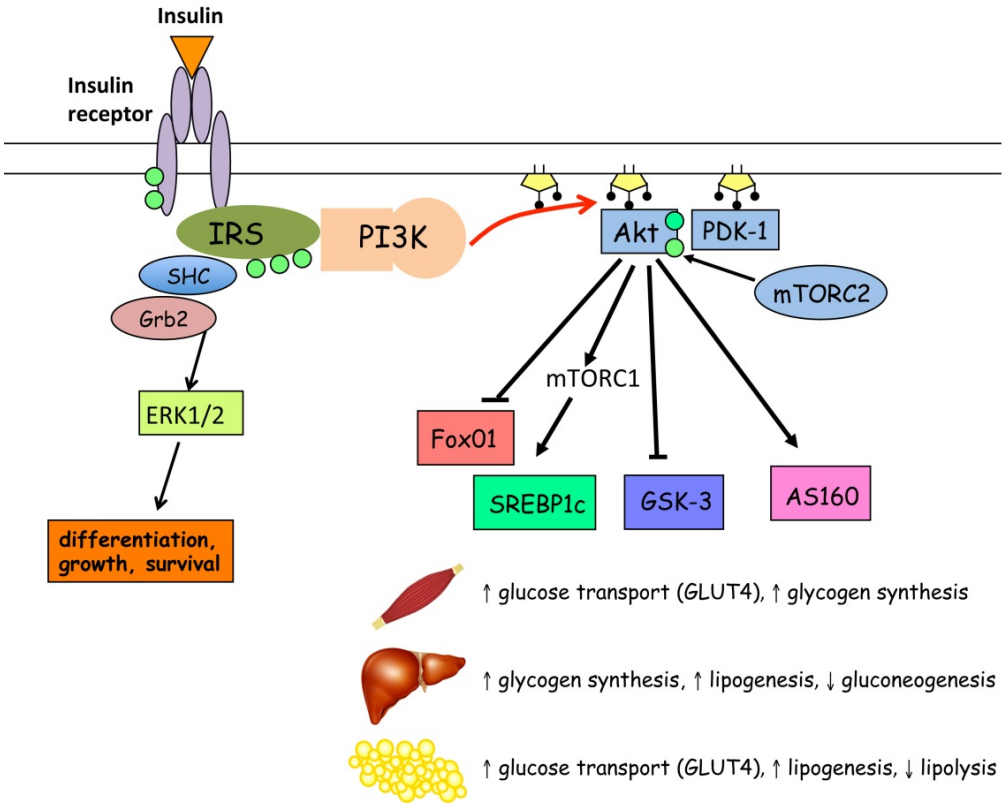

Figure 1.6: **Insulin Signalling Pathway. Taken from (Turner, 2013)**

Phosphorylation of the IR recruits IRS proteins to the membrane. IRS-1 is phosphorylated resulting in binding to the p85 regulatory subunit of PI3K. PI3K then catalyses the production of PIP3 at the plasma membrane. PIP3 recruits PDK1 which causes AKT activation. Activated AKT then phosphorylates various substrates (Turner, 2013).

1.3.2 Insulin Resistance and Obesity

An obese adult is classified as having a Body Mass Index equal or greater than 30 (Alberti and Zimmet, 1998). Obesity is believed to be caused by an imbalance between energy ingested in food and the energy expended (Bray, 2004). This excess energy is then stored in adipocytes, which over time will increase in number and size. Adipocytes, in addition to having a role as lipid storage depots, are an active endocrine organ regulating fat mass and nutrient homeostasis (Yadav et al., 2012). Adipocytes are therefore critical for modulating fat mass but as a person gets heavier and the adipocytes enlarge, these control mechanisms become dysregulated, macrophages accumulate in the adipose tissue and inflammation ensues (Greenberg and Obin, 2006), resulting in macrophages constituting up to 40 % of adipose tissue. This chronic inflammation results in cytokine and adipokines, adipose tissue related cytokines, production resulting in a number of pathologies associated with obesity including T2D. Up to 65% of cases of T2D can be attributed to obesity. Furthermore, two thirds of diabetic deaths may be caused by obesity (Bray, 2004).

Adipokines include hormones such as leptin, resistin, adiponectin, and inflammatory cytokines such as TNF-α, monocytes chemoattractant protein-1 (MCP-1) and interleukin 6 (IL-6) (Wozniak et al., 2009). TNF-α expression in adipocytes of obese animals is markedly increased and there is a significant correlation between BMI and plasma TNF-α concentrations (Dandona et al., 2004). TNF-α causes an inhibition of the auto-phosphorylation of tyrosine residues of the IR and an induction of serine phosphorylation of IRS-1, which in turn causes serine phosphorylation of the insulin receptor in adipocytes and inhibits tyrosine phosphorylation. This is suggested to occur through activation of c-Jun N-terminal protein kinase (JNK), as illustrated in Figure 1.7 (Hirosumi et al., 2002). IL-6 has been shown to inhibit insulin signal transduction in hepatocytes. This effect has been shown to be related to suppressor of cytokine signalling-3 (SOCS-3), a protein that associates with the IR, inhibits its autophosphorylation, the tyrosine phosphorylation of IRS-1, the association of p85 subunit of PI3K to IRS-1 and the subsequent activation of AKT (Dandona et al., 2004).

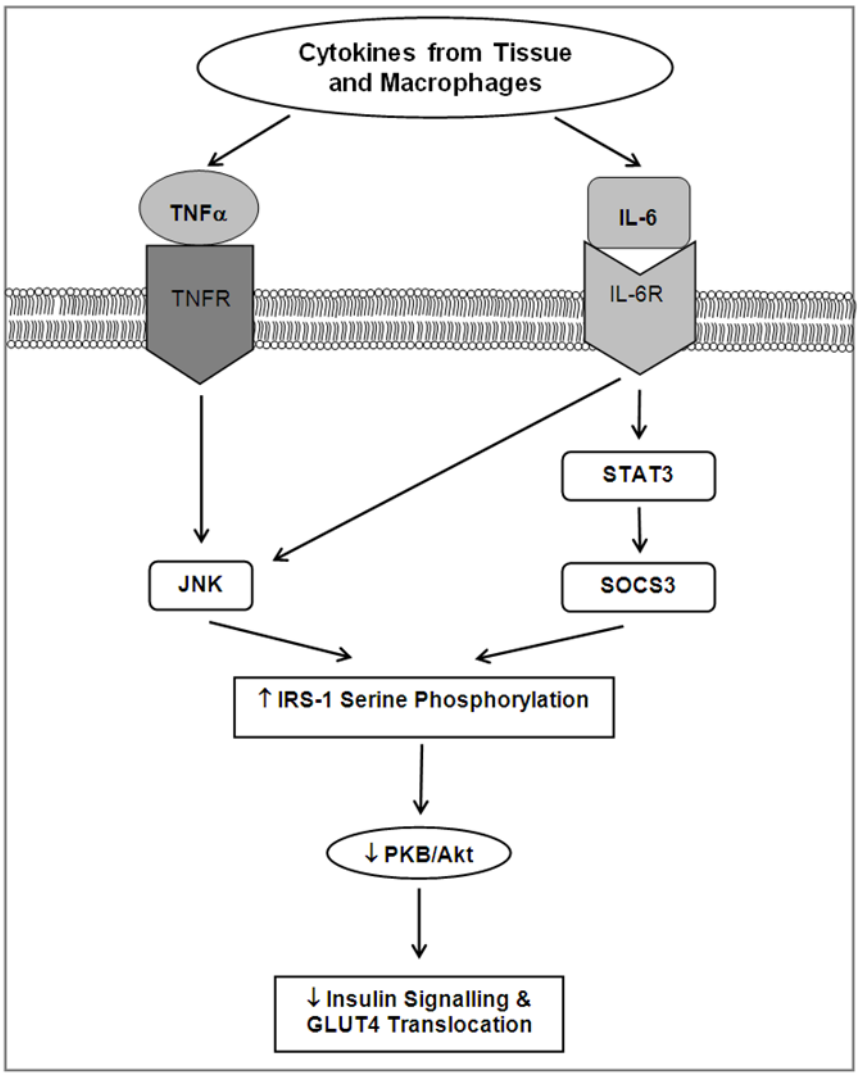

Figure 1.7: Proposed Mechanism for Inflammation Induced Insulin Resistance in Muscle. Taken from (Toit and Donner, 2012)

IL-6 activates the STAT3-SOCS3 pathways while TNF-α activates JNK to phosphorylate IRS-1. Serine phosphorylation of IRS-1 inhibits GLUT4 translocation to the membrane and attenuates the insulin signalling pathway (Toit and Donner, 2012).

1.3.3 RBP and T2D

The significance of the RBP system, especially in terms of human health, reached an enhanced level of interest with the claim that RBP is deeply implicated in the genesis of insulin resistance and T2D – specifically, that elevated levels of RBP attenuate intracellular responses to insulin by a mechanism independent of insulin levels or insulin-receptor interactions. The hypothesis holds that RBP causes a reduction in the expression and translocation of GLUT4 which results in the development or worsening of insulin resistance. Down regulation of GLUT4 in adipose tissue is seen in nearly all insulin-resistant pathologies and increasing GLUT4 in adipose tissue has been shown to protect the body against insulin resistance (Yang et al., 2005). It has been shown that GLUT4 levels in adipose tissue and RBP levels correlate inversely in T2D patients (Graham et al., 2006). RBP may affect GLUT4 expression by inducing the expression of phosphoenolpyruvate carboxykinase (PEPCK), a regulatory enzyme of gluconeogenesis, which reduces insulin action and suppresses glucose production in hepatocytes (Yang et al., 2005). PEPCK catalyses the first step of gluconeogenesis and the increase in this enzyme alone is sufficient to induce the metabolic pathway and finally to cause insulin resistance (Valera et al., 1994).

Serum TTR is also elevated in T2D. It is believed that increased amounts of the RBP: TTR complex may contribute to RBP elevation in T2D as TTR prevents the renal clearance of RBP (Klöting et al., 2007). Fenretinide (an anti-cancer synthetic retinoid), which accelerates RBP urinary excretion (and hence reduces serum levels), reduces insulin resistance and improves insulin sensitivity and glucose tolerance in obese mice (Yang et al., 2005). Furthermore, a study in approximately 6,500 aging adults showed that a gain-of-function single nucleotide polymorphism (SNP) in the RBP promoter is associated with a 2-fold-increased risk of T2D (van Hoek et al., 2008). The data provide some mechanistic insights into RBP mediated insulin resistance, but the underlying cellular mechanisms are not known.

Emerging evidence suggests RBP may cause insulin resistance by development of the inflammatory state. RBP was shown to induce cytokine production in

macrophages. These cytokines include TNF-α, IL-6, MCP-1, IFN-γ, Granulocyte-Macrophage Colony Stimulating Factor (GM-CSF), Interleukin-1 beta (IL-1β), Interleukin-2 (IL-2), and Interleukin-12p70 (IL-12p70) (Norseen et al., 2012). As already mentioned, TNF-α is a JNK activator, which in turn phosphorylates IRS-1 at Ser 307 (Hirosumi et al., 2002). A JNK specific inhibitor reversed the RBP dependent inhibition of insulin signalling. Toll-like receptor 4 (TLR4) has also been suggested to be involved in RBP mediated insulin resistance. In TLR4−/− macrophages, IL-6 and TNF-α secretion is attenuated by 60 to 80 %. TLR4 has previously been linked to insulin resistance (Shi et al., 2006). RBP attenuates insulin signalling independent of its binding to retinol. As STRA6 is not expressed in macrophages, this effect is also independent of STRA6. This is a novel alternative mechanism for RBP action and highlights differences in RBP signalling in adipocytes and macrophages. However, both direct and indirect effects of RBP on adipocyte insulin signalling may contribute to insulin resistance (Norseen et al., 2012).

A recent publication put forward evidence displaying how RBP, acting extracellularly but producing an intracellular effect, regulates energy homeostasis and insulin responses through a RBP-retinol/STRA6/JAK2/STAT5 signalling cascaded that induces the expression of STAT target genes including *SOCS3*, which, as already mentioned, inhibits insulin signalling (Berry et al., 2011, Berry and Noy, 2012). This will be discussed in more detail in relevant chapters.

1.4 STRA6

STRA6 is a 74 kDa multitransmembrane protein, encoded by a gene originally identified as a retinoic acid-stimulated gene in cancer cell lines (Szeto et al., 2001). It is a new class of transmembrane protein, with no similarity to any other protein receptor (Kawaguchi et al., 2007). The predicted topology of STRA6 is illustrated in Figure 1.8. STRA6 is highly conserved among mammals and other vertebrates

(Bouillet et al., 1997). STRA6 specifically binds holo-RBP and is crucial in the delivery of retinol to the target tissues. The existence of a specific receptor for RBP was shown experimental in the 1970s using retinal pigment epithelium (Heller, 1975). Its role in RBP binding and retinol uptake was characterised (Sivaprasadarao and Findlay, 1988a, Sivaprasadarao et al., 1994, Sivaprasadarao et al., 1998). The groups of Dollé and Chambon, identified STRA6 as the product of a retinoic acid inducible gene and suggested that it might have a transport – related function (Bouillet et al., 1997). Subsequently, the over expression of the gene was seen in human tumours (Szeto et al., 2001) with, interestingly, a potential connection to Wnt-1 signalling (Tice et al., 2002). Using purified RBP derivatized with an ultraviolet crosslinking agent, Kawaguchi et al., were able to identify STRA6 as a protein present in membrane preparations from RPE cells that bound specifically to RBP (Kawaguchi et al., 2007). Although the existence of an RBP receptor previously was a contentious subject (Noy, 2000), it is now widely accepted that such a receptor exists and its role in retinol uptake (Sivaprasadarao and Findlay, 1988b) has now been validated (Kawaguchi et al., 2007). The crystal structure of STRA6 has yet to be elucidated and any other functions STRA6 may have are yet to be clarified.

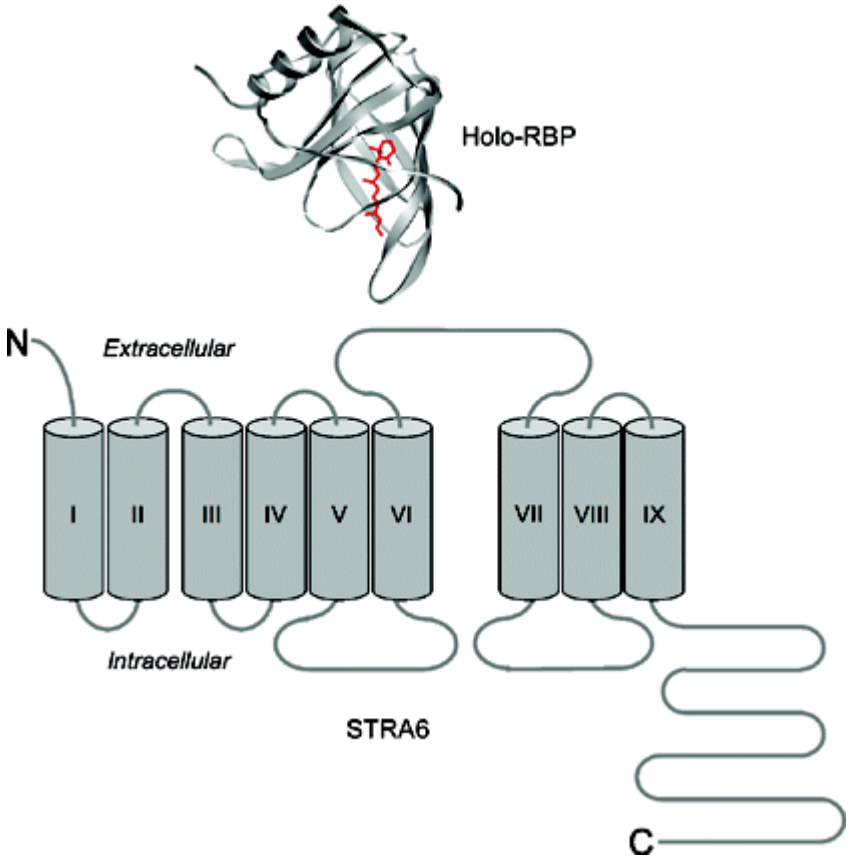

Figure 1.8: Holo-RBP and the RBP Receptor STRA6. Taken from (Kawaguchi et al., 2008b).

The high affinity cell surface receptor for RBP, STRA6, predicted topology. Crystal structure of holo-RBP is based on structure 1HBP in the Protein Data Bank (PDB). The predicted 9 transmembrane domains for STRA6 are indicated with roman numerals (Kawaguchi et al., 2008b).

1.4.1 STRA6 in Disease

A number of natural STRA6 human mutations have been identified which give rise to devastating abnormalities, most of which are fatal (Pasutto et al., 2007, Golzio et al., 2007). These mutations cause a variety of serious malformations and dysfunctions most noticeably in the eye, diaphragm, lungs and heart, often accompanied by moderate to severe mental retardation. Foetal or early death or termination of pregnancy is the usual outcome. Some effects can clearly be related to disruption of the potential supply of retinol which remains bound to RBP and is not delivered in sufficient quantity to the developing tissues. Whether there is also a separate or associated signalling function which is affected remains to be discovered. Some of these mutations produce stop codons and absence of the protein altogether; others are predicted to occur in extramembranous regions such as the loops between transmembrane segments or the N- and C- terminal "tails" (Pasutto et al., 2007). It has been postulated that these alterations may affect the architecture and or trafficking of the protein, e.g. by extending the transmembrane helices (Golzio et al., 2007). STRA6 has been shown to be potentially important in cancer biology, as *STRA6* mRNA levels are highly elevated in mammory gland tumours and human colorectal tumours (Szeto et al., 2001).

1.4.2 STRA6 Mediated Retinol Transport

STRA6 binds holo-RBP, facilitates the dissociation of the protein-ligand complex, and transfers retinol directly from extracellular RBP to cellular retinol binding protein (CRBP; also known as CRBP-1). Apo-RBP, which has lower affinity for the receptor (Sundaram et al., 1998), then dissociates from STRA6 and is excreted in the kidney since its affinity for TTR is also markedly reduced. The next holo-RBP will bind STRA6 and hereby the process continues. STRA6 thus employs a transport mechanism that is distinct from that of other transporters of small lipids (Kawaguchi

et al., 2007). STRA6 mediated retinol uptake is tightly coupled to intracellular retinoid storage proteins, CRBP and LRAT (Kawaguchi et al., 2011). CRBP is involved in the intracellular trafficking of retinol (Franzoni et al., 2010) and delivers retinol to LRAT (Ong, 1994), an enzyme that catalyses retinyl ester synthesis (Jin et al., 2007). The coupling of STRA6 and LRAT enhances retinol uptake by converting it to its ester form (Amengual et al., 2012). LRAT and CRBP, therefore, provide high specificity in cellular uptake of retinol and prevent the excessive accumulation of free retinol (Kawaguchi et al., 2011).

CRBP is widely distributed, found in almost all organs, particularly abundant in certain cells known to process considerable amounts of retinol, such as the pigment epithelial cells of the eye (Ghyselinck et al., 1999) as well as HSCs (Blomhoff and Blomhoff, 2006). CRBP is indispensable for efficient RE synthesis and storage, this is particularly evident under conditions of dietary retinol deprivation (Ghyselinck et al., 1999). Mutant mice, with the CRBP gene knocked out, are healthy and fertile when fed a retinol enriched diet. However, when reared on a retinol deficient diet, mice fully exhaust their RE stores within 5 months, and develop abnormalities characteristic of post-natal retinol deficiency (Ghyselinck et al., 1999). LRAT was the first protein shown to enhance STRA6's vitamin A uptake activity (Kawaguchi et al., 2007) and is essential for retinol esterification: knockout mice have reduced retinyl esters, shown to be reduced in the liver by more than 10,000-fold, and dramatically attenuated visual functions due to the lack of retinyl esters in the eye (Batten et al., 2004).

STRA6 has been shown to function as a bidirectional transporter to mediate release of retinol under certain conditions (Sivaprasadarao and Findlay, 1988b). STRA6 catalyses both retinol release from holo-RBP and loading of free retinol into apo-RBP. This exchange occurs between intracellular holo-CRBP and extracellular holo-RBP, both of which bind to STRA6 (Kawaguchi et al., 2012, Sundaram et al., 1998). LRAT expression is required to drive STRA6 mediated retinol transport directionally toward uptake rather than efflux (Amengual et al., 2012). It is unclear to what extent this efflux happens and in what context. STRA6's retinol exchange

may serve to refresh the intracellular retinoid pool to guard against depletion due to gradual oxidation occurring during long-term storage (Kawaguchi et al., 2012) or for times of retinol deficiency so retinol can be used for critically dependent tissues (Sivaprasadarao and Findlay, 1988b).

1.4.3 Other Functions of STRA6

A recent publication has proposed that STRA6 is not only a retinol transporter but also a cell-surface signalling receptor activated by the RBP–retinol complex, as illustrated in Figure 1.9. The belief is that association of holo-RBP with STRA6 triggers tyrosine phosphorylation of STRA6, resulting in recruitment and activation of JAK2 and the transcription factor STAT5. Activation of STAT5 results in the expression STAT target genes, including *SOCS3*, which inhibits insulin signalling, and *PPARγ*, which enhances lipid accumulation (Berry et al., 2011). The group went on to suggest that STRA6-mediated uptake of retinol and transduction of a phosphorylation cascade are interdependent (Berry et al., 2012b).

The authors believe that this signalling cascade is inhibited by TTR, as it blocks the ability of holo-RBP to associate with STRA6 (Berry et al., 2012a). The ability of TTR to block holo-RBP association with STRA6 has previously been discovered (Sivaprasadarao and Findlay, 1988b). The authors suggests that STRA6 functions only under circumstances where the plasma RBP level exceeds that of TTR and that, in addition to preventing the loss of RBP, TTR plays a central role in regulating holo-RBP/STRA6 signalling (Berry et al., 2012a).

These findings remain controversial and have been contradicted by other groups. Chen et al. and Farjo et al. found that the signalling cascade occurred independent of retinol. Kawaguchi et al., heavily criticised the STRA6 antibody used by Berry et al., and their technique of producing holo-RBP (Kawaguchi et al., 2012).

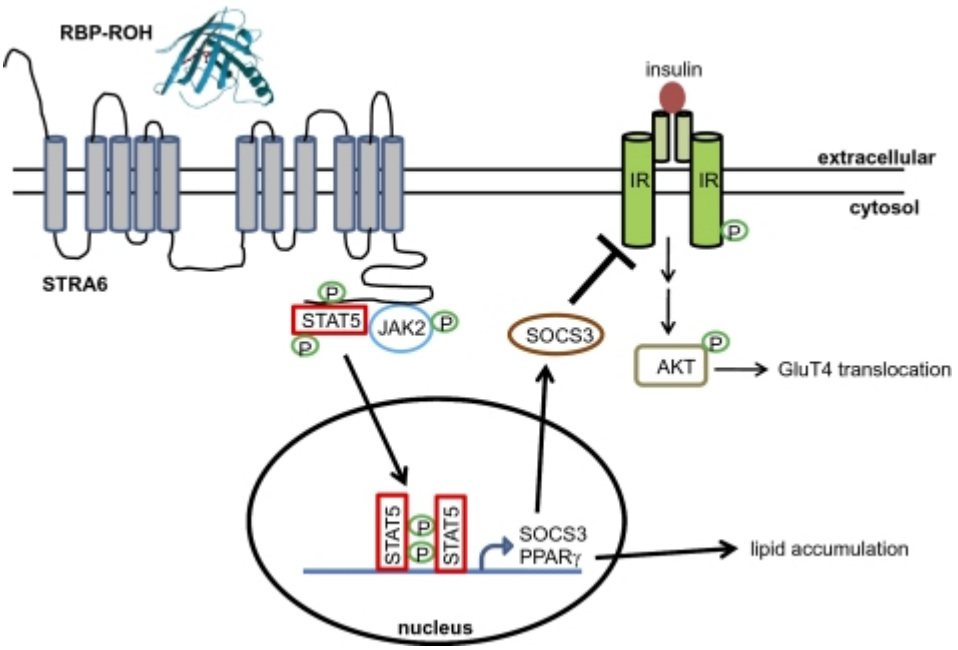

Figure 1.9: Model of the RBP-ROH/STRA6/JAK/STAT Pathway. Taken from (Berry et al., 2011).

Binding of holo-RBP to STRA6 triggers tyrosine phosphorylation within an SH2 domain-binding motif in the receptor's cytosolic domain. Phosphorylated STRA6 recruits and activates JAK2, which in turn, phosphorylates STAT5. Activated STAT5 translocates to the nucleus to regulate the expression of target genes, including *SOCS3*, which inhibits insulin signalling and *PPARγ*, which enhances lipid accumulation (Berry et al., 2011).

1.4.4 STRA6 Domains

STRA6's predicted topology suggests 19 distinct regions, including 5 extracellular loops, 9 transmembrane segments and 5 intracellular loops (Kawaguchi et al., 2008a). STRA6 is known to bind RBP. A number of imitational experiments were performed in hopes of discovering the RBP binding domain of STRA6, resulting in the discovery of three key residues. Mutations in these three residues, on STRA6's third extracellular loop (EC3), abolish RBP binding: Tyr 336, Gly, 340 and Gly 342 (Kawaguchi et al., 2008a). STRA6 also associates with CRBP (Sundaram et al., 1998, Redondo et al., 2008) and the binding domain (intracellular loop 3, residues 235 to 295) has been identified (Berry et al., 2012b) located in which is the human polymorphism $P^{293}L$, shown to elicit a broad spectrum of severe birth defects. Interestingly, the unusually large C-terminus for this protein accounts for almost one third of the molecular weight of the full-length ~ 74 kDa receptor and within which the human polymorphisms $T^{644}M$ and $R^{655}C$ are located (Pasutto *et al.*, 2007).

Aims and Objectives

STRA6 has been identified as the specific membrane receptor for RBP, mediating cellular retinol uptake from holo-RBP (Kawaguchi et al., 2007). The existence of a receptor for RBP has been controversial (Noy, 2000) and STRA6's function remains at present to be characterised (Blaner, 2007). The vital necessity of STRA6 has been underlined by the discovery of human mutants of STRA6 which cause massive, devastating and ultimately fatal tissue malformations (Pasutto et al., 2007, Golzio et al., 2007). Given that STRA6 is not homologous to any other protein in the human genome and has been implicated in disease the elucidation of its actual purpose in the body is imperative.

The objective of the work undertaken in this thesis is toward a greater understanding of STRA6, with specific interest in function, directed at the identification of novel protein interactions. To this end, the MYTH was utilized to detect protein interactions and detected interactions were subsequently to be validated independently of the yeast based assay, described in Chapters 3 and 4.

STRA6's predicted topology suggests the presence of a large third intracellular loop. The presence of such a domain lends itself to the possibility of intracellular protein: protein interactions. Studies aimed at understanding the role of this region in relation to STRA6's function should prove instructive. Characterization of the third intracellular loop of STRA6 is described in Chapter 5. Finally, a summarizing discussion aims to place the findings outlined within this thesis in the context of the literature reviewed above.

Chapter 2

Materials and Methods

2.1 Chemicals and Reagents

All chemicals, reagents, and proteins were obtained from Sigma unless otherwise stated. Enzymes and buffers were purchased from New England Biolabs, Fermentas, Promega and Stratagene. All oligonucleotides used were acquired from Sigma.

Size markers for DNA and protein gels were supplied by Fermentas. Plasmid DNA isolation and purification kits were procured from Fermentas, Invitrogen and Qiagen.

IPTG was purchased from Ambion. *E. coli* strains were bought from Invitrogen. FuGENE® 6 transfection reagents were attained from Roche. Lipofectamine 2000 was obtained from Invitrogen. Dulbecco's Modified Eagle's Medium (DMEM) was supplied by Fisher. T75 Tissue culture flasks were purchased from Sarstedt.

Protein purification was performed using Glutathione Sepharose™ 4 Fast Flow purchased from GE Healthcare, Ni-NTA agarose or Strep-Tactin Superflow Plus, both of which were acquired from Qiagen. In the detection of proteins, ECL Western blotting substrate was supplied by Roche, stripping buffer was procured from ThermoScientific. PVDF transfer membrane was bought from GE healthcare.

Antibodies were purchased from Sigma (α-rabbit-HRP, α-His-HRP), Origene (α – DDK), Cell Signalling (α-myc), Promega (α-mouse-HRP), Abnova (α-STRA6), Dako (α -RBP), Covance (α-HA) and Santa Cruz Biotechnology Inc. (α -CRBP).

2.2 Vectors, Host Strains and Cell Lines

The coding sequence for human STRA6 (UniProt entry Q9BX79) was obtained in the pPICZA vector (OriGene), incorporating a C-terminal GFP and 6xHis tag. This vector was used in attempts to express the full length receptor in *Pichia pastoris.* The coding sequence for human STRA6 (UniProt entry Q9BX79) was also obtained in the pcDNA3.1 vector (Invitrogen), incorporating a C-terminal 6xHis tag, in the

pcDNA4 vector (Invitrogen), incorporating a C-terminal Myc and 6xHis tag and in the pN-TGSH vector (Dualsystems Biotech AG) incorporating a HA and STREPII tag. These vectors were used in attempts to express the full length receptor in Human Embryonic Kidney 293T (HEK293T) cells. All expression attempts are described further in Chapter 4.

The STRA6-ICL3 construct (in pETd9) and Im7 construct (in pTrc99A) were a kind gift from Dr. Conor Breen & Dr. Werner Vos, NUI Maynooth.

The RBP construct (in pPICZ-α A) and CRPB construct (in pGEX-4T-3) were a kind gift from Dr. José Angel Campos-Sandoval and Dr. Lyndsey Brown.

HEK293T lysates overexpressing [C-C motif chemokine 2 (CCL2), CXCL14, interferon-induced transmembrane protein 1 (IFITM1), interferon-induced transmembrane protein 3 (IFITM3), macrophage migration inhibitory factor (MIF), **S**tress-associated Endoplasmic Reticulum (ER) protein 1 (SERP1) and proteolipid protein 2 (PLP2)] were all obtained from Origene. Ovarian Cancer Immuno Reactive Antigen Domain Containing Protein 2 (OCIAD2) and osteopontin constructs (in pCMV6-Entry) were supplied by Origene.

The coding sequences for human CD63 (UniProt entry P08962) and PDZK1-Interacting Protein 1 (PDZK1-IP1) (UniProt entry Q13113) were obtained in the pcDNA3.1 vector, incorporating a C-terminal HA tag. These vectors were used in attempts to express the full length proteins in HEK293T cells.

For cloning and plasmid amplification, supercompetent *E. coli* strain TOP10 cells were used. Expression of full length human STRA6 was carried out in the *P. pastoris* strain KM71H and mammalian HEK293T cells (Invitrogen). STRA6-ICL3, Im7 and CRBP were expressed in the *E. coli* strain BL21(DES). Expression of human RBP was carried out in *P. pastoris* strain KM71H. Expression of CD63, PDZK1-IP1, OCIAD2 and osteopontin were carried out in mammalian HEK293T cells.

2.3 Subcloning

Subcloning of the coding sequences of interest into appropriate vectors was by amplification from the host vector by polymerase chain reaction. Both PCR product and destination vector were linearized by double restriction digestion, followed by ligation of the coding sequence into the destination vector. Competent *E. coli* cells were transformed with plasmid DNA and spread onto LB agar plates containing appropriate antibiotics for growth and selection.

Methods will be explained in more detail hereafter and in relevant chapters.

2.3.1 The Polymerase Chain Reaction (PCR)

DNA template (10 ng) was incubated with each of the primers (at a final concentration of 0.4 µM) and dNTPs (at a final concentration of 0.2 mM each), in the appropriate 1x reaction buffer [20 mM Tris-HCl (pH 8.8), 2 mM $MgSO_4$, 10 mM KCl, 10 mM $(NH_4)_2SO_4$, 0.1% Triton® X-100, 0.1 mg/ml nuclease-free bovine serum albumin (BSA)] to a final volume of 49 µL. After thorough mixing, 1 µL (at a final concentration of 0.05 U) Pfu Turbo Hot Start DNA polymerase (Strategene) was added.

Following polymerase activation at 95 °C for 5 minutes, PCR was performed for thirty cycles of denaturation at 95 °C for 30 seconds, annealing at the 5 °C below lowest primer Tm °C for 30 seconds and extension at 72 °C for 1 min/kb. Total reaction mixture was analysed on a 0.8 % (w/v) agarose gel [50 ml 1x Tris base, acetic acid and ethylenediaminetetraacetic acid (EDTA) buffer (TAE), 0.4 g agarose] as described in 2.3.11.

Where a single PCR product of expected size was observed, the band was excised under UV light and purified using the QIAquick gel extraction kit (Qiagen) according to the manufacturer's instructions.

2.3.2 Restriction Digestion

Purified PCR product was digested with the appropriate restriction enzymes. The PCR product was incubated with both enzymes (at a final concentration of 0.17 U) and BSA (at a final concentration of 100 ng/mL) in a 1x reaction buffer [MULTI-CORE™ Buffer (Promega), 25mM Tris-acetate (pH 7.5 at 37 °C), 100 mM potassium acetate, 10 mM magnesium acetate, 1 mM dithiothreitol (DTT)] for at least four hours at 37 °C. The destination vector was digested with the same restriction enzymes.

The double digested vector and insert were analysed on a 0.8 % (w/v) agarose gel as described in 2.3.11. The bands were excised under UV light and purified using the QIAquick gel extraction kit (Qiagen) according to manufacturer's instructions.

2.3.3 Zero Blunt TOPO Cloning

For a number of constructs, plasmids were initially ligated into pTOPO (Invitrogen) before ligation into the destination vector. Gel extracted PCR product concentrations were determined using a UV-Vis Spectrophotometer (NanoDrop™ 1000 Spectrophotometer, Thermo Scientific) and 10 ng-50 ng of PCR product added to 1 µl pCR®-Blunt II-TOPO® vector (10 ng/µL plasmid DNA in 50 % glycerol, 50 mM Tris-HCl, pH 7.4, 1 mM EDTA, 2mM DTT, 0.1 % Triton X-100, 100 µg/mL BSA, 30 µM bromophenol blue) in the presence of 1 µl salt solution (1.2 M NaCl, 0.06 M $MgCl_2$) and made up to 5 µl with water. The reaction was gently mixed and incubated for 5 minutes at room temperature (20-22 °C). 2 l of the reaction mixture were added to TOP10 chemically competent *E.coli* cells and incubated on ice for 5 minutes. Cells were then heat-shocked at 42 °C for 30 seconds before being returned to ice for a further 2-3 minutes. 250 µL super optimal broth with catabolite repression (SOC) medium (20 g/L bacto tryptone, 5 g/L bacto yeast extract, 0.5 g/L

sodium chloride, 0.186 g/L potassium chloride, 0.932 g/L magnesium chloride, 1.2 g/L $MgSO_4$, 3.603 g/L glucose, pH 7) was added prior to incubation at 37 ℃, with shaking (200-250 rpm) for one hour.

Following this incubation period, approximately 200 µL of the transformation mixture were spread onto an Luria-Bertani (LB) agar plate (10 g/L tryptone, 5 g/L yeast extract, 10 g/L NaCl, pH 7.0, 10 g/L agar) containing 50 µg/mL kanamycin (for the selection of transformants), followed by incubation overnight at 37 ℃. A number of resulting colonies were cultured and the plasmid DNA isolated as described in 2.2.8 and 2.2.9 respectively. Successful insertion of the coding sequence into the destination vector was determined by restriction digestion and subsequent analysis by agarose gel electrophoresis as described in 2.3.2 and 2.3.11 respectively. Successful constructs were independently sequenced (Eurofins) to verify the coding sequence was correct, in frame and free of errors.

2.3.4 Ligation Reaction

Approximately 100 ng of vector and a 1 to 9 fold molar excess of insert were mixed in a 1x ligation buffer (50 mM Tris-HCl, 10 mM MgCl2, 1 mM Adenosine 5'-triphosphate (ATP), 10 mM DTT, pH 7.5), to which 1 µL (400 U) T4 DNA Ligase (NEB) (in 10 mM Tris-HCl, 50 mM KCl, 1 mM DTT, 0.1 mM EDTA, 50 % glycerol, pH 7.4 @ 25 ℃) was added. Total reaction mix was incubated at 16 ℃ overnight and competent TOP10 cells subsequently transformed with ligation products as described in 2.3.5.

2.3.5 Transformation of *E.coli* Cells

E.coli cells [TOP10 or BL21(DES)] were thawed on ice and 50 µL transferred to a 15 ml tube. To this tube, 1 µL (10 ng) of ligation product was added, followed by

incubation on ice for 5 minutes. Cells were then heat-shocked at 42 °C for 30 seconds before being returned to ice for a further 2-3 minutes. 250 µL SOC medium was added prior to incubation at 37 °C with shaking (200-250 rpm) for one hour.

Following this incubation period, approximately 200 µL of the transformation mixture was spread onto a LB agar plate containing the appropriate antibiotic for the selection of transformants, followed by incubation overnight at 37 °C. A number of resulting colonies were cultured and the plasmid DNA isolated as described in 2.3.8 and 2.3.9 respectively. Successful insertion of the coding sequence into the destination vector was determined by restriction digestion and subsequent analysis by agarose gel electrophoresis as described in 2.3.2 and 2.3.11 respectively. Successful constructs were independently sequenced to verify the coding sequence was correct, in frame, and free of errors.

2.3.6 Preparation of Seed Stocks

50 l of TOP10 competent cells were streaked onto an super optimal broth (SOB) agar plate (20 g/L bacto tryptone, 5 g/L bacto yeast extract, 0.5 g/L sodium chloride, 0.186 g/L potassium chloride, 0.932 g/L magnesium chloride, 3.603 g/L glucose, 10 g/L agar, pH 7) and incubated overnight at room temperature (20-22 °C). A single colony was used to inoculate 2 ml of SOB medium (20 g/L bacto tryptone, 5 g/L bacto yeast extract, 0.5 g/L sodium chloride, 0.186 g/L potassium chloride, 0.932 g/L magnesium chloride, 3.603 g/L glucose, pH 7) and incubated overnight at room temperature (20-22 °C) with shaking (220rpm). 15 % glycerol (0.44 g/2ml) was added to the culture, which was then aliquoted and placed in a dry ice/ethanol bath for 5 minutes before storage at -80 °C.

2.3.7 Preparation of Competent Cells

250 ml of SOB medium was inoculated with 1 vial of the seed stocks, as described in 2.3.6, and grown at 20 °C till the culture reached an OD_{600} of 0.3. The culture was then centrifuged (3000 g at 4 °C for 10 minutes) and the pellet resuspended in 80 ml of ice cold CCMB80 buffer (0.98 g/L potassium acetate, 8.88 g/L calcium chloride, 4 g/l magnesium chloride, 10 % glycerol, pH 6.4). Following incubation on ice for 20 minutes, centrifugation was repeated (3000 g at 4 °C for 10 minutes). The pellet was resuspended in 10 ml of ice cold CCMB80 buffer. Chilled CCMB80 was added to yield a final OD_{600} of 1.0 to 1.5. The culture was incubated for 20 minutes on ice and then aliqouted before being stored at -80 °C.

2.3.8 Growth of Bacterial Cultures

For plasmid DNA amplification, homemade TOP10 *E. coli* competent cells, as described in 2.2.6 and 2.2.7, were used throughout. Colonies were selected on LB agar plates containing the appropriate antibiotic.

All vectors used confer ampicillin or kanamycin resistance to *E. coli* transformants. Ampicillin was added to both liquid and solid media (final concentration 100 µg/mL) for selection and maintenance. Kanamycin was added to both liquid and solid media (final concentration 50 µg/mL) for selection and maintenance.

From LB agar plates, 3 mL starter cultures were inoculated with single colonies of transformed cells, as described in 2.3.5, and grown overnight at 37 °C with shaking (200-250 rpm). For large-scale purification, cultures were subsequently diluted 1:500 in fresh medium and growth continued overnight prior to isolation of plasmid DNA.

2.3.9 Isolation of Plasmid DNA from *E. Coli*

Large-scale (midi-prep) and mini-prep plasmid DNA preparations were carried out using the S.N.A.P. Midiprep (Invitrogen) and GeneJet Plasmid Miniprep (Fermentas) kits respectively. Both procedures are based on the alkaline lysis method but use a support column to purify isolated plasmid DNA. Lysis is obtained with a 1 % sodium dodecyl sulfate (SDS), 0.2 M NaOH solution; the alkaline mixture ruptures the cells and the detergent breaks apart the lipid membranes and solubilises the cellular proteins. The NaOH also denatures the DNA, generating single strands. The lysate is supplemented with potassium acetate (3 M) which neutralises the pH, allowing the DNA strands to renature. The potassium acetate also precipitates the SDS, along with the cellular debris. The *E. coli* chromosomal DNA, a partially renatured tangle at this step, is also trapped in the precipitate. The plasmid DNA remains in solution. The centrifuged samples are then applied to a silica membrane in spin columns, the plasmid DNA binds to the silica matrix of the columns allowing repeated washes with an ethanol-based buffer. The purified DNA is then eluted from the silica resin with dH_2O and verified by restriction digestion and subsequent analysis by agarose gel electrophoresis, as described in 2.3.2 and 2.3.11.

2.3.10 Quantification of Plasmid DNA

Concentration and purity of final DNA preparations were assessed by agarose gel electrophoresis, as described in 2.3.11, and verified by UV-Vis spectroscopy (NanoDrop™ 1000 Spectrophotometer, Thermo Scientific).

2.3.11 Agarose Gel Electrophoresis of DNA

Agarose gel electrophoresis was used to determine the size of PCR products, estimate concentration of DNA, confirm restriction digestion and for verification of successful ligation of inserts into destination vectors.

0.8 % agar was dissolved in 1x TAE by heating. The solution was allowed to cool prior to the addition of SYBR Safe DNA stain (40 mM Tris-acetate, 1 mM EDTA, pH ~8.3, Invitrogen) to facilitate visualisation of DNA. Gels were subsequently poured, covered in aluminium foil and allowed to set at room temperature (20-22 °C) for one hour before use. Samples were prepared in a 6x DNA loading buffer (10 mM Tris-HCL pH 7.6, 0.03 % bromophenol blue, 0.03 % xylene cyanol FF, 60 % glycerol, 60 mM EDTA). Agarose gels were electrophoresed in 1x TAE buffer at 100 volts and DNA visualised under UV light once sufficient migration and separation had occurred. 1 Kbp O'GeneRuler DNA ladder (10 mM Tris-HCL pH 7.6, 10 mM EDTA, 0.005 % bromophenol blue, 0.005 % xylene cyanol FF, 10 % glycerol) was used for estimation of fragment length and DNA concentration.

2.4 Protein Expression and Purification

2.4.1 Protein Expression in *E.coli*

Competent cells from the *E. coli* host strain BL21(DES) were used for protein expression.

Starter cultures were inoculated with a single colony and incubated overnight, then diluted 1:100 with fresh medium and grown to an OD_{600} of 0.6-0.7. Protein expression was induced by the addition of Isopropyl β-D-1-thiogalactopyranoside (IPTG) to a final a 0.1 mM, and growth continued for a further 4 hours, or till they

reached an OD_{600} of 2.8, prior to harvesting of cells by centrifugation (4000 g at 4 °C for 10 minutes).

The supernatants were discarded and the pellets resuspended in an appropriate volume of ice-cold wash buffer (300 mM Na_2HPO_4, 300 mM NaCl) (~ 5 mL per gram of culture) supplemented with protease inhibitors [1x EDTA-free protease inhibitor cocktail, 1 mM Tris (2-carboxyethyl) phosphine hydrochloride (TCEP), 1 mM phenylmethylsulfonyl fluoride (PMSF), 10 mM β-mercaptoethanol]. Resuspended cells were centrifuged (4000 g at 4 °C for 10 minutes). The supernatants were aspirated to waste, the pellets were weighted and stored at -80 °C or proceeded to cell lysis.

The cell pellets were resuspended in 3-5 ml of lysis buffer (300 mM Na_2HPO_4, 300 mM NaCl, 1x EDTA-free protease inhibitor cocktail, 1 mM TCEP, 1 mM PMSF, 10 mM β-mercaptoethanol, 1% Triton X-100, 1 mg/ml lysozyme) per gram of wet cell pellet. The sample was passed through a 18-gauge needle fitted to a 20ml syringe twice. The suspensions were incubated at 4 °C for 60 minutes under gentle agitation by rotation. Suspended cells were sonicated over ice in short bursts until the lysate cleared. The sample was passed through a 25-gauge needle fitted to a 20ml syringe until no longer viscous. The cell suspension was centrifuged (12,000 g at 4 °C for 20 minutes). The volume of supernatant was noted, the protein purified and the pellet was discarded. Samples were taken at each step for subsequent analysis by sodium dodecyl sulphate polyacrylamide gel electrophoresis (SDS-PAGE) and Western blotting.

2.4.2 Protein Purification

Since all proteins under investigation were expressed as 6xHis, StrepII or Glutathione-S-transferase (GST) fusions, purification was carried out using affinity chromatography.

Protein was purified by affinity chromatography using Ni-NTA agarose (Qiagen), Strep-tactin Superflow Plus (Qiagen) or Glutathione Sepharose™ 4 Fast Flow resin (GE Healthcare). The soluble fraction from the bacterial lysate, containing the protein of interest, was incubated with the appropriate affinity resin overnight or for 90 minutes at 4 °C. Following incubation, resin was loaded onto a 5 mL disposable column and the flow-through containing unbound material collected and stored at 4 °C for subsequent analysis by SDS-PAGE and Western blotting.

Packed resin was then washed in 2 x 5 bed volumes of a suitable wash buffer, prior to elution of the protein.

Purification methods will be discussed in more detail in relevant chapters.

2.4.3 Transfection of HEK293T Cells using FuGENE® 6

HEK293T cells were cultured at 37 °C in a humidified atmosphere (5 % CO_2 / 95 % O_2) in DMEM (supplemented with 10 % (v/v) heat-inactivated foetal calf serum (FCS), penicillin and streptomycin [1 % (v/v)] and 1 % glutamine). Cells were grown as adherent monolayers to between 60-70 % confluence prior to transfection. HEK293T cells were transiently transfected using FuGENE® 6, according to the manufacturer's instructions.

Briefly, FuGENE® 6 was first diluted in serum-free medium, mixed to homogeneity by brief vortex mixing, and incubated at room temperature (20-22 °C) for 5 minutes. Plasmid DNA was then added and incubation continued for 20 minutes, to allow the formation of lipid: DNA complexes. The transfection reagent: DNA complex was then added to cells drop-wise, prior to incubation at 37 °C (5 % CO_2 / 95 % O_2).

At 48 hours post-transfection, growth medium was removed and cells washed in ice-cold phosphate buffer saline (PBS) [10 mM NaH_2PO_4 (pH 7.4), 0.14 M NaCl, 3 mM

KCl]. Flasks were agitated until all cells were in suspension, at which time cells were harvested by centrifugation (700 g for 5 minutes).

2.4.4 Transfection of HEK293T Cells using Lipofectamine™ 2000

FuGENE® 6 was replaced with Lipofectamine™ 2000 as the transfection reagent of choice as FuGENE® 6 became unavailable commercially in Ireland.

HEK293T cells were cultured at 37 °C in a humidified atmosphere (5 % CO_2 / 95 % O_2) in DMEM (supplemented with 10 % (v/v) heat-inactivated FCS, penicillin and streptomycin [1 % (v/v)] and 1 % glutamine). Cells were grown as adherent monolayers to between 60-70 % confluence prior to transfection. HEK293T cells were transiently transfected using Lipofectamine™ 2000 Transfection Reagent according to the manufacturer's instructions.

Briefly, cells were seeded 24 hours pre-transfection so that they were approximately 70 % confluent at time of transfection. Lipofectamine™ 2000 and the plasmid DNA were first diluted separately in serum-free medium, mixed to homogeneity by brief vortex mixing, and incubated at room temperature (20-22 °C) for 5 minutes. Plasmid DNA was then added to Lipofectamine™ 2000 and incubation continued for 20 minutes, to allow the formation of lipid: DNA complexes. The transfection reagent: DNA complex was then added to cells drop-wise, prior to incubation at 37 °C (5 % CO_2 / 95 % O_2).

At 24 hours post-transfection, growth medium was removed and cells washed in ice-cold PBS. Flasks were agitated until all cells were in suspension, at which time cells were harvested by centrifugation (700 g for 5 minutes).

2.5 Detection and Analysis of Proteins

2.5.1 SDS-PAGE

Separation of proteins according to molecular mass was achieved by SDS-PAGE to allow detection of expression and estimation of purity.

Protein was electrophoresed in 8-12 % (w/v) acrylamide or 8-20 % gradient gels. Samples were prepared in 5x loading buffer [250 mM Tris-HCl, pH 6.8, 50 % (v/v) glycerol, 10 % (w/v) SDS, 500 mM β-mercaptoethanol, 0.5 % bromophenol blue]. Electrophoresis was carried out in 1x Tris-Glycine SDS buffer (025 mM Tris, 250 mM glycine pH 8.3, 0.1 % SDS) for 90 minutes at 100 volts. PageRuler Plus Prestained Protein Ladder (Thermo Scientific) [62.5 mM Tris-H_3PO_4 (pH 7.5 at 25°C), 1 mM EDTA, 2 % SDS, 10 mM DTT, 1 mM NaN_3, 33 % glycerol] was used for estimating the molecular mass of the protein.

2.5.2 Coomassie Brilliant Blue and Silver Staining

Proteins present at ≥ 0.1 µg or ≥ 1 ng were visualised by Coomassie Brilliant Blue or silver staining, respectively. Staining in Coomassie Brilliant Blue [0.1 % (w/v) Coomassie Brilliant Blue, 40 % (v/v) methanol, 10 % (v/v) acetic acid] was carried out for a minimum of 2 hours, prior to destaining [40 % (v/v) methanol, 10 % (v/v) acetic acid] overnight.

Silver staining was carried out using Pierce Silver Stain Kit according to the manufacturer's instructions. Gels were first washed twice in ultrapure water, then fixed [30 % (v/v) ethanol, 10 % (v/v) acetic acid], rinsed [10 % (v/v) ethanol, followed by ddMilliQ water twice], sensitised (0.2 g/L Na_2SO_3), rinsed a second time (ddMilliQ water) and incubated with silver nitrate. Gels were then rinsed in ddMilliQ and developed to the desired intensity. Development was terminated with 5 % acetic acid and gels stored in ddMilliQ.

2.5.3 Western Blotting

The specific detection of proteins of interest was achieved by Western blotting, more specifically, semi-dry or wet electroblotting.

2.5.3.1 Semi-Dry Western Blotting

Gels were washed for 5 minutes in ultrapure water followed by 2 x 5 minute washes in transfer buffer [10 mM CAPS, pH 11, 10 % (v/v) methanol]. Proteins were transferred from SDS-PAGE gels onto a polyvinylidene fluoride (PVDF) membrane in this transfer buffer for one hour at constant amperage of 78 mA using a semi-dry transfer unit at room temperature (20-22 °C). Membranes were then blocked in 10 % (w/v) dried skimmed milk (Marvel) in PBS-t [10 mM NaH_2PO_4 (pH 7.4), 0.14 M NaCl, 3 mM KCl, 0.05 % (v/v) Tween-20] for one hour at room temperature (20-22 °C) or overnight at 4 °C. Membranes were subsequently washed in PBS-t (5 minutes) and incubated with the appropriate antibody or antibodies for one hour at room temperature (20-22 °C) or overnight at 4 °C. After washing in PBS-t (3 x 5 minutes), membranes were incubated with appropriate secondary antibody for one hour at room temperature (20-22 °C). After washing in PBS-t (5 x 5 minutes), membranes were developed by incubation for 90 seconds with chemiluminescent (ECL) Western blotting substrate, and signal detected by X-ray film exposure (Kodak) for variable periods of time.

2.5.3.2 Wet Western Blotting

Gels were washed for 5 minutes in ultrapure water followed by 2 x 5 minute washes in transfer buffer. Proteins were transferred from SDS-PAGE gels onto a PVDF membrane in transfer buffer at constant amperage of 78 mA for two hours using a

wet transfer unit at 4 °C. Membranes were then blocked in 10 % (w/v) dried skimmed milk in PBS-t for one hour at room temperature (20-22 °C) or overnight at 4 °C. Membranes were subsequently washed in PBS-t (5 minutes) and incubated with the appropriate antibody or antibodies, for one hour at room temperature (20-22 °C) or overnight at 4 °C. After washing in PBS-t (3 x 5 minutes), membranes were incubated with appropriate secondary antibody for one hour at room temperature (20-22 °C). After washing in PBS-t (5 x 5 minutes), membranes were developed by incubation for 90 seconds with chemiluminescent (ECL) Western blotting substrate (Roche), and signal detected by X-ray film exposure (Kodak) for variable periods of time.

2.5.4 Stripping and Reprobing PVDF Membranes

In order to visualise two bands on the same membrane or, where an antibody failed to detect any protein and an alternative was available, PVDF membranes were stripped using Restore Western Blot Stripping Buffer (ThermoScientific) and reprobed.

Membranes were washed in PBS-t to remove ECL, prior to incubation with Restore Western Blot Stripping Buffer for 15 minutes at room temperature (20-22 °C).

Following incubation, membranes were washed in PBS-t and subsequently blocked [10 % dried skimmed milk] for one hour at room temperature (20-22 °C) or overnight at 4 °C. Stripped membranes were then probed with alternative antibodies.

Chapter 3 Membrane Yeast Two Hybrid

3.1 Introduction

Integral membrane proteins, such as STRA6, represent one of the most biologically important protein classes, having key roles in a diverse range of processes including cell signalling, recognition and adhesion, molecular transport, cellular metabolism and maintenance of cellular structure. Approximately one-third of the predicted proteins of an organism are believed to be anchored in the lipid bilayer, with many involved in functions linked to disease. This has made membrane proteins of considerable diagnostic and therapeutic importance, and indeed approximately 60 % of currently available therapeutics are directed towards membrane receptors and ion channels (Arinaminpathy et al., 2009, Terstappen and Reggiani, 2001). As such, obtaining a thorough understanding of the function and mechanism of action of membrane proteins is of crucial importance. The high-throughput identification of membrane protein 'interactomes', maps of the protein–protein interactions, are crucial for understanding the function of an uncharacterised protein, particularly when interacting proteins have known functions and deductions about the potential role of the uncharacterised protein can be made. However, the construction of these interactomes is particularly challenging, as the hydrophobic nature of many membrane-spanning proteins makes them difficult to analyse using conventional interaction assays, particularly those suitable for use in a high-throughput format.

The yeast two hybrid (YTH), system is one of the most popular and powerful tools to study protein-protein interactions. Since its introduction fourteen years ago, it has developed from a simple assay for the analysis of interactions between known proteins, into a routine system for the high throughput identification of novel protein interactions using libraries. However the traditional YTH, the Gal4/LexA system, depends on the analysed proteins localizing to the yeast cell nucleus and is therefore not suitable for studying membrane proteins. To address this problem an alternative system has been developed, known as the membrane yeast two hybrid assay

(MYTH), by Stagljar et al. (Stagljar et al., 1998). The MYTH was originally developed by Johnsson and Varshavsky but was intended for the detection of interactions between soluble proteins (Johnsson and Varshavsky, 1994). The MYTH represents a powerful tool to facilitate the characterisation of membrane protein interactions and takes advantage of the concept of 'split ubiquitin', the observation that ubiquitin, a conserved 76 amino-acid protein that serves as a tag for proteins targeted for degradation by the 26S proteasome, can be divided into two stable moieties, an N-terminal fragment called NubI and a C-terminal fragment called Cub, which are capable of spontaneous *in vivo* reassociation into a stable full-length quasi-native ubiquitin, or "split ubiquitin". A point mutation in the N-terminal domain of ubiquitin (NubG), isoleucine 13 to glycine, reduces the affinity of the two halves for each other, such that NubG and Cub fail to assemble into split ubiquitin when coexpressed in yeast. In the MYTH, this principle is adapted for use as a 'sensor' of protein-protein interactions (PPIs). A membrane protein of interest serves as the 'bait' and is tagged at its N- or C- terminus with a moiety consisting of Cub linked to an artificial transcription factor, comprising the *Escherichia coli* DNA-binding domain LexA and the activation domain of VP16 from *herpes simplex* virus. Preys are tagged at either their N- or C- terminus with the NubG fragment. For high-throughput screening applications, entire prey libraries can be generated from sources such as genomic or cDNA. The bait and prey are then coexpressed in an *S. cerevisiae* host. An interaction between these proteins brings the Cub and NubG moieties into close contact, allowing for reconstitution of split ubiquitin. The reporter protein is released by ubiquitin binding proteases (UBPs) responsible for the deconjugation of ubiquitin from modified proteins through the hydrolysis of the amide bond formed between the protein and the C-terminal residue of ubiquitin. Once released, the reporter molecule enters the nucleus where it will activate expression of reporter genes (*HIS3*, *ADE2* and *lacZ*) under the control of promoters containing LexA binding sites. *HIS3* and *ADE2* activation enables the yeast to grow on defined minimal media lacking histidine and adenine. *LacZ*, encoding the enzyme

β-galactosidase, activation results in a colour development in the β-galactosidase assay.

In the absence of a protein-protein interaction, the *ADE2* reporter gene is not transcribed and therefore, a red-coloured intermediate accumulates in the adenine metabolic pathway. Activation of the *ADE2* gene by a protein-protein interaction leads to expression of the *ADE2* gene product and unblocks the pathway. For this reason, NMY51 cells expressing an interacting protein pair will display a very faint pink to white colour, depending on the strength of the interaction. In the absence of a protein-protein interaction, the NMY51 cells display a pink colour, similar to strains carrying an ade2 mutation. Use of appropriate selective media thus allows for convenient and highly specific selection of cells containing interacting bait-prey pairs.

The MYTH permits large-scale screening of interactions between full-length membrane proteins, membrane associated proteins and cytoplasmic proteins from a range of organisms; the only requirement being that these membrane proteins have their N- and/or C- terminus located in the cytosol (Snider et al., 2010b). This system maintains eukaryotic proteins in an environment close to their physiological norm and allows post-translational modifications to occur, permitting the expression of correctly folded proteins (Causier, 2004). Reports of PPIs using this system are becoming commonplace in the literature (Hooker et al., 2007, Egaña et al., 2009, Felkl and Leube, 2008, Paumi et al., 2008). The MYTH has been successfully used to detect both transient and stable interactions of exogenously and endogenously expressed proteins from a variety of organisms (Stagljar and Fields, 2002, Snider et al., 2010b, Snider et al., 2010a).

Aims and Objectives

A cell surface receptor for RBP was first described in the 1970s and further characterised in the 1980s and 1990s by a number of groups (Chen and Heller, 1977, Heller, 1975, Sivaprasadarao and Findlay, 1988a, Sivaprasadarao and Findlay, 1988b, Sivaprasadarao et al., 1994). The molecular identify of this receptor remained elusive until 2008, when *STRA6* was identified, coding for the high affinity cell-surface receptor for RBP (Kawaguchi et al., 2008a). *STRA6* was originally identified as a retinoic acid-stimulated gene in cancer cell lines, leading to suggestions that it may potentially be important in cancer biology (Bouillet et al., 1997). Homozygous mutations in the human *STRA6* gene have been shown to cause a pleitropic, multisystem malformation syndrome (Pasutto et al., 2007), thus highlighting the importance of this receptor. Furthermore, STRA6 has recently been linked to JAK2/STAT5 signalling and insulin resistance (Berry and Noy, 2012). Given that STRA6 is not homologous to any other protein in the human genome and many questions regarding the receptors function remain unanswered (Blaner, 2007) possible protein interactions for the receptor were explored.

To detect proteins that interact with full-length STRA6, a human kidney and a human brain library were screened using the MYTH in yeast. The DNA encoding the full-length human STRA6 was cloned in-frame with the C-terminal half of ubiquitin and the LexA-VP16 transcription factor in the pBT3-Suc vector. This construct was then used to screen for possible interactors in an adult human brain library and human kidney library, fused to the mutated form of ubiquitin in the pPR3-N vector (Dualsystems Biotech AG). The human kidney screen was repeated in the presence of RBP-ROH to identify any protein interactions dependent on the presence of holo-RBP.

3.2 Materials and Methods

3.2.1 Preparation for Library Screen using STRA6 as Bait

3.2.1.1 MYTH Constructs

The coding sequence for full-length human STRA6 (UniProt entry Q9BX79) obtained in the expression vector pBT3-SUC (Dualsystems Biotech) was a kind gift from Dr. Monika Wysocka-Kapcinsk. The plasmid incorporates an N-terminal signal sequence derived from the *Saccharomyces cerevisiae* invertase (*SUC2*) gene, to allow expression and translocation of membrane proteins in yeast as well as a C-terminal LexA DNA binding domain. The plasmid also incorporates a *Herpes simplex* VP16 transactivator domain in combination with the C-terminal (Cub), amino acids 34-76, of yeast ubiquitin and a CYC1 promoter to drive gene expression. Additionally, the pBT3-SUC vector contains the auxotrophic growth marker *LEU2* which allows yeast expressing pBT3-SUC to grow on minimal media lacking leucine, as well as the ampicillin resistance marker.

Control vectors, pCCW-Alg5, pAL-Alg5 and pDL2-Alg5 were provided by DUALsystems Biotech. pCCW-Alg5 contains the auxotrophic growth marker *LEU2* which allows yeast expressing pCCW-Alg5 to grow on minimal media lacking leucine. pAL-Alg5 and pDL2-Alg5 contain the auxotrophic growth marker *TRP1* which allows yeast expressing pAL-Alg5 or pDL2-Alg5 to grow on minimal media lacking tryptophan. The three vectors also contain the kanamycin resistance marker. The pAI-Alg5 construct expresses a fusion of the yeast ER protein Alg5 and the wild type N-terminal (NubI), amino acids 1-38, of yeast ubiquitin. pDL2-Alg5 expresses a fusion of the same protein along with the mutated N-terminal (NubG), amino acids 1-38, of yeast ubiquitin.

pPR3-N, the library vector, was provided by DUALsystems Biotech and contains the auxotrophic growth marker *TRP1* which allows yeast expressing pPR3-N to grow on

minimal media lacking tryptophan. The vector contains the kanamycin resistance marker, a CYC1 promoter to drive gene expression, as well as the mutated N-terminal (NubG), amino acids 1-38, of yeast ubiquitin.

3.2.1.2 Determination of the Optimum pH for NMY51 Growth

NMY51 cells previously transfected with the bait construct were streaked onto an yeast extract, peptone, adenine sulphate, dextrose (YPAD) agar plate (10 g/L bacto yeast extract, 20 g/L bacto peptone, 20 g/L glucose monohydrate, 40 mg/L adenine sulphate, 20 g/L bacto agar, pH 6) and incubated for 3 days at 30 °C. Single colonies were used to inoculate 10 ml selective dropout (SD) medium (6.7 g/L yeast nitrogen base without amino acids, 0.6 g/L dropout mix, 20 g/L glucose monohydrate), supplemented with uracil (Ura, 0.02 g/L), adenine (Ade, 0.02 g/L), tryptophan (Trp, 0.02 g/L), and histidine (His, 0.02 g/L) and lacking leucine (Leu, 0.02g /L), with pHs of 6, 6.5, 7, or 7.5. The cultures were grown for 8 hours at 30 °C with shaking (200-250 rpm). The OD_{546} was taken for the 4 cultures and the optimum pH determined.

3.2.1.3 Transformation of Yeast with the Bait Construct and Control Plasmids

NMY51 cells were streaked onto a YPAD agar plate and incubated for 3 days at 30 °C. A single colony was used to inoculate 50 ml of YPAD medium (10 g/L bacto yeast extract, 20 g/L bacto peptone, 20 g/L glucose monohydrate, 40 mg/L adenine sulphate, pH 6) and grown overnight at 30 °C with shaking (200-250 rpm). Once the culture reached an OD_{546} of 0.6-0.8, the culture was centrifuged (5 minutes at 2500 g) and resuspended in 2.5 ml water. 1.5 µg of DNA (bait construct, pCCW-Alg5, pPR3-N, pAL-Alg5 or pDL2-Alg5) was added to a 1.5 ml tubes. 300 µl of the

polyethylene glycol (PEG)/ lithium acetate (LiOAc) master mix (240 µl 50 % PEG, 36 µl 1M LiOAc, 30 µl single-stranded carrier DNA) was added to each tube and vortexed briefly. 100 µl of the resuspended yeast cells were added to each tube and vortexed to thoroughly mix all the components. The mix was incubated in a 42 °C water bath for 45 minutes. The reaction was centrifuged (5 minutes at 700 g), pellets resuspended in 100 µl 0.9 % NaCl and plated onto SD agar plates (6.7 g/L yeast nitrogen base without amino acids, 0.6 g/L dropout mix, 20 g/L glucose monohydrate, 20 g/L bacto agar), supplemented with Ade, Trp, His, and Ura and lacking Leu (bait construct and pCCW-Alg5) or SD agar plates supplemented with Ade, His, Leu and Ura and lacking Trp (pPR3-N, pAL-Alg5 and pDL2-Alg5).

All agar plates were incubated for 3-4 days at 30 °C.

3.2.1.4 Verifying Bait Expression and Functionality

As in 3.2.1.3 with minor changes; DNA used was bait construct and pAI-Alg5 or bait construct and pDL2-Alg5. Pelleted reactions were resuspended in 100 µl 0.9 % NaCl and plated onto SD agar plates supplemented with Ade, His, and Ura and lacking Leu and Trp, SD agar plates supplemented with Ade and Ura and lacking Trp, Leu and His, as well as SD agar plates supplemented with Ura and lacking Ade, Trp, Leu and His. All agar plates were incubated for 3-4 days at 30°C.

3.2.1.5 Optimizing the Screening Stringency using a Pilot Screen

NMY51 cells previously transfected with the bait construct were streaked onto an YPAD agar plate and incubated for 3 days at 30 °C. A single colony was used to inoculate 10 ml SD medium supplemented with Ade, Trp, His, and Ura and lacking Leu. The culture was grown for 8 hours at 30 °C with shaking (200-250 rpm). The culture was used to inoculate 100 ml SD medium supplemented with Ade, Trp, His,

and Ura and lacking Leu. The culture was grown overnight at 30 °C with shaking (200-250 rpm). A 1 ml aliquot of the culture was centrifuged (2500 g for 5 minutes) and the pellet resuspended in 1 ml water. The OD_{546} was measured and the amount of culture needed for 22.5 OD units calculated. This volume was aliquoted and centrifuged (700 g for 5 minutes). The pellet was resuspended in 150 ml 2x YPAD (20 g/L bacto yeast extract, 40 g/L bacto peptone, 40 g/L glucose monohydrate, 40 mg/L adenine sulphate, pH 6). The cells were grown at 30 °C with vigorous shaking (250 rpm) to an OD_{546} of 0.6-0.7.

The 150 ml culture was split into three 50 ml tubes and centrifuged (700 g for 5 minutes). The pellets were resuspended in 30 ml of sterile water by vortexing and centrifuged again (700 g for 5 minutes). The supernatants were removed and each pellet was resuspended in 1 ml LiOAc/ Tris EDTA (TE) master mix [110 µl 1M LiOAc, 110 µl 10x TE (100 ml/L 1 M Tris-Cl pH 7.5, 20 ml/L 0.5 M EDTA pH 8.0), 0.78 ml water] and transferred to a 1.5 ml tube. The reactions were centrifuged (700 g for 5 minutes), the supernatants removed and the pellets resuspended in 600 µl of LiOAc/TE master mix (66 µl 1 M LiOAc, 66 µl 10x TE pH 7.5, 468 µl water). To each 50 m tube; 7 µg of pPR3-N, 100 µl of single stranded carrier DNA, 600 µl of cells and 2.5 ml of PEG/LiOAc mix (0.25 µl 1M LiOAc, 0.25 µl 10x TE pH7.5, 2 ml 50 % PEG) were added.

The reactions were vortexed for 1 minute to thoroughly mix all components and incubated at 30 °C for 45 minutes (mixing briefly every 15 minutes). 160 µl DMSO was added to each tube and mixed immediately by shaking (200-250 rpm). The tubes were incubated at 42 °C for 20 minutes. The cells were centrifuged (700 g for 5 minutes) and resuspended in 3 ml 2x YPAD and pooled. The cells were incubated at 30 °C for 90 minutes with slow shaking (150 rpm) and centrifuged (700 g for 5 minutes). The pellet was resuspended in 3.6 ml 0.9 % NaCl. 300 µl of cells were spread onto SD agar plates supplemented with Ade and Ura and lacking Leu, Trp and His with 0, 1, 2, 5, 7.5 and 10 mM 3-amino-1 2 3-triazole (3-AT) and SD agar plates supplemented with Ura and lacking Leu, Ade, Trp and His with 0, 1, 2, 5, 7.5

and 10 mM 3-AT. 3-AT is a competitive inhibitor of imidazole-glycerol-phosphate dehydratase, the *HIS3* gene product (Lalonde et al., 2008). The remaining resuspended cells were used to prepare 1:100, 1:1000 and 1:10,000 dilutions in 0.9 % NaCl and 100 µl of each dilution plated onto a 100 mm diameter SD agar plate supplemented with Ade, His, and Ura and lacking Leu and Trp (used later to calculate the transformation efficiency). All agar plates were incubated at 30 °C for 3-4 days.

3.2.1.6 RBP Expression and Purification

Pichia pastoris KM71H cells previously transformed with RBP, in the expression vector pPICZ-αA with a HA and 6xHis tag, were a kind gift from Dr Campos-Sandoval. A single colony was used to inoculate a 1 L culture of yeast extract peptone dextrose (YPG) (10 g/L yeast extract, 20 g/L peptone, 2 % dextrose). The culture was incubated overnight at 30 °C. Once the culture had reached an OD_{600} of 6 the culture were centrifuged (10,900 g for 15 minutes at 4 °C). Each pellet (from 250 ml of culture) was used to inoculate 1 L of yeast extract peptone methanol (YPM) (10 g/L yeast extract, 20 g/L peptone, 1 % methanol) and the cultures were incubated overnight at 30 °C. After 16 hours, methanol was added to a final concentration of 1 % and incubation continued overnight at 30 °C. The cultures were centrifuged and the supernatant filtered (0.65 µM filter), as the protein is secreted into the supernatant. After filtering, the culture was incubated with pre-equilibrated Ni-NTA agarose (1 ml/4 L culture) overnight at 4 °C with gentle agitation by rotation. The culture was feed into a 50 ml column. The flow-through was collected and the resin was washed with 20 ml PBS. Protein was eluted using 20 ml elution buffer (120 g/L NaH_2PO_4, 29 g/L NaCl, 34 g/L imidazole, pH 7.5). The protein was dialysed against 1x PBS.

3.2.1.7 Functional Characterisation of RBP

The binding of retinol to RBP was monitored by fluorimetric titration in a Cary Eclipse fluorescence spectrophotometer (Varian). The purified recombinant protein was diluted to a concentration of 2 μM in PBS buffer and small increments of retinol were added. The two were mixed and allowed to incubate for 5 min before recording the fluorescence emission of the retinol–RBP complex. For titration of RBP with retinol, excitation wavelength was 335 nm and emission was recorded at 470 nm.

3.2.2 Library Screen using STRA6 as Bait

3.2.2.1 Library Transformation and Selection of Interactors

NMY51 cells previously transfected with the bait construct were streaked onto an YPAD agar plate and incubated for 3 days at 30 °C. A single colony was used to inoculate 10 ml SD medium supplemented with Ade, Trp, His, and Ura and lacking Leu. The culture was grown for 8 hours at 30 °C with shaking (200-250 rpm). The culture was used to inoculate 100 ml SD medium supplemented with Ade, Trp, His, and Ura and lacking Leu. The culture was grown overnight at 30 °C with shaking (200-250 rpm), a 1 ml aliquot of the culture was centrifuged (2500 g for 5 minutes) and the pellet resuspended in 1 ml water. The OD_{546} was measured and the amount of culture needed for 22.5 OD units calculated. This volume was aliquoted and centrifuged (700 g for 5 minutes). The pellet was resuspended in 150 ml 2x YPAD. The cells were grown at 30 °C with vigorous shaking (250 rpm) to an OD_{546} of 0.6-0.7. The culture was split between four 50 ml tubes and centrifuged (700 g for 5 minutes). The pellets were resuspended in 30 ml of sterile water by vortexing and centrifuged again (700 g for 5 minutes). The supernatants were removed and each pellet was resuspended in 1 ml LiOAc/TE master mix and transferred to a 1.5 ml tube. The reactions were centrifuged (700 g for 5 minutes), the supernatants removed

and the pellets resuspended in 600 µl of LiOAc/TE master mix. To each 50 ml tube; 7 µg of library plasmid, 100 µl of single stranded carrier DNA, 600 µl of cells and 2.5 ml of PEG/LiOAc mix was added.

The reaction was vortexed for 1 minute to thoroughly mix all components and incubated at 30 °C for 45 minutes (mixing briefly every 15 minutes). 160 µl DMSO was added to each tube and mixed immediately by shaking (200-250 rpm). The tubes were incubated at 42 °C for 20 minutes. The cells were centrifuged (700 g for 5 minutes) and resuspended in 3 ml 2x YPAD and pooled. The cells were incubated at 30 °C for 90 minutes with slow shaking (150 rpm) and centrifuged (700 g for 5 minutes). The pellet was resuspended in 4.8 ml 0.9 % NaCl. 300 µl of cells were spread onto SD agar plates supplemented with Ade and Ura and lacking Leu, Trp and His with 2 mM 3-AT and SD agar plates supplemented with Ura and lacking Leu, Ade, Trp and His with 2 mM 3-AT. The remaining resuspended cells were used to prepare 1:100, 1:1000 and 1:10,000 dilutions in 0.9 % NaCl and 100 µl of each dilution plated onto a 100 mm diameter SD agar plate supplemented with Ade, His, and Ura and lacking Leu and Trp (used later to calculate the transformation efficiency). All agar plates were incubated at 30 °C for 3-4 days. All resulting colonies were restreaked onto SD agar plates supplemented with Ura and lacking Leu, Ade, Trp and His with 2 mM 3-AT and incubated at 30 °C for 3-4 days.

3.2.2.2 Assay for the Detection of β-Galactosidase Activity

One circular filter paper was fitted directly onto the agar plate containing the yeast colonies, from 3.2.2.1, and incubated for 10 minutes. Each filter, and the corresponding agar plate, was marked with a number so each filter could be matched with the corresponding agar plate. The orientation of the filter relative to the agar plate was also marked. The filters were placed in liquid nitrogen for 5 minutes. The filters were then put into the lid of a Petri dish, colony side up and let thaw for 5 minutes. Each filter was covered with overlay mix [5 g/L agarose, 1 ml/L bromo-

chloro-indolyl-galactopyranoside (X-gal) stock solution (0.1 g x-gal, 1 ml N,N-dimethylformamide), 1x PBS pH 7.4] and incubated at room temperature (20-22 °C) overnight.

3.2.2.3 Plasmid Recovery from Yeast and Retransformation in *E. coli*

3 ml of SD medium supplemented with Ade, His and Ura and lacking Leu and Trp was inoculated with a positive clone and incubated overnight at 30 °C with shaking (200-250 rpm). 2 ml of the culture was transferred to a 2 ml tube. The culture was centrifuged (5 minutes at 4000 g) and 250 µl resuspension buffer (GeneJet Plasmid Miniprep kit) added to the cell pellet and resuspended by vortexing. 100 µg of acid-washed glass beads were added to the tube and vortexed for 5 minutes. Mini-prep plasmid DNA preparations were carried out using the GeneJet Plasmid Miniprep kit. TOP10 cells were transformed with 10 ng of DNA, the entire mixture plated onto a LB agar plate supplemented with 100 µg/ml ampicillin and incubated at 37 °C overnight. Plasmid DNA from two independent colonies was prepared using the GeneJet Plasmid Miniprep kit. Minipreps were digested with *sfi 1* to release the insert of each prey.

3.2.2.4 Confirmation of Positive Interactors

NMY51 cells previously transfected with the bait construct were streaked onto an YPAD agar plate and incubated for 3 days at 37 °C. A single colony was used to inoculate SD medium (2 ml per bait/prey pair to be assayed) supplemented with Ade, Trp, His, and Ura and lacking Leu. The cells were grown at 30 °C with vigorous shaking (220 rpm) to an OD_{546} of 0.6-0.7. The culture was centrifuged (700 g for 5 minutes) and the pellet resuspended in 1/20 volume sterile water. For each prey to be assayed, 1.5 µg prey plasmid was added to a tube along with 300 µl of PEG/LiOAc

mix (240 µl 50 % PEG, 35 µl 1M LiOAc, 25 µl single stranded carrier DNA) and 100 µl of cells.

The reactions were vortexed for 1 minute to thoroughly mix all components and incubated at 30 °C for 45 minutes (mixing briefly every 15 minutes). The tubes were incubated at 42 °C for 45 minutes. The cells were centrifuged (700 g for 5 minutes) and each pellet resuspended in 200 µl 0.9 % NaCl. 100 µl of cells were spread onto a SD agar plate supplemented with Ade, His and Ura and lacking Leu and Trp with 2 mM 3-AT and SD agar plates supplemented with Ura and lacking Leu, Ade, Trp and His with 2 mM 3-AT. All agar plates were incubated at 30 °C for 3-4 days. Subsequent analysis for the detection of β-Galactosidase activity was performed as 3.2.2.2

3.2.2.5 Library Transformation and Selection of Interactors in the Presence of Holo-RBP

NMY51 cells previously transfected with the bait construct were transfected with a human kidney library both in the presence and absence of RBP-ROH, to identify proteins that interact with STRA6 in the presence and absence of RBP-ROH. Library transformation and confirmation of positive interactors, as described in 3.2.2.1 and 3.2.2.4 respectively, were performed as before with the inclusion of RBP-ROH on all agar plates. The RBP-ROH complex, at a 1:1 molar ratio, was added at the concentration of 2.3 M (normal levels of RBP in human serum range approximately between 1.9 M and 2.9 M).

3.2.3 Detection of Protein Expression

Protein expression was analysed by SDS-PAGE and Western blotting. In the detection of RBP, α-His-HRP (Roche) was used.

3.3 Results and Discussion

3.3.1 Preparation for Library Screen using STRA6 as Bait

3.3.1.1 Determination of the Optimum pH for NMY51 Growth

NMY51 cells, previously transformed with the bait construct, were cultured in SD medium with a pH of 6, 6.5, 7 or 7.5. The OD_{546} was measured for the 4 cultures and the optimum pH determined. The culture with a pH of 6 had an OD_{546} of 0.850. The yeast colonies were bright red, as expected. The culture with a pH of 6.5 had an OD_{546} of 0.845, again cells were bright red. The culture with a pH of 7.0 had an OD_{546} of 0.763. The yeast cells were pinkish, which is not expected as this should only occur if an interacting bait-prey pair is present. In the absence of a protein-protein interaction, the *ADE2* reporter gene is not transcribed and therefore, a red-coloured intermediate accumulates in the adenine metabolic pathway. Activation of the *ADE2* gene by a protein-protein interaction leads to expression of the *ADE2* gene product and unblocks the pathway. For this reason, NMY51 cells expressing an interacting protein pair will display a very faint pink to white colour, depending on the strength of the interaction. In the absence of a protein-protein interaction, NMY51 displays a pink colour; similar to strains carrying an ade2 mutation. The culture with a pH of 7.5 had an OD_{546} of 0.641. The yeast cells were white in colour, which is not expected as this should only occur if a strongly interacting bait-prey pair is present. It was therefore concluded that the optimum pH was 6 and this was used for all subsequent assays.

3.3.1.2 Transformation of Yeast with the Bait Construct and Control Plasmids

NMY51 cells were transformed with the bait construct or control constructs; pCCW-Alg5, pPR3-N, pAL-Alg5 or pDL2-Alg5, and streaked onto SD selective agar plates.

NMY51 cells successfully transformed with the bait construct or pCCW-Alg5 will grow on minimal media lacking Leu as these constructs contain the *LEU2* auxotrophic growth marker. Likewise, NMY51 cells successfully transformed with pPR3-N, pAL-Alg5 or pDL2-Alg5 will grow on minimal media lacking Trp as these constructs contain the *TRP1* auxotrophic growth marker. After 3-4 days the selective agar plates (lacking Leu, Bait and pCCW-Alg5 or Trp, pPR3-N, pAL-Alg5 and pDL2-Alg5) had over one hundred colonies, indicating transformation was successful. The transformed yeast cells were also spread on SD selective agar plates lacking both Leu and Trp. As expected, there was no growth on these agar plates indicating that growth on selective agar plates lacking Leu or Trp were specific and not due to contaminants.

3.3.1.3 Verifying Bait Expression and Functionality

The pAI-Alg5 construct expresses a fusion of the yeast ER protein Alg5 and the wild type Nub portion of yeast ubiquitin, whereas pDL2-Alg5 expresses a fusion of the same protein to the Nub portion bearing the isoleucine to glycine mutation at position 13 (NubG). If the bait is properly inserted into the membrane of yeast and the Cub-LexA-VP16 moiety is located on the cytosolic side of the membrane, coexpression of the bait with pAI-Alg5 results in rapid formation of split ubiquitin due to the strong affinity of wild type Nub for Cub. Consequently, the reporter genes are activated by LexA-VP16 cleaved off the bait by the UBPs. Reporter gene activation is assayed by growing the yeast transformants on selective media. Coexpression of the bait with pDL2-Alg5 should not lead to split ubiquitin formation as NubG has low affinity for Cub and the bait is unlikely to interact with Alg5. Consequently, yeast coexpressing the bait and Alg5-NubG should not grow on selective media and should be negative in the β-galactosidase assay. The control assay determines whether the bait is functional in the assay and whether it displays any Nonspecific background.

As illustrated in Figure 3.1, coexpression of the bait together with Alg5-NubI resulted in over one hundred colonies being present after transformation, signifying that the bait is expressed in the MYTH. Coexpression of the bait together with pDL2-Alg5 resulted in no colonies on selective agar plates, signifying there is no nonspecific background.

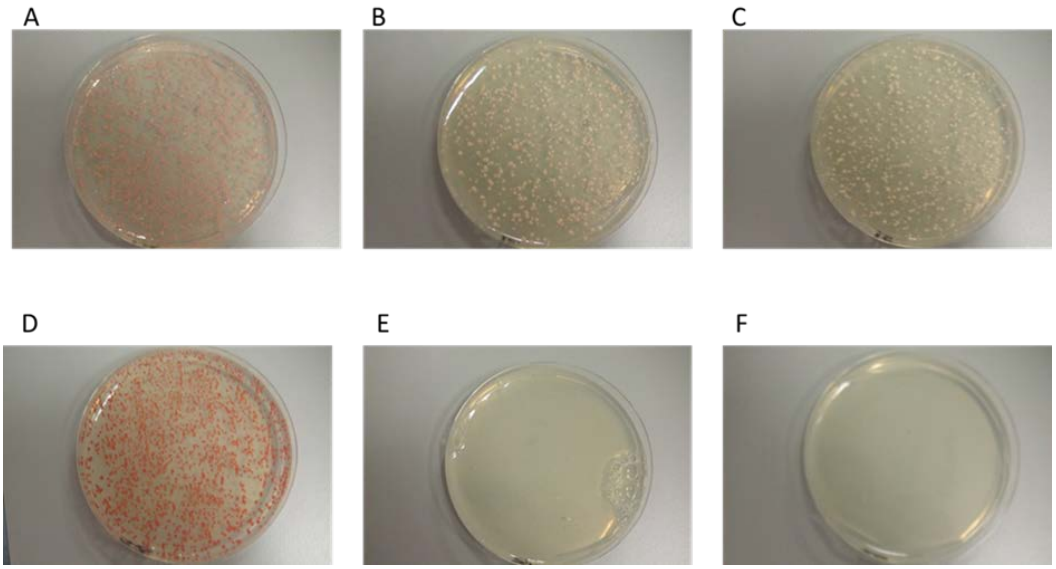

Figure 3.1: Verification of Bait Expression and Functionality

Bait and pAL-Alg5 coexpressed in yeast and streaked on selective agar plates lacking **(A)** Leu and Trp, **(B)** Leu, Trp and His, **(C)** Leu, Trp, His and Ade.

Bait and pDL2-Alg5 coexpressed in yeast and streaked on selective agar plates lacking **(D)** Leu and Trp, **(E)** Leu, Trp and His, **(F)** Leu, Trp, His and Ade.

Only coexpression of STRA6 with pAL-Alg5 resulted in growth on selective agar plates lacking Leu, Trp, His and Ade, indicating STRA6 is expressed.

3.3.1.3 Optimizing the Screening Stringency using a Pilot Screen

The pilot screen simulates the conditions of a library screen but instead of a cDNA library, the corresponding empty library vector is transformed into the bait-bearing strain. The transformation mixture is then plated onto selective agar plates of increasing stringency supplemented with different amounts of 3-AT. Only when the bait construct and library vector interact should there be growth on agar plates lacking Leu, Trp, Ade and His. This is due to the fact that the reporter genes used in the MYTH are two auxotrophic growth markers (*HIS3* and *ADE2*), whose activation enables the yeast to grow on defined minimal media lacking His or Ade, this is in addition to the auxotrophic growth markers (*LEU2* and *TRP1*) expressed when NMY51 is successfully transformed with the two constructs. Since the bait is coexpressed with unfused NubG (expressed in the empty library vector pPR3-N), any colonies that arise on the selective agar plates must be background. Any background is due to the slight leakiness of the *HIS3* gene. The pilot screen aims to adjust the screening conditions such that, in the following library screen, the absolute minimum of false positives are possible. Slight background growth on the selection agar plates can be removed by the addition of 1-10 mM 3-AT to the selection medium. As a competitive inhibitor of the *HIS3* gene product, increasing levels of 3-AT increase the stringency of *HIS3* selection.

NMY51 cells were transformed with the bait construct and the empty library vector and streaked onto selective agar plates. To find the optimal 3-AT concentration, selection agar plates were supplemented with 0, 1, 2, 5, 7.5 and 10 mM 3-AT. 2mM 3-AT was found to eradicate all background, illustrated in Figure 3.2, and was therefore used in all subsequent assays.

Figure 3.2: Use of 3-Aminotriazole to Increase the Stringency of *HIS3* Selection

3-AT was used to remove any background due to leakiness of the *HIS3* gene. The bait construct and the empty library vector were coexpressed in yeast and streaked on selective agar plates lacking Leu, Trp, His and Ade with increasing amounts of 3-AT, (A) O mM (B) 1 mM (C) 2 mM. 2 mM 3-AT was found to eradicate all background colonies and was used for subsequent experiements.

3.3.1.4 Expression of RBP

A large amount of soluble and active recombinant human RBP was required for use in the MYTH. Human RBP has been purified from plasma or urine, or produced as a recombinant protein expressed as inclusion bodies in *Escherichia coli*. In the first case, its affinity for TTR makes it long-winded to purify from blood, involving first a partial purification of the RBP–TTR complex and then a separation of both proteins by various methods. In the second, the recombinant RBP is expressed as inclusion bodies so requires a denaturation and refolding process to be active. Fortuitously, RBP has recently been successfully expressed using the methylotrophic yeast *P. Pastoris* (Wysocka-Kapcinska et al., 2010) without the need for laborious separation or refolding techniques and this system was employed. The human recombinant RBP, with an N-terminal His-tag to aid efficient purification, was successfully expressed under the control of the alcohol oxidase (AOX1) methanol inducible promoter and was secreted into the medium through the cell wall by the *S. cerevisiae* α-factor signal sequence, using the pPICZ-αA expression vector. Protein was purified using Ni-NTA agarose, as illustrated in Figure 3.3. Protein was in large enough quantities, ~ 15 mg/ 4 L culture, and sufficiently pure to proceed to the functional characterisation.

Figure 3.3: Purification of RBP

Representative Western blot showing fractions from the purification of RBP, as detected by *α*-His-HRP antibodies. 5 µl loaded per well. RBP was expressed in *P. Pastoris.* The protein was secreted into the medium, filtered to remove contaminants and incubated with Ni-NTA agarose. The supernatant **(FT)** was collected and the resin washed once **(W)** prior to elution of any bound material **(ELUT).** RBP was found to be migrating at an expected ~ 21 kDa and was found to be predominantly in the eluate.

3.3.1.5 Functional Characterisation of RBP

The functionality of recombinant RBP was evaluated by testing its capacity to bind increasing concentrations of retinol. Upon excitation at 280 nm, the protein exhibited the typical fluorescence of the holo form: one peak with a maximum at 335 nm caused by the protein itself, and a second with a maximum at 470 nm, due to retinol bound to the protein. Retinol quenches the intrinsic RBP tryptophan fluorescence due to energy transfer to the vitamin resulting in an emission fluorescence peak at 470 nm.

3.3.2 Library Screen using STRA6 as Bait

3.3.2.1 Library Transformation and Selection of Interactors

An oligo(dT)-primed, size-selected (0.4–5 kb; average insert size, 1.3 kb) human cDNA library (kidney or brain) with 3×10^6 independent clones was constructed in the prey vector, pPR3-N, by Dualsystems Biotech and inserted N-terminally (in the case of the kidney library) and C-terminally (in the case of the second kidney library and the brain library) to the NubG sequence, generating the library in X-NubG and NubG-X orientation respectively (where X is a genomic DNA). The yeast reporter strain NMY51 expressing the C-terminal tagged STRA6 bait was transformed with the cDNA library, yielding transformation efficiencies in the range of 5×10^5 to 2×10^6 clones/µg DNA. Transformed NYM51 cells were streaked on selective agar plates to select for colonies containing interacting bait-prey pairs. Library plasmids were isolated from positive clones and further processed for β-Galactosidase activity.

3.3.2.2 Assay for the Detection of β-Galactosidase Activity

In addition to the growth reporters *HIS3* and *ADE*, the MYTH has the colour reporter *lacZ*. The *lacZ* gene encodes the bacterial enzyme β-galactosidase, which converts

the substrate X-gal into a blue compound. Yeast cells expressing β-galactosidase therefore turn blue when incubated with X-gal.

β-Galactosidase expression was monitored using a colony lift filter assay with X-gal. Colonies expressing interacting bait-prey pairs were picked and restreaked on selective agar plates for the β-galactosidase assay, as illustrated in Figure 3.4. All clones positive for β-galactosidase were isolated, amplified in *Escherichia coli*, and analysed by restriction analysis for insert sizes.

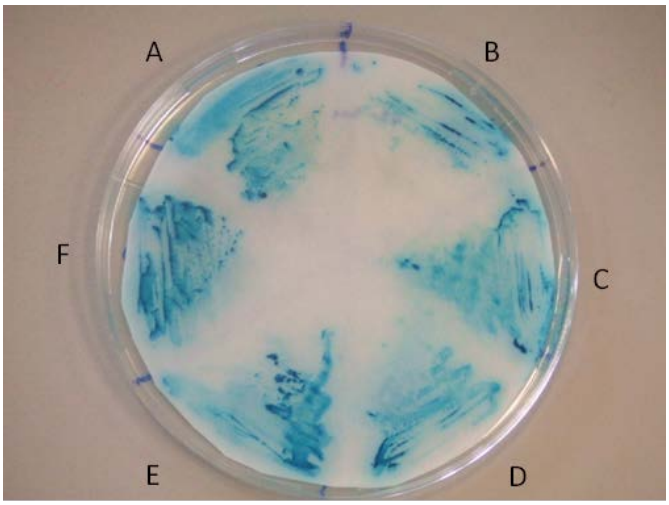

Figure 3.4: Assay for the Detection of β-Galactosidase Activity

The bait construct and prey plasmids, (A) Stress Associated Endoplasmic Reticulum Protein 1 (SERP1) (B) CD63, (C) PDZK1-Interacting protein 1(PDZK1-IP1), (D) Proteolipid Protein 2 (PLP2), (E) osteopontin, (F) Ovarian Cancer Immuno Reactive Antigen Domain Containing Protein 2 (OCIAD2), were coexpressed in yeast and streaked on minimal medium lacking Leu, Trp, His and Ade. Colonies were isolated using filter paper and the assay for β-Galactosidase activity was performed. **(A)** - **(F)** Interacting bait-prey pairs, all positive in the β-Galactosidase activity assay, indicating that a strong interacting occurs.

3.3.2.3 Plasmid Recovery from Yeast and Retransformation in *E. coli*

After the identification of colonies containing interacting bait-prey pairs, the next step is to isolate the library plasmid encoding the putative interactor. Each interactor was cultured in liquid medium, the yeast lysed and the bait and library plasmids purified. *E. coli* was transformed with the plasmid mix and the library plasmid selectively propagated on LB agar plates containing the antibiotic kanamycin. Since the library plasmids carry a kanamycin marker, whereas the bait plasmid carries an ampicillin marker, only *E. coli* which have taken up a library plasmid are able to grow under selection.

As yeast can take up several plasmids during the transformation procedure, two *E. coli* colonies were picked from each transformation. Plasmids were prepared and digested with the restriction enzyme *Sfi* I, releasing the cDNA insert. If only one library plasmid was originally introduced into yeast, both digests will show an insert of the same size, illustrated in Figure 3.5. If the two inserts differ in size, the original yeast clone contained more than one library plasmid and both plasmids are then used for the confirmation assay as described in 3.2.2.5.

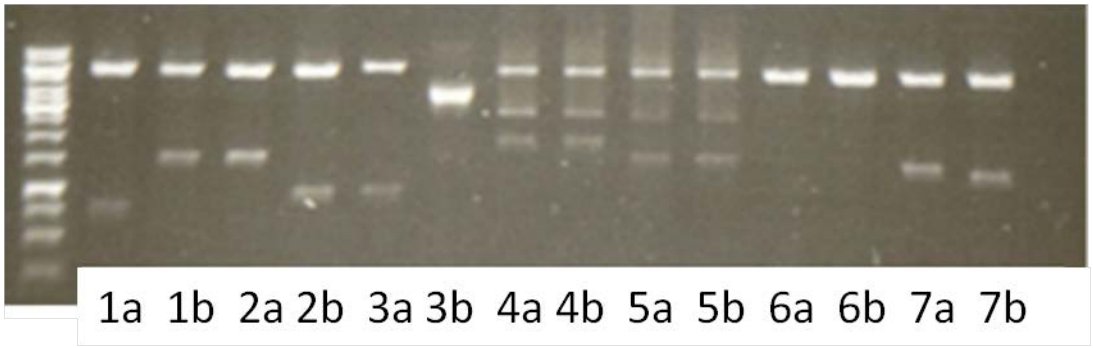

Figure 3.5: Isolation of Prey Plasmids

Transformed NYM51 cells were streaked on selective agar plates to select for colonies containing interacting bait-prey pairs. Library plasmids were isolated from positive clones and digested with the restriction enzyme *Sfi* I, releasing the cDNA insert. If only one library plasmid was originally introduced into yeast, both digests will show an insert of the same size. If the two inserts differ in size, the original yeast clone contained more than one library plasmid and both plasmids are then analysed further. 1-7 (a and b) represent positive clones, with some having inserts of the same size (such as 4a and 4b) and others (such as 1a and 1b) have inserts of different sizes.

3.3.3 Confirmation of Positive Interactors

3.3.3.1 Confirmation of Positive Interactors (Kidney Library)

Like any genetic selection system, the MYTH will isolate a certain number of false positives. These clones will result in growth on selective agar plates independent of a true interaction between the bait and a prey. False positives are eliminated by retransforming the isolated prey plasmids with the original bait plasmid. Only preys that yield colonies on selective agar plates when coexpressed with the bait are considered as true positives, as illustrated in Figure 3.6, and analysed further.

The kidney library (X-NubG and NubG-X) contained a total of 130 colonies which scored as positives for the activation of the *HIS3/ADE2/lacZ* reporter genes. 47 of these potential hits were found to be true positives following retransformation into yeast along with the bait construct and subsequent assay for the detection of β-Galactosidase activity. The plasmids were sent for sequencing and the prey plasmid identified using basic local alignment search tool (BLAST). The plasmids encoded: SERP1 (isolated from four colonies), CD63 (isolated from two colonies) and PDZK1-IP1 (isolated from one colony).

All other potential hits were either expected hits such as ubiquitin, common false positives such as 3-beta-hydroxysteroid-Delta(8),Delta(7)-isomerase, which appears in approximately 22 % of screens, or partial hits which are not considered to be true interactors. Partial hits contain only part of the open reading frame of a protein.

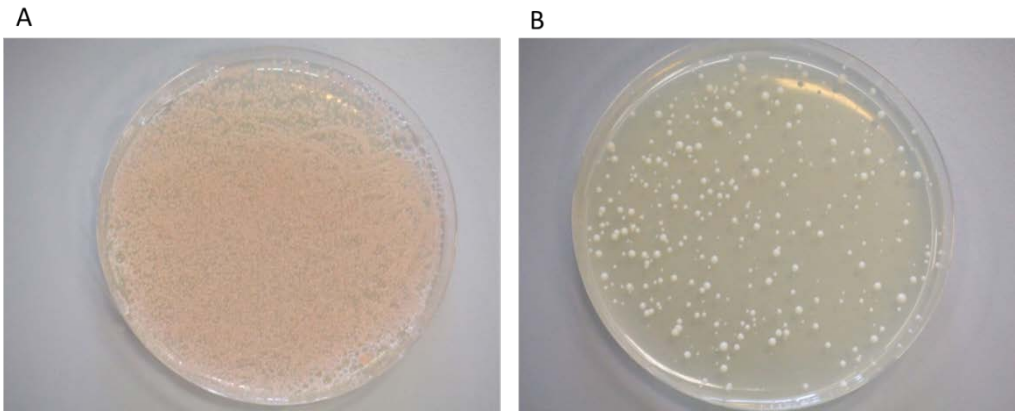

Figure 3.6: Confirmation of Positive Interactors

The bait construct and isolated prey plasmid coexpressed in yeast and plated on selective agar plates lacking **(A)** Leu and Trp, **(B)** Leu, Trp, His and Ade (with 2mM 3-AT).

3.3.3.2 Confirmation of Positive Interactors (Brain Library)

The brain library (NubG-X) contained 104 colonies which scored as positives for the activation of the *HIS3/ADE2/lacZ* reporter genes. 40 of these potential hits were found to be true positives following retransformation into yeast along with the bait construct and subsequent assay for the detection of β-Galactosidase activity. The plasmids were sent for sequencing and the prey plasmids identified using BLAST. The plasmids encoded: CD63 (isolated from three colonies), SERP1 (isolated from fourteen colonies), PDZK1-IP1 (isolated from one colony) and PLP2 (isolated from one colony).

All other potential hits were either expected such as ubiquitin, common false positives such as B-cell receptor-associated protein 31, which appears in approximately 25% of screens, or partial hits which are not considered to be true interactors.

3.3.3.3 Confirmation of Positive Interactors (Kidney Library +/-RBP-ROH)

NMY51 cells were transformed with the bait construct and the human kidney library (X-NubG and NubG-X) and streaked on selective agar plates supplemented with holo-RBP. After isolation, resulting prey plasmids were reintroduced into yeast with the original bait plasmid and again the cells were streaked on selective agar plates supplemented with holo-RBP. Prey plasmids were also streaked on selective agar plates that were not supplemented with holo-RBP. All prey-bait pairs that had growth on selective agar plates supplemented with holo-RBP also grew on selective agar plates that did not contain holo-RBP. This implies that the interactions are not dependent on the presence of holo-RBP.

The kidney library (X-NubG and NubG-X) contained a total of 144 colonies which scored as positives for the activation of the *HIS3/ADE2/lacZ* reporter genes. 30 of

these potential hits were found to be true interactors following reintroduction of prey plasmids and the bait construct in yeast and subsequent analysis for the detection of β-Galactosidase activity. The plasmids were sent for sequencing and the hits identified using BLAST. The plasmids encoded: SERP1 (isolated from four colonies), PDZK1-IP1 (isolated from two colonies), OCIAD2 (isolated from one colony), CD63 (isolated from two colonies), MIF (isolated from one colony), CCL2 (isolated from one colony), osteopontin (isolated from one colony), IFITM1 (isolated from two colonies), IFITM3 (isolated from one colony) and CXCL14 (isolated from one colony). All other potential hits were either expected hits such as ubiquitin, common false positives or partial hits which are not believed to be true interactors.

3.4 Concluding Discussion

To elucidate any other role STRA6 may play in the body, novel protein interactions for STRA6 were explored. Proteins of known function tend to cluster together, with 63 % of interactions occurring between proteins with a common functional assignment. Possible functions can therefore be assigned to a protein based on the known functions of its interacting partners (Schwikowski et al., 2000).

The MYTH was employed to identify novel protein interactions for STRA6. Three screens were performed using STRA6 as the bait; a human kidney library screen, a human brain library screen and a human kidney library screen in the presence of holo-RBP. These libraries were chosen as STRA6 is expressed in both the kidney and brain (Bouillet et al., 1997). The kidney library was also screened in the presence of holo-RBP, in order to detect any protein interactions dependent on the presence of holo-RBP. Interestingly, it was recently reported that STRA6 interacts with CRBP only in the presence of holo-RBP (Berry et al., 2012b).

All three screens resulted in 117 clones that induced activation of reporter genes in the presence of the STRA6. Only clones encoding full-length sequences in-frame with the N-terminal half of ubiquitin in pPR3-N were considered to be potential true interactors. Common false positives were also eliminated using information provided by Dualsystems Biotech, resulting in 11 unique protein interactors for STRA6. The human kidney library identified CD63, PDZK1-IP1 and SERP1 as potential STRA6 interactors. The human brain library identified CD63, PDZK1-IP1, SERP1 and PLP2 as potential STRA6 interactors. The human kidney library, in the presence of RBP-ROH, identified CD63, PDZK1-IP1 and SERP1 as potential STRA6 interactors as well as previously undetected proteins; MCP-1, CCL2, CXCL14, IFITM1, IFITM3, MIF, OCIAD2, and osteopontin. These 11 proteins, 3 of which appeared in all three screens, need now to be verified independently of the MYTH and their biological relevance explored, this will be discussed in the next chapter.

Chapter 4 Hit Verification

4.1 Introduction

The MYTH was used to identify potential PPIs for STRA6, the RBP receptor. The gene coding for this receptor was identified in 2008 (Kawaguchi et al., 2007) and since then a large amount of work has been conducted, aimed at identifying any other function the receptor may have (Kawaguchi et al., 2012, Berry and Noy, 2012, White et al., 2008). However, many questions regarding STRA6 remain unanswered, such as, does STRA6 act to regulate insulin responsiveness (Berry and Noy, 2012) and if so, how does STRA6 play a role in mediating insulin resistance and T2D? Furthermore, what role does STRA6 play in cancer biology (Szeto et al., 2001) and are the devastating consequences of human mutations only related to the disruption of the potential supply of retinol to the developing tissues (Pasutto et al., 2007) or are they a consequence of the interruption of other functions STRA6 may have. What is more, due to its implication in these disease states, STRA6, or any protein(s) which regulates its function, may potentially be drug targets.

Undoubtedly, the function of STRA6 and its implication in disease needs to be established. Exploring interactions for STRA6 may answer these questions. Since PPIs play a role in nearly all events that take place in a cell, clues to the function of an uncharacterised protein can be obtained by investigating its interaction with other proteins whose functions are already known, termed “guilt by association” (Auerbach et al., 2002). The MYTH was chosen owing to the success of the YTH in detecting PPIs: it has been estimated that more than 50 % of all interactions described in the literature have been detected by the YTH (Xenarios et al., 2001). Using the MYTH, 11 novel protein interactions for STRA6 were detected.

Generally, proteins are more likely to be true interactors, and are therefore considered to be potentially biologically relevant, if they share common features including, colocalization, functional correlation and shared interaction partners. The MYTH only detects protein interactions with cytosolic or membrane proteins as both Cub and NubG need to be located in the cytosol for the activation of reporter genes. Secreted hits include CCL2, CXCL14, and MIF. CCL2 is one of the key chemokines that regulate migration and infiltration of macrophages and is induced in various

diseases (Deshmane et al., 2009). CXCL14 is a member of the CXC chemokine family with unknown function (Wente et al., 2008). MIF is released by immune cells and activates ERK1/ERK2 signalling, upregulates TLR4 expression, suppresses p53 activity and inhibits JABY activity (Calandra and Roger, 2003). As secreted proteins, CCL2, CXCL14 and MIF are not located at the plasma membrane with STRA6. These proteins may interact with STRA6 in the ER and could have a regulatory role in the trafficking of STRA6.

SERP1 was the only hit detected that is expressed solely in the ER. SERP1, also known as ribosome-associated membrane protein 4 (RAMP4), is a Sec61-associated polypeptide that is induced by ER stress. SERP1 controls the glycosylation of major histocompatbility complex class II–associated invariant chain and interacts directly with calnexin, a membrane protein and molecular chaperone in the ER (Yamaguchi et al., 1999). Again, as an ER protein, SERP1 is not located at the plasma membrane with STRA6. This protein may interact with STRA6 in the ER and could have a regulatory role in the trafficking of STRA6.

MYTH hits which are classed as; integral membrane proteins, membrane-associated proteins or cytoplasmic proteins could possibly interact with STRA6 at the plasma membrane. CD63 and PDZK1-IP1, both of which appeared in all 3 screens, as well as PLP2 are all integral membrane/membrane-associated proteins. CD63 is a ubiquitously expressed protein found in late endocytic organelles and on the plasma membrane (Latysheva et al., 2006) and is a member of the tetraspanins, a large family of four transmembrane domain proteins (Tugues et al., 2013). Tetraspanins are believed to control compartmentalization of associated receptors into specialized protein networks or microdomains (also called tetraspanin-enriched microdomains, or TERMs). TERMs have been shown to regulate cell motility, trigger homotypic cell aggregation, and participate in various types of cell fusion and signalling through their ability to act as “molecular facilitators”, grouping specific cell-surface proteins and thus increasing the formation and stability of functional signalling complexes (Hemler, 2001, Maecker et al., 1997). CD63 may function as a specific anchor of proteins in TERMs (Latysheva et al., 2006). PDZK1-IP1 or MAP17 is a 17 kDa membrane associated protein expressed on both the plasma membrane and

golgi. The protein was first identified as a PDZK1 interacting protein in a yeast two hybrid screen (Kocher et al., 1998) and may regulate PDZK1 turnover (Silver et al., 2003). Considering the previously reported function of these proteins, CD63 and PDZK1-IP1 may act to regulate the activity of STRA6 or/and anchor the protein in TERMs. Proteolipid protein 2 (PLP2) or A4 associates with chemokine receptor 1 (CCR1) on the plasma membrane and may be involved in chemotaxis mediated by CCR1 (Lee et al., 2004). PLP2 has appeared before in numerous MYTH screens and may be a common false positive in the MYTH (Pope and Lee, 2005, Lee et al., 2004).

IFITM1 and IFITM3 are also cell membrane proteins (Tanaka et al., 2005) and are both members of the interferon-inducible transmembrane protein family 9 (Yount et al., 2012). IFITM1 and IFITM3 play a key role in the antiproliferative action of Interferon- γ (IFN- γ). Considering the previously reported function of these proteins, it is unclear why they would interact with STRA6 and to what end. Osteopontin (OPN) or secreted phosphoprotein 1 (SPP1) (Fernández et al., 2011) is an highly phosphorylated, glycosylated protein, and cytokine, found in all body fluids and the extracellular matrix of mineralised tissues (Huang et al., 2004, Denhardt and Noda, 1998), but is now known to have an intracellular function. Intracellular OPN can contribute to the diverse biological activities of OPN involving developmental, regenerative processes, immune defence and tumour-cell survival and metastasis (Sodek et al., 2002). OPN is a negative regulator of osteogenesis by inhibiting both proliferation and differentiation of osteoblastic cells (Huang et al., 2004). Interestingly, OPN expression has been found to be induced by RA (Park et al., 1997, Sodek et al., 2002, Harada et al., 1995). This provides a potential link to STRA6, as STRA6 is also induced by RA (Bouillet et al., 1997). OCIAD2 is a member of the OCIAD domain family. OCIAD2 was originally identified by its sequential similarity with ovian carcinoma immunoreactive antigen 1. However, the biological function of OCIAD2 has not been elucidated (Ishiyama et al., 2007). OCIAD2 was previously detected by a colleague, Dr. Conor Breen, in an assay to identify any protein(s) that copurify with STRA6. In this assay, STRA6 was overexpressed in HEK293T cells and purified using a strep-tactin resin. Any proteins that copurified with STRA6 were identified using mass spectrometry

(unpublished data). OCIAD2 was the only protein detected in both assays and for this reason, OCIAD2 is of particular interest.

Aims and Objectives

The MYTH enables the identification of proteins that interact with a plasma membrane protein of interest. Using STRA6 as the bait, we have screened a human kidney library, both in the presence and absence of holo-RBP and a human brain library in the absence of holo-RBP, to identify 117 protein sequences, or hits, that interact with STRA6. After the elimination of partial sequences and common false positives, 11 proteins remained. In the MYTH, due to overexpression and the elimination of proteins residing in different cellular compartments, detection of interactions that do not occur *in vivo* can occur. Therefore all potential interactions need to be verified independently of the MYTH (Lalonde et al., 2008)

A stable HEK293T cell line inducibly expressing STRA6, containing HA (YPYDVPDYA) and StrepII tags (WSHPQFEK) on either the N- or C-terminus, was generated. The StrepII tag allows affinity purification of STRA6 on a Strep-Tactin resin, an engineered form of Streptavidin. This cell line was used to verify STRA6's interaction with the hits. HEK293T lysates overexpressing the hits, purchased from Origene, were incubated with STRA6 bound to the Strep-Tactin resin. Any nonspecifically bound proteins were removed by washing the resin or alternatively, the rapid centrifugation through oil. Proteins interacting with STRA6 were eluted from the resin along with STRA6 by the addition of elution buffer containing imidazole or 2xSDS buffer. Samples were taken for subsequent analysis by SDS-PAGE and Western blotting. In addition, CD63, PDZK1-IP1, OCIAD2 and osteopontin were obtained in mammalian expression vectors (pcDNA3.1; for CD63 and PDZK1-IP1, along with a HA tag, or pCMV6-entry; for OCIAD2 and osteopontin, along with Myc and DDK tags). The stable HEK293T cell line inducibly expressing STRA6 was transfected with vectors coding for CD63, PDZK1-IP1, OCIAD2 or osteopontin. STRA6 was purified using the Strep-Tactin resin. Any nonspecifically bound proteins were removed by washing the resin or alternatively, rapid centrifugation through oil. Proteins interacting with STRA6 were eluted from the resin along with STRA6 by the addition of elution buffer containing imidazole or 2xSDS buffer. Samples were taken for subsequent analysis by SDS-PAGE and Western blotting. CD63 and PDZK1-IP1 were expressed along with

STRA6 as they were considered to be in all likelihood true interactors due to their location at the plasma membrane and the fact that they were detected in all three screens. OCIAD2 and osteopontin were expressed along with STRA6 as they were believed to be of particular interest as osteopontin is induced by RA and OCIAD2 was previously detected by Dr. Conor Breen in a mass spectrometry screen to identify proteins that copurify with STRA6 (unpublished data). Expression of these hits along with STRA6 in mammalian cells, given that the interaction is first verified by pull-down assays, allows for subsequent characterisation of the interaction, such as co-localization and knock-out studies.

4.2 Materials and Methods

4.2.1 Expression and Purification of STRA6 in *Pichia pastoris*

4.2.1.1 Expression of STRA6

The coding sequence for human STRA6 (UniProt entry Q9BX79), in the expression vector pPICZA, designed to incorporate the gene encoding a green fluorescent protein (GFP) from the jellyfish *Aequorea victoria* as a marker of gene expression and a 6xHis tag, was a kind gift from Dr. Conor Breen. *P. pastoris* cells previously transformed with the STRA6 construct were streaked on a YPDS agar plate (10 g/L yeast extract, 20 g/L peptone, 182.2 g/L sorbitol, 2 % dextrose, 20 g/L agar) supplemented with 2 mg/ml Zeocin and incubated at 30 °C for 48 hours. One colony was used to inoculate 10 ml BMGY (10 g/L yeast extract, 20 g/L peptone, 100 ml/L 1M potassium phosphate buffer, 6.9 g/L yeast nitrogen base with ammonium sulfate without amino acids (YNB), 0.04 mg/L biotin, 10 ml/L glucose, pH 6.0) and incubated for 48 hours at 30 °C with shaking (220 rpm). The 10 ml culture was transferred to 400 ml BMMY (10 g/L yeast extract, 20 g/L peptone, 182.2 g/L sorbitol, 10 ml/L methanol) and incubated for 4 hours at room temperature (20-22 °C) with constant shaking (220 rpm). After 4 hours, 0.5 % methanol (2 ml) was added to the culture and incubation continued for 24 hours at room temperature (20-22 °C) with shaking (220 rpm). After 24 hours, 1 % methanol (4 ml) was added to the culture and incubation continued for 48 hours at room temperature (20-22 °C) with constant shaking (220 rpm). After 48 hours, an additional 1 % methanol (4 ml) was added to the culture and incubation continued for 24 hours at room temperature (20-22 °C) with constant shaking (220 rpm). The culture was centrifuged (700 g for 10 minutes at 4 °C) and the supernatant was aspirated to waste. The pellet was resuspended in 15 ml cold wash buffer (4.585 g/L TES, 7.948 g/L NaCl, 0.022 g/L KCL, 0.575 g/L Na_2HPO_4, 0.131 g/L NaH_2PO_4, 2.92 g/L 1x EDTA, pH 8.0). The cells were centrifuged (700 g for 10 minutes at 4 °C) and the supernatant aspirated to waste. The pellets were weighed and yeast spaghetti produced by pressing yeast through a 50 ml tube with small holes into a beaker filled with liquid nitrogen. The holes were punched into the bottom of a 50 ml tube containing 10-20 ml of pellet

yeast. Pressure was created by manually inserting a piston of a 60 ml disposable syringe into the tube. The yeast spaghetti was stored at -80 °C prior to lysis and purification.

4.2.1.2 Lysis and Purification of STRA6

A ball mill (Retsch MM301) was used for cryogenic disruption of yeast cells. The yeast spaghetti, in a 50 ml tube, was cooled in liquid nitrogen along with a stainless steel grinding jar and grinding ball. Once cooled, the grinding jars were removed from the bath and emptied. The yeast spaghetti and grinding ball was transferred into the grinding jar. The jar was closed and transferred back into the liquid nitrogen bath for five minutes before being installed on the ball mill. The jar clamps were tightened. Grinding was done in five cycles of 3 minutes at 30 hz. Between each grinding cycle, the jars were removed from the mill and submerged into the liquid nitrogen bath. Grinding was continued once the bath boiling had subsided. Ground yeast cells were transferred into a 50 ml tube and resuspended in 5 ml lysis buffer (4.585 g/L TES, 7.948 g/L NaCl, 0.022 g/L KCL, 0.575 g/L Na_2HPO_4, 0.131 g/L NaH_2PO_4, 10µM EDTA, 0.5 g/L TCEP, 0.78 g/L β-mercaptoethanol, 1x EDTA-free protease inhibitor cocktail, 0.174 g/L PMSF, pH 8.0). The mixture was incubated for 60 minutes at 4 °C under gentle agitation by rolling. The mixture was centrifuged (10 minutes at 1,500 g at 4 °C). The supernatant was added to a 5 ml pollyallomer Optiseal tube (Beckman) and centrifuged (150,000 g for 90 minutes at 4 °C) to isolate the membranes. The supernatant was aspirated to waste and the pellet was stored at -80 °C or preceded to solubilisation and purification.

300 l of membrane solubilisation buffer (4.585 g/L TES, 7.948 g/L NaCl, 0.022 g/L KCL, 0.575 g/L Na_2HPO_4, 0.131 g/L NaH_2PO_4, 0.5 g/L TCEP, 0.78 g/L β-mercaptoethanol, 1x EDTA-free protease inhibitor cocktail, 0.174 g/L PMSF, 10 % v/v glycerol, 3 % DDM, pH 8.0) was added to the pellet and the pellet resuspended with the aid of a paintbrush. The resuspended cells were transferred to a new tube. 300 l of membrane solubilisation buffer was used twice more to rinse the original tube and all 900 µl pooled. The resuspended cell membranes were passed through a

25-gauge needle twice and added to 4.1 ml of membrane solubilisation buffer. The mixture was incubated for 3 hours at 4 °C. 1.5 ml Ni-NTA agarose was pre-equilibrated in column binding buffer (4.585 g/L TES, 7.948 g/L NaCl, 0.022 g/L KCL, 0.575 g/L Na_2HPO_4, 0.131 g/L NaH_2PO_4, 0.5 g/L TCEP, 0.78 g/L β-mercaptoethanol, 1x EDTA-free protease inhibitor cocktail, 0.174 g/L PMSF, 2.72 g/L imidazole, 0.1 % DDM, pH 8.0) before being added to the solubilised pellet and incubated for 90 minutes at 4 °C. The mixture was added to a 5 ml column at 4 °C. The resin was allowed to settle and the flow-through was collected. The column was washed with 5 ml wash buffer 1 (4.585 g/L TES, 66.39 g/L NaCl, 0.022 g/L KCL, 0.575 g/L Na_2HPO_4, 0.131 g/L NaH_2PO_4, 0.5 g/L TCEP, 0.78 g/L β-mercaptoethanol, 1x EDTA-free protease inhibitor cocktail, 0.174 g/L PMSF, 10 % (v/v) glycerol, 2.72 g/L, 1 % DDM, pH 8.0) and 5 ml wash buffer 2 (4.585 g/L TES, 7.948 g/L NaCl, 0.022 g/L KCL, 0.575 g/L Na_2HPO_4, 0.131 g/L NaH_2PO_4, 0.5 g/L TCEP, 0.78 g/L β-mercaptoethanol, 1x EDTA-free protease inhibitor cocktail, 0.174 g/L PMSF, 1 % DDM ,6.8 g/L imidazole, pH 8.0). The protein was eluted by the addition of 5 ml elution buffer (4.585 g/L TES, 7.948 g/L NaCl, 0.022 g/L KCL, 0.575 g/L Na_2HPO_4, 0.131 g/L NaH_2PO_4, 0.5 g/L TCEP, 0.78 g/L β-mercaptoethanol, 1x EDTA-free protease inhibitor cocktail, 0.174 g/L PMSF, 10.21 g/L imidazole, 1 % DDM, pH 8.0) to the column. Protein was dialysed to remove imidazole. Protein was concentrated and resuspended in a buffer (4.585 g/L TES, 7.948 g/L NaCl, 0.022 g/L KCL, 0.575 g/L Na_2HPO_4, 0.131 g/L NaH_2PO_4) supplemented with glycerol and DDM to give a final concentration of 10 % glycerol with 1 % DDM. Samples were taken for subsequent analysis by Coomassie Brilliant Blue staining of SDS-PAGE gels and Western blotting.

4.2.2 Expression and Purification of 6xHis Tagged STRA6 in Mammalian Cells

4.2.2.1 Expression of STRA6

STRA6 (UniProt Q9BX79) with a 6xHis tag in the mammalian expression vector pcDNA3.1 was a kind gift from Dr. Darren Martin

HEK293T cells were cultured at 37 °C in a humidified atmosphere (5 % CO_2 / 95 % O_2) in DMEM (supplemented with 10 % (v/v) heat-inactivated foetal bovine serum (FBS), penicillin and streptomycin [1 % (v/v)] and 1 % glutamine). Cells were grown as adherent monolayers to between 60-70 % confluence prior to transfection with empty vector or the STRA6 construct. HEK293T cells were transiently transfected using FuGENE® 6, according to the manufacturer's instructions.

At 48 hours post-transfection, growth medium was removed and cells washed in ice-cold PBS. Flasks were agitated until all cells were in suspension, at which time cells were harvested (700 g for 5 minutes). The supernatant was removed and discarded. Cells were stored at -80 °C or used to determine protein expression; Pellets were resuspended in 2 ml PBS, 80 µL of which was added to 20 µL of 5x SDS buffer. Cells were sonicated for 10 seconds at 10 % power on ice and heated at 70 °C for 5 minutes. Cells were centrifuged (17,000 g for 5 minutes) and the supernatants collected. Protein expression was determined by SDS-PAGE and Western blotting.

4.2.2.2 Lysis and Purification of STRA6

Cell pellets were resuspended in 2 ml hypotonic buffer (47.66 g/L HEPES, 2.86 g/L $MgCl_2$, 14.92 g/L KCl, 1.54 g/L DTT, 0.5 g/L TCEP, 0.78 g/L β-mercaptoethanol, 1x EDTA-free protease inhibitor cocktail, 0.174 g/L PMSF). The cells were ruptured by sonicating the sample for 1 minute at 20 % power on ice. The mixture was converted to a 5 ml pollyallomer optiseal tube and centrifuged (1 hour at 100,000 g at 4 °C). The supernatant was discarded and the pellet was resuspended in 250 µl lysis buffer (6.9 g/L $NaH_2PO_4H_2O$, 17.54 g/L NaCl, 0.68 g/L imidazole, 3 % DDM,

1x EDTA-free protease inhibitor cocktail, pH 8.0). The resuspended pellet was passed through a 25-gauge needle using a 1 ml syringe. The mixture was incubated on ice for 30 minutes and agitated occasionally. The mixture was sonicated at 10 % power for 30 seconds on ice and centrifuged (5 minutes at 17,000 g) to remove the insoluble fraction. 500 µl of Ni-NTA agarose was re-equilibrated in wash buffer (6.9 g/L $NaH_2PO_4H_2O$, 17.54 g/L NaCl, 1.36 g/L imidazole, 0.5 % DDM, 1x EDTA-free protease inhibitor cocktail, pH 8.0). The resin was added to the solubilised pellet and incubated overnight or for 90 minutes at 4 °C. The resin was centrifuged (700 g for 5 minutes) and the supernatant was collected. The resin was washed twice with 500 µl wash buffer, centrifuged (700 g for 5 minutes) and the washes collected. The protein was incubated with 300 µl elution buffer (6.9 g/L $NaH_2PO_4H_2O$, 17.54 g/L NaCl, 0.68 g/L imidazole, 0.5 % DDM, 1x EDTA-free protease inhibitor cocktail, pH 8.0) for 5 minutes, centrifuged (700 g for 5 minutes) and the eluate collected. Protein expression was determined by SDS-PAGE and Western blotting. Following purification, protein concentrations were determined using the BCA assay (Smith *et al.*, 1985).

4.2.3 Expression and Purification of Myc/6xHis Tagged STRA6 in Mammalian Cells

4.2.3.1 STRA6 Construct Design

The coding sequence for human STRA6 (UniProt entry Q9BX79), in the expression vector pPICZA, was previously used for STRA6 expression in *Pichia pastoris*. The coding sequence was amplified by PCR using the primers:

$^{5'}$-AGCTGGGAATTCGCCACCATGTCGTCC -$_{3'}$ which incorporates an *EcoRI* restriction site (underlined), and $^{5'}$- CGGCTTCTAGAGGGCTGGGCACCATT -$_{3'}$ which incorporates a *Xba1* restriction site, (also underlined).

Following purification from an agarose gel, the STRA6 insert and the Myc (EQKLISEEDL)/6xHis gene fusion expression vector, pcDNA4, were digested with the restriction endonucleases, *EcoRI* and *Xba1*, and further purified from agarose gels. The digested insert was subsequently ligated into pcDNA4.

Successful subcloning was confirmed by digestion, and further verified by sequencing.

4.2.3.2 Expression of STRA6

HEK293T cells were cultured at 37 °C in a humidified atmosphere (5 % CO_2 / 95 % O_2) in DMEM (supplemented with 10 % (v/v) heat-inactivated FBS, penicillin and streptomycin [1 % (v/v)] and 1 % glutamine). Cells were grown as adherent monolayers to between 60-70 % confluence prior to transfection with empty vector or the STRA6 construct. HEK293T cells were transiently transfected using FuGENE® 6, according to the manufacturer's instructions.

At 48 hours post-transfection, growth medium was removed and cells washed in ice-cold PBS. Flasks were agitated until all cells were in suspension, at which time cells were harvested (700 g for 5 minutes). The supernatant was removed and discarded. Cells where stored at -80 °C or used to determine protein expression.

Protein expression was determined by SDS-PAGE and Western blotting.

4.2.3.3 Lysis and Purification of STRA6

As given in 4.2.2.2

4.2.4 STRA6 Stable Cell Line

4.2.4.1 STRA6 Stable Cell Line Induction

Stable HEK293T cells inducibly expressing STRA6, in expression vector pN-TGSH along with a HA and StrepII tag on either the N- or C-terminus, were cultured at 37 °C in a humidified atmosphere (5 % CO_2 / 95 % O_2) in DMEM (supplemented with 10 % (v/v) heat-inactivated FBS, penicillin and streptomycin [1 % (v/v)], 1 % glutamine, 100 g/ml hygromycin B and 15 g/ml blasticidin) Cells were grown as adherent monolayers to between 60-70 % confluence prior to induction in DMEM

(supplemented with 10 % (v/v) heat-inactivated FBS, penicillin and streptomycin [1 % (v/v)], 1 % glutamine and 1 g/ml tetracycline).

At 24 hours post-induction, growth medium was removed and cells washed in ice-cold PBS. Flasks were agitated until all cells were in suspension, at which time cells were harvested (700 g for 5 minutes). The supernatant was removed and discarded. Cells where stored at -80 °C or used to determine protein expression.

Protein expression was determined by SDS-PAGE and Western blotting.

4.2.4.2 Purification of STRA6

Cell pellets were resuspended in 1 ml of NP buffer (6.90 g/L $NaH_2PO_4H_2O$, 17.54 g/L NaCl, 1.54 g/L DTT, 0.5 g/L TCEP, 0.78 g/L β-mercaptoethanol, 1x EDTA-free protease inhibitor cocktail, 0.174 g/L PMSF, pH 8) supplement with 1 % Trition-X-100. Once resuspended, the cells were incubated at 4 °C for 1 hour with constant agitation. The sample was then centrifuged (12,000 g for 20 minutes at 4 °C). Following centrifugation, the supernatant was harvested and the pellet discarded.

Avidin was added to the cleared lysate at 5 µg/ml. STRA6 was purified using Strep-Tactin superflow plus. 200 µl of a 50 % slurry of Strep-Tactin superflow plus was re-equilibrated in NP buffer. The cleared lysate was incubated with the resin for 90 minutes at 4 °C. The resin was centrifuged (700 g for 3 minutes at 4 °C) and the supernatant collected. The resin was washed twice with 200 µl NP buffer supplement with 0.5 % Trition-X-100, the resin was centrifuged (700 g for 3 minutes at 4 °C) and the washes collected. The resin was incubated with 200 µl NPD buffer (6.90 g/L $NaH_2PO_4H_2O$, 17.54 g/L NaCl, 0.54 g/L desthiobiotin, 0.5 % Trition-X-100, pH 8) for 5 minutes. The resin was centrifuged (700 g for 3 minutes at 4 °C) and the eluate collected. Each fraction was analysed by SDS-PAGE and Western blotting. Following purification, protein concentrations were determined using the BCA assay (Smith *et al.*, 1985).

4.2.5 STRA6 Binding Capacity of MYTH Hits

4.2.5.1 STRA6 Binding Capacity of MYTH Hits with Washing

Stable HEK293T cells, inducibly expressing STRA6 (as well as un-induced cells as a control), were centrifuged and resuspended in 1 ml of NP buffer supplement with 1 % Trition-X-100. Once resuspended, the cells were incubated at 4 °C for 1 hour with constant agitation. The two samples were then centrifuged (12,000 g for 20 minutes at 4 °C). Following centrifugation, the supernatants were harvested and the pellets discarded.

Avidin was added to the cleared lysates at 5 µg/ml. 2 x 200 µl of a 50 % slurry of Strep-Tactin resin was re-equilibrated in NP buffer. The cleared lysates were incubated with the resins for 90 minutes at 4 °C. The resins were centrifuged (700 g for 3 minutes at 4 °C) and the supernatants collected. The resins were washed once with 200 µl NP buffer supplement with 0.5 % Trition-X-100, the resins were centrifuged (700 g for 3 minutes at 4 °C) and the washes collected. A HEK293T lysate overexpressing one of the MYTH hits (CCL2, CXCL14, IFITM1, IFITM3, MIF, PLP2 or SERP1) was added and incubated with the resins for 45 minutes at 4 °C. The resins were centrifuged (700 g for 3 minutes at 4 °C) and the supernatant collected. The resins were washed once with 200 µl NP buffer supplement with 0.5 % Trition-X-100, the resins centrifuged (700 g for 3 minutes at 4 °C) and the washes collected. The resin was incubated with NPD buffer for 5 minutes, the resins centrifuged (700 g for 3 minutes at 4 °C) and the eluate collected. Each fraction was analysed by SDS-PAGE and Western blotting to determine if a specific interaction had occurred.

4.2.5.2 STRA6 Binding Capacity of MYTH Hits without Washing

As in 4.2.5.1, however following incubation, instead of a tradition wash step to remove nonspecifically bound material, reactions were carefully resuspended prior to rapid centrifugation (6,800 g for 5 minutes) through an oil layer. A 3:2 dibutyl phthalate: dinonyl phthalate preparation was used to separate the aqueous, oil and

agarose layers. The pellet was incubated with 2x SDS sample buffer for 5 minutes at 70 °C, prior to analysis of the supernatant by SDS-PAGE and Western blotting.

4.2.6 Construct Design of MYTH Hits for Coexpression in Mammalian Cells with STRA6

4.2.6.1 Construct Design of CD63

The coding sequence for human CD63 (UniProt entry P08962), in the expression vector pPR3-N, had been previously used for CD63 expression in the MYTH. The coding sequence was amplified by PCR using the primers:

$^{5'}$- AGCTGGAAGCTTGCCACCATGGCGGTGGAAGGAGG -$_{3'}$ which incorporates an *HindII* restriction site (underlined), and $^{5'}$-CGGCTGGCGGCCGCTTA**AGCGTAATCTGGAACATCGTATGGGTA**CATC ACCTCGTAGCCACTTCTG -$_{3'}$ which incorporates a *Not1* restriction site (also underlined) and a HA tag (in bold).

Following purification from an agarose gel, CD63 and the mammalian expression vector pcDNA3.1 were digested with the restriction endonucleases, *HindII* and *Not1*, and further purified from agarose gels. The digested insert was subsequently ligated into pcDNA3.1. Successful subcloning was confirmed by digestion, and further verified by sequencing.

4.2.6.2 Construct Design of PDZK1-IP1

The coding sequence for human PDZK1-IP1 (UniProt entry Q13113), in the expression vector pPR3-N, had been previously used for PDZK1-IP1 expression in the MYTH. The coding sequence was amplified by PCR using the primers:

$^{5'}$- AGCTGGAAGCTTGCCACCATGTCGGCCCTCAGC -$_{3'}$ which incorporates a *HindII* restriction site (underlined), and $^{5'}$-

CGGCTGGCGGCCGCTTA**AGCGTAATCTGGAACATCGTATGGGTA**CATC GGGGTGCTGC -3' which incorporates a *Not1* restriction site (also underlined) and a HA tag (in bold).

Following purification from an agarose gel, PDZK1-IP1 and the mammalian expression vector pcDNA3.1 were digested with the restriction endonucleases, *HindII* and *Not1*, and further purified from agarose gels. The digested insert was subsequently ligated into pcDNA3.1. Successful subcloning was confirmed by digestion, and further verified by sequencing.

4.2.6.3 Construct Design of OCIAD2 and Osteopontin

The coding sequence for OCIAD2 (UniProt Q56VL3) and osteopontin (UniProt P10451), in the mammalian expression vector pCMV6-Entry incorporating a c-terminal Myc (EQKLISEEDL) and DDK (DYKDDDDK) tag, were purchased from Origene.

4.2.7 STRA6 Binding Capacity of Coexpressed MYTH Hits

4.2.7.1 STRA6 and MYTH Hits Expression

Stable HEK293T cells inducibly expressing STRA6, in expression vector pN-TGSH along with a HA and StrepII tag on either the N- or C-terminus, were cultured at 37 °C in a humidified atmosphere (5 % CO_2 / 95 % O_2) in DMEM (supplemented with 10 % (v/v) heat-inactivated FBS, penicillin and streptomycin [1 % (v/v)], 1 % glutamine, 100 g/ml hygromycin B and 15 g/ml blasticidin). Cells were grown as adherent monolayers to between 60-70 % confluence prior to transfection with CD63, PDZK1-IP1, OCIAD2 or osteopontin. HEK293T cells were transiently transfected using Lipofectamine™ 2000 Transfection reagent according to the manufacturer's instructions.

Four hours after transfection, medium was changed, to DMEM (supplemented with 10 % (v/v) heat-inactivated FBS, penicillin and streptomycin [1 % (v/v)], 1 % glutamine and 1 µg/ml tetracycline) to induce STRA6 expression. At 24 hours post-transfection, growth medium was removed and cells washed in ice-cold PBS. Flasks were agitated until all cells were in suspension, at which time cells were harvested (700 g for 5 minutes). The supernatant was removed and discarded. Cells where stored at -80 °C or used to determine protein expression.

Protein expression was determined by SDS-PAGE and Western blotting.

4.2.7.2 STRA6 Binding Capacity of MYTH Hits with Washing

Stable HEK293T cells, inducibly expressing STRA6 (as well as un-induced cells as a control) and transiently expressing PDZK1-IP1, CD63, OCIAD2 or osteopontin were centrifuged and resuspended in 1 ml of NP buffer supplement with 1 % Trition-X-100. Once resuspended, the cells were incubated at 4 °C for 1 hour with constant agitation. The two samples were then centrifuged (12,000 g for 20 minutes at 4 °C). Following centrifugation, the supernatants were harvested and the pellets discarded.

Avidin was added to the cleared lysates at 5 µg/ml. 2 x 200 µl of a 50 % slurry of Strep-Tactin resin was re-equilibrated in NP buffer. The cleared lysates were incubated with the resins for 90 minutes at 4 °C. The resins were centrifuged (700 g for 3 minutes at 4 °C) and the supernatants collected. The resins were washed once with 200 µl NP buffer supplement with 0.5 % Trition-X-100, the resins were centrifuged (700 g for 3 minutes at 4 °C) and the washes collected. The resin was incubated with NPD buffer for 5 minutes, the resins centrifuged (700 g for 3 minutes at 4 °C) and the eluate collected. Each fraction was analysed by SDS-PAGE and Western blotting to determine if a specific interaction had occurred.

4.2.7.3 STRA6 Binding Capacity of MYTH Hits without Washing

As in 4.2.7.2, however following incubation, reactions were carefully resuspended prior to rapid centrifugation (6,800 g for 5 minutes) through an oil layer, a 3:2 dibutyl phthalate: dinonyl phthalate preparation, to separate the aqueous, oil and agarose layers. The pellet was incubated with 2x SDS sample buffer for 5 minutes at 70 °C, prior to analysis of the supernatant by SDS-PAGE and Western blotting.

4.2.8 Detection of Protein Expression

Protein expression was analysed by SDS-PAGE and Western blotting. In the detection of STRA6, α-His-HRP (Roche), α-myc (Cell Signalling), α-HA (Covance), α-mouse-HRP (Promega), α-STRA6 (Abnova) and α-rabbit-HRP (GE Healthcare) antibodies were used where appropriate. Lysates overexpressing the hits, purchased from Origene, were detected using α-myc and α-mouse-HRP antibodies. CD63 and PDZK1-IP1 constructs were detected using α-HA and α-mouse-HRP antibodies. OCIAD2 and osteopontin were detected using α-myc and α-mouse-HRP antibodies.

4.3 Results

4.3.1 Expression and Purification of STRA6 in *Pichia pastoris*

4.3.1.1 Expression of STRA6

Pichia pastoris is an industrial methylotrohic yeast initially chosen for production of single-cell protein because of its ability to grow to very high cell density in simple defined medium. The advantage of using *P. pastoris,* as opposed to other eukaryotic expression systems such as insect and mammalian cells, is the comparatively high yields obtained from the yeast system, which allows recombinant proteins to be expressed at relatively low cost, without the need of a complex growth medium or culture conditions. What's more, as a eukaryotic organism, *P. Pastoris* is capable of producing soluble, correctly folded recombinant proteins that have undergone all the posttranslational modifications required for functionality. With its proven ability to express more than 300 proteins, *P. Pastoris* has become a consistent choice for heterologous protein production and is now the most commonly used host for eukaryotic membrane proteins (Hedfalk, 2013, Goncalves et al., 2013).

The coding sequence for human STRA6, in the expression vector pPICZA, was designed to incorporate the coding sequence for GFP as a marker of gene expression and a 6xHis tag. Protein expression was determined by SDS-PAGE and Western blotting. After expression, a large quantity of STRA6 was obtained, approximately 25 g/L, and continued onto lysis and purification.

4.3.1.2 Lysis and Purification of STRA6

A ball mill (Retsch MM301) was used for cryogenic disruption of yeast cells. Since STRA6 was expressed as a 6xHis fusion protein, purification was carried out using affinity chromatography. Protein was purified by immobilised metal ion affinity chromatography (IMAC) using Ni-NTA agarose. Eluted fractions contained a large quantity of protein, as illustrated in Figure 4.1. Protein was aliqouted before storage at -20 °C. However protein was not soluble after storage at -20 °C and could no

longer be detected after two days of storage, presumably due to degradation. After considerable attempts to prevent degradation the decision was made to express STRA6 in HEK293T cells for subsequent binding assays.

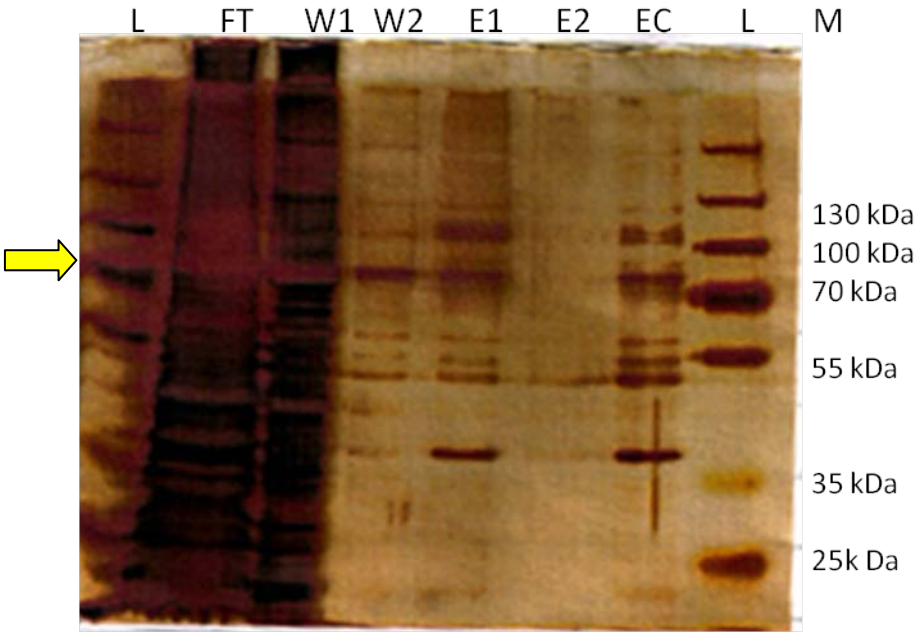

Figure 4.1 **STRA6 Purification using Ni-NTA**

Silver stained (12%) SDS-PAGE gel showing the purification of STRA6. 5 µl loaded per well. The soluble fraction after lysis was incubated with Ni-NTA agarose and the flow-through **(FT)** collected. The resin was washed twice **(W1 and W2)** prior to elution **(E1).** The elution step was repeated **(E2)** and the eluates pooled and concentrated **(EC)**. Molecular weight markers **(M)** revealed STRA6 migrating at an expected ~ 74 kDa in the flow-through, washes and in the eluted fraction with some contamination.

4.3.2 Expression and Purification of STRA6 in Mammalian Cells

HEK293T cells express STRA6 in its native form and thus represent an ideal mammalian expression system for overexpression of the recombinant receptor. In addition, HEK293T cells are easy to grow and tend to transfect readily.

After transfecting HEK293T cells with the STRA6 construct, expression remained unsuccessful or at least, undetectable by Western blotting, using α-STRA6 antibodies, despite different combinations of conditions including DNA concentration, transfection reagent and collection time. Membrane isolation and Ni-NTA purification were performed to isolate and concentrate any recombinant STRA6 present in the cells. Attempts were further encumbered by the presence of a Nonspecific band, using the α-his-HRP antibody, at approximately 74 kDa, the expected molecular weight for STRA6, as illustrated in Figure 4.2. This Nonspecific band was present in both transfected and untransfected cells to the same degree. Transfection efficiency may have been low resulting in the untransfected cell population outgrowing the transfected, resulting in a low yield of the protein of interest. It was therefore decided to design a new STRA6 construct with both a 6xHis tag for purification and a Myc tag for detection.

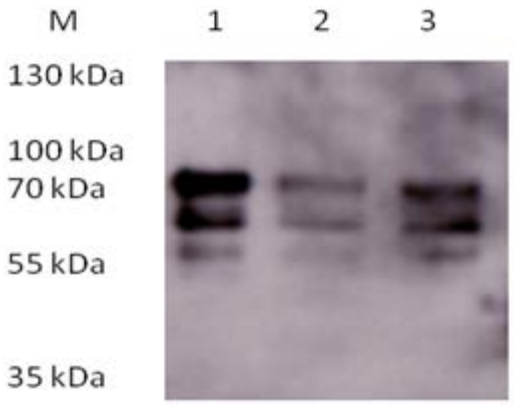

Figure 4.2: STRA6 Expression in HEK293T Cells

Representative Western blot showing fractions from the expression of STRA6 as detected by α-His-HRP antibodies. 5 µl loaded per well. HEK293T cells were transfected with the STRA6 construct **(1).** Untransfected cells **(2)** and cells transfected with the empty vector **(3)** were used as a control. Cells were harvested and the soluble fraction, after lysis, applied to the gel. Molecular weight markers **(M)** revealed a band at the expected molecular weight, ~ 74 kDa, of STRA6 in all three lanes. The presence of this band in untransfected cells and cells transfected with the empty vector indicates that this band does not represent STRA6. STRA6 may not be expressed in transfected cells or is difficult to detect due to the presence of this nonspecific band.

4.3.3 Expression and Purification of Myc/ 6xHis Tagged STRA6 in Mammalian Cells

4.3.3.1 STRA6 Construct Design

Following PCR, a band at the expected size, approximately 2000 bp, was visualised on an agarose gel. The PCR band was extracted, purified and ligated into pcDNA4_myc/his. Successful subcloning was confirmed by digestion and further verified by sequencing.

4.3.3.2 Expression and Purification of STRA6

HEK293T cells were transfected with the STRA6 construct. The cells were lysed and STRA6 immobilised on Ni-NTA agarose. After incubation, the resin was washed twice and any bound protein eluted. As illustrated in Figure 4.3, STRA6 was detectable in transfected cells at the expected molecular weight of 74 kDa and in sufficient quantities for downstream experiments, ~ 100 µg/ T75 flask. However, it was later decided to use a HEK293T cell line inducibly expressing STRA6 which had unexpectedly become available. Inducible expression resulted in higher levels of STRA6 expression than that observed using transient expression.

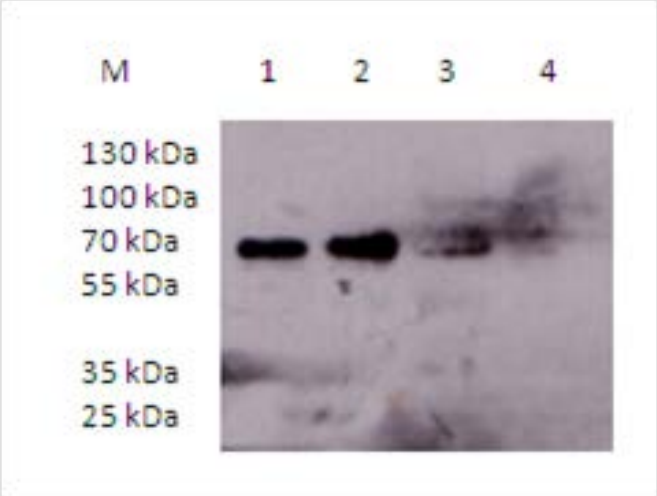

Figure 4.3: Expression of Myc-Tagged STRA6

Representative Western blot showing fractions from the expression of STRA6 as detected by *α*-myc and *α*-mouse-HRP antibodies. 5 µl loaded per well. HEK293T cells were transfected with the STRA6 construct using a number of different DNA concentrations, 2 µg **(1),** 5 µg **(2),** 7 µg **(3).** Untransfected cells **(4)** were used as a control. Cells were harvested and the soluble fraction, after lysis, applied to the gel. Molecular weight markers **(M)** revealed a band at the expected molecular weight, ~ 74 kDa, of STRA6 in lanes 1-3, with no band in lane 4, indicating transfection was a success.

4.3.4 STRA6 Stable Cell Line

4.3.4.1 Stable Cell Line Induction and Purification

The stable HEK293T cell line inducibly expressing STRA6 along with a HA and StrepII tag on either the N- or C-terminus, using expression vector pN-TGSH, was generated by Dr. Conor Breen. The StrepII tag allows affinity purification of STRA6 on a Strep-Tactin resin. The epitope tags were placed either at the N- or C-terminus of STRA6 as these epitope tags may inhibit STRA6 binding with other proteins. Therefore both constructs were used in binding assays.

Cells were cultured and expression induced at 60-70 % confluency. At 24 hours post-transfection, cells were harvested. Cells were stored at -80 ℃ or used to determine protein expression. Protein expression was determined by SDS-PAGE and Western blotting, using α-HA and α-mouse-HRP antibodies. Once expression of the construct had been verified, the protein was purified using a Strep-Tactin resin. A large quantity of STRA6 was present in the eluted fraction, ~ 150 μg/ T75 flask, with little lost in the washes, illustrated in figure 4.4.

Figure 4.4: STRA6 Purification using Strep-Tactin Resin

Representative Western blot showing fractions from the purification of STRA6 as detected by α-HA and α-mouse-HRP antibodies. 5 µl loaded per well. STRA6 contains either an N- **(NT)** or C- **(CT)** terminal HA/strepII epitope tag allowing for the purification of STRA6 using Strep-Tactin superflow plus agarose. Untransfected cells **(Untraf)** were used as a control. The soluble fractions of the cleared HEK293T lysates were incubated with the Strep-Tactin resin. The supernatants **(FT)** were then collected and the resins washed **(W)** followed by elution of bound proteins from the resins **(E).** Molecular weight markers **(M)** revealed STRA6 migrating at an expected ~ 74 kDa in both elutions with no protein lost in the FT or W.

4.3.5 STRA6 Binding Capacity of Hits

4.3.5.1 STRA6 Binding Capacity of MYTH Hits with Washing

Stable HEK293T cells inducibly expressing STRA6 were cultured, (un-induced cells were used as a control), harvested, lysed and the cleared lysates bound to the Strep-Tactin resin, ~ 5 µg of protein. Avidin was added to the cleared lysate to prevent biotin present in the lysate binding the resin. Any nonspecifically bound proteins were removed by washing the resins with NP buffer. A HEK293T lysate overexpressing one of the hits (CCL2, CXCL14, IFITM1, IFITM3, MIF, PLP2 or SERP1), ~ 5 µg of protein, was incubated with the resins. The resins were washed again to remove any nonspecifically bound proteins and the protein eluted from the resin. The binding assay was performed at 4 °C to prevent aggregation of proteins. Each fraction was analysed by SDS-PAGE and Western blotting to determine if a specific interaction occurred. STRA6 was eluted from the resin alone, all hits were present in the supernatant, indicating that an interaction did not occur or a weak interaction occurred which could not be captured in this assay. STRA6 and PLP2 binding assay is illustrated in Figure 4.5 as an example of the results obtained

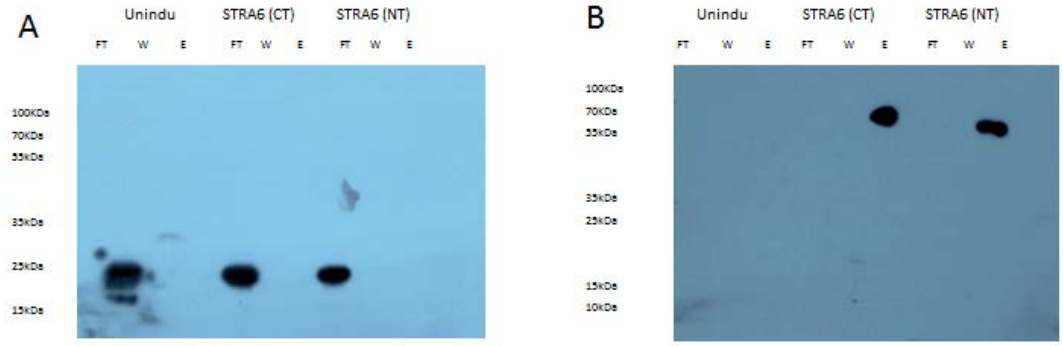

Figure 4.5: STRA6 and PLP2 Binding Assay

Representative Western blot showing lack of STRA6 binding capacity for PLP2, as detected by α-Flag **(A),** α-HA **(B)** and α-mouse-HRP antibodies. 5 µl loaded per well. STRA6 contains either an N- **(NT)** or C- **(CT)** terminal HA/StrepII epitope tag. Un-induced cells **(Unindu)** were used as a control. The soluble fraction of the cleared HEK293T lysates were incubated with a Strep-Tactin resin, before the addition of the overexpressed PLP2 cleared lysate The supernatants **(FT)** were then collected and the resins washed **(W)** followed by elution of any bound proteins from the resins **(E).** Molecular weight markers **(M)** revealed PLP2 migrating at an expected ~ 17 kDa and STRA6 migrating at an expected ~ 74 kDa as expected. STRA6 is present in the elution. PLP2 is present in the FT, indicating no interaction occurred.

4.3.5.2 STRA6 Binding Capacity of MYTH Hits without Washing

Stable HEK293T cells inducibly expressing STRA6 were cultured, harvested, lysed and the cleared lysates immobilised on a Strep-Tactin resin, ~ 5 µg of protein. Any nonspecifically bound proteins were removed by washing the resin. HEK293T lysate overexpressing one of the hits (CCL2, CXCL14, IFITM1, IFITM3, MIF, PLP2 or SERP1), ~ 5µg of protein, was incubated with the resin. Nonspecifically bound proteins were removed by the rapid centrifugation through oil, a 3:2 dibutyl phthalate: dinonyl phthalate preparation. This circumvents the wash step of traditional pull-down protocols, allowing even low affinity interactions to be detected (Sivaprasadarao and Findlay, 1988b). A 3:2 dibutyl phthalate: dinonyl phthalate preparation has a combined density of ~ 1.09 g/mL, whereas Strep-Tactin Superflow Plus has a higher density and free hits are of lower density than the oil mix, resulting in separation of hits from hits bound to STRA6 immobilised on the Strep-Tactin resin. Previously, the binding assay was performed at 4 °C to prevent aggregation of proteins and using a wash step to remove nonspecifically bound proteins. However, this did not result in any detectable interactions. STRA6 and PLP2 binding assay is illustrated in Figure 4.6 as an example of the results obtained. Performing the binding assay at 4 °C may inhibit STRA6 binding, therefore, the second binding assay, eliminating the wash step, was performed at room temperature.

Each fraction was analysed by SDS-PAGE and Western blotting to determine if a specific interaction occurred. STRA6 was eluted from the resin alone, all hits were present in the aqueous phase, indicating that an interaction did not occur.

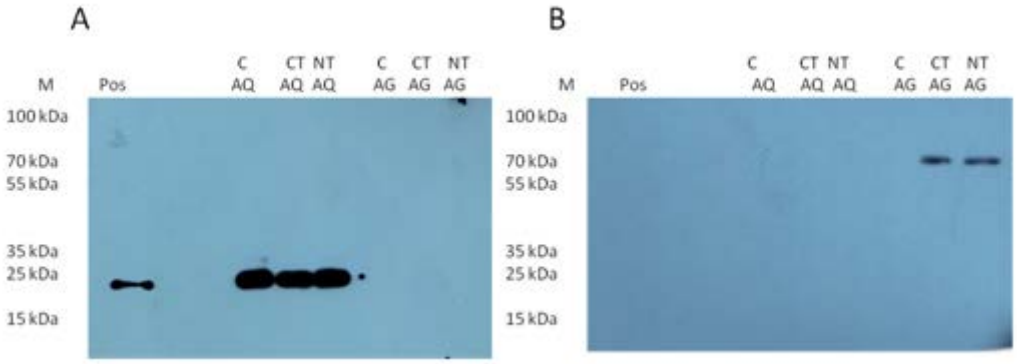

Figure 4.6: STRA6 and PLP2 Binding Assay without Washing

Representative Western blot showing lack of STRA6 binding capacity for PLP2, as detected by α-Flag **(A),** α-Ha **(B)** and α-mouse-HRP antibodies. 5 µl loaded per well. STRA6 contains either an N- **(NT)** or C- **(CT)** terminal HA/StrepII epitope tag. Un-induced cells **(C)** were used as a control. Positive control for PLP2 **(Pos)** was also loaded. The soluble fraction of the cleared HEK293T lysates were incubated with a Strep-Tactin resin, before the addition of the overexpressed PLP2 cleared lysates. The mixture was added to an oil preparation and spun to separate the aqueous **(AQ)** phase and the agarose **(AG)** phase, containing the bound protein. Molecular weight markers **(M)** revealed PLP2 migrating at an expected ~ 17 kDa and STRA6 migrating at an expected ~ 74 kDa as expected. STRA6 is present in the agarose phase. PLP2 is present in the aqueous phase, indicating no interaction occurred.

4.3.6 STRA6 Binding Capacity of Coexpressed MYTH Hits

4.3.6.1 CD63 and PDZK1-IP1 Construct Design

Following PCR, a band at the expected size, 700 bp for CD63 and 350 bp for PDZK1-IP1, was visualised on an agarose gel. PCR band was extracted, digested, purified and ligated into pcDNA3.1. Successful subcloning was confirmed by digestion, as illustrated in Figure 4.7, and further verified by sequencing.

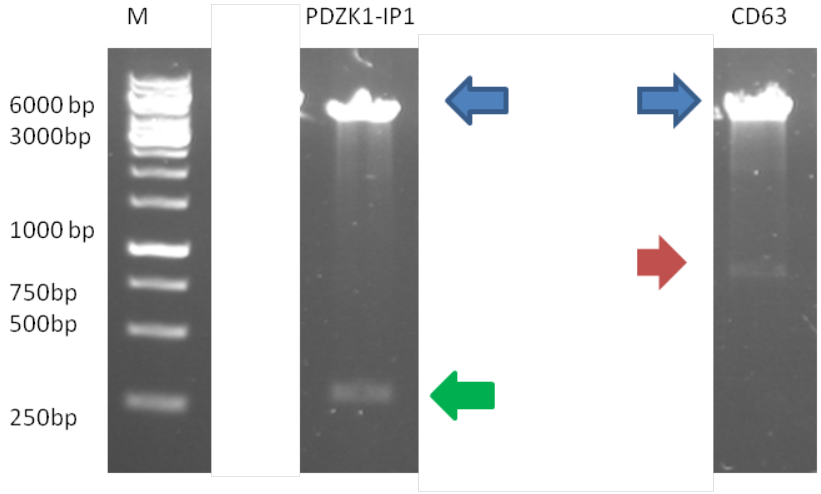

Figure 4.7: CD63 and PDZK1-IP1 Construct Design

CD63 and PDZK1-IP1 were both ligated into pcDNA3.1. Following ligation, digestion was performed to ensure successful subcloning. Digestions were loaded onto a 0.8 % agarose gel. A band at the expected size, 700 bp, for CD63 (highlighted by red arrow) and 350 bp for PDZK1-IP1 (highlighted by green area), were detected, as well as a band at the expected size, 5428 bp, for the empty vector, pcDNA3.1 (highlighted by blue arrow).

4.3.6.2 STRA6 and MYTH Hits Expression

Stable HEK293T cells with inducible STRA6 were cultured, transfected with PDZK1-IP1, CD63, OCIAD2 or osteopontin and STRA6 expression was induced (un-induced cells were used as a control). Cells were harvested 24 hours later and lysed. Protein expression was determined by SDS-PAGE and Western blotting. Expression of STRA6 with PDZK1-IP1 is illustrated in Figure 4.8. The MYTH hits were expressed along with STRA6 to ensure that if any intermediate protein(s) or *in vivo* post-translational modification(s) (PTM) were involved, the interaction would be captured.

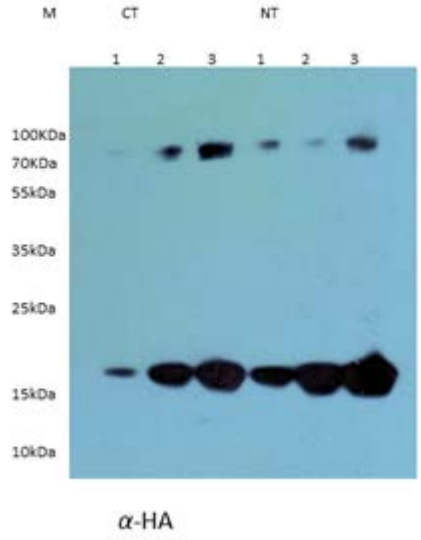

Figure 4.8: Expression of PDZK1-IP1 and STRA6

Representative Western blot showing STRA6 expression with PDZK1-IP1, as detected by *α*-HA and *α*-mouse-HRP antibodies. STRA6 contains either an N- **(NT)** or C- **(CT)** terminal HA/StrepII epitope tag. **(1-3)** 2 µl, 4 µl and 8 µl respectively of lysed cells loaded per well. Molecular weight markers **(M)** revealed PDZK1-IP1 and STRA6 migrating at ~ 17 kDa and ~ 74 kDa respectively, as expected.

4.3.6.3 STRA6 Binding Capacity of PDZK1-IP1 with Washing

Once expression of PDZK1-IP1, both in the presence (induced cells) and absence of STRA6 (un-induced cells), was verified, the cleared lysates were incubated with a Strep-Tactin resin. Nonspecifically bound proteins were removed from the resin by washing and bound material eluted from the resin, ~ 10 µg of protein. The binding assay was performed at 4 °C to prevent aggregation of proteins. Each fraction was analysed by SDS-PAGE and Western blotting to determine if a specific interaction occurred. STRA6 was present in the eluted fraction for the induced sample and PDZK1-IP1 was present in the supernatant indicating that the two did not interact, illustrated in Figure 4.9.

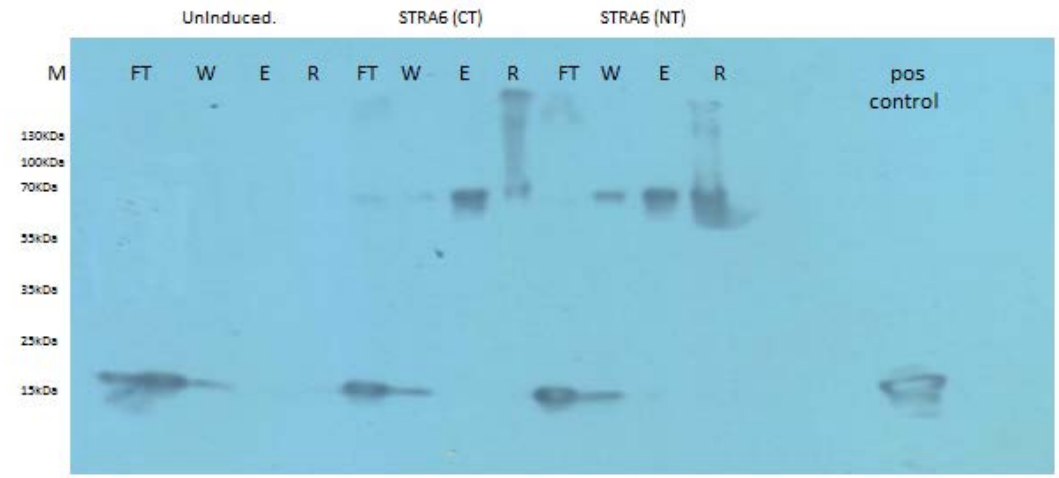

Figure 4.9: STRA6 and PDZK1-IP1 Binding Assay

Representative Western blot showing lack of STRA6 binding capacity for PDZK1-IP1, as detected by α-HA and α-mouse-HRP antibodies. 5 µl loaded per well. STRA6 contains either an N- **(NT)** or C- **(CT)** terminal HA/StrepII epitope tag. Un-induced cells **(Uninduced)** were used as a control. The soluble fraction of the cleared HEK293T lysates expressing both STRA6 and PDZK1-IP1 were incubated with a Strep-Tactin resin, as well as un-induced cells expressing only PDZK1-IP1. The supernatants **(FT)** were then collected and the resins washed **(W)** followed by elution of any bound proteins from the resins **(E).** Any protein still bound to the resin **(R)** was also loaded onto the gel. Molecular weight markers **(M)** revealed PDZK1-IP1 migrating at an expected ~ 17 kDa and STRA6 migrating at an expected ~ 74 kDa as expected. STRA6 is present in the elution. PDZK1-IP1 is present in the FT and washes, indicating no interaction occurred. 5 µl of the HEK293T lysate expressing only PDZK1-IP1 was used as a positive control **(pos control).**

4.3.6.4 STRA6 Binding Capacity of CD63 with Washing

As in 4.3.6.3, however PDZK1-IP1 was replaced with CD63. STRA6 was present in the eluted fraction for the induced sample and CD63 was present in the supernatant, indicating that the two do not interact, illustrated in Figure 4.10.

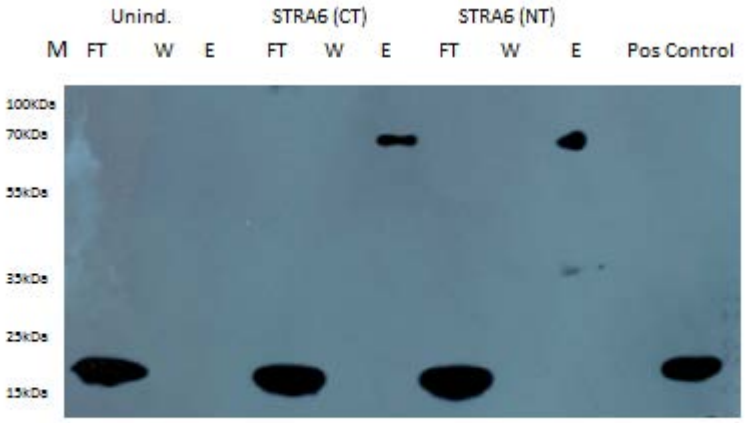

Figure 4.10: STRA6 and CD63 Binding Assay

Representative Western blot showing lack of STRA6 binding capacity for CD63, as detected by α-HA and α-mouse-HRP antibodies. 5 µl loaded per well.STRA6 contains either an N- **(NT)** or C- **(CT)** terminal HA/StrepII epitope tag. Un-induced cells **(Unind)** were used as a control. The soluble fraction of the cleared HEK293T lysates expressing both STRA6 and CD63 were incubated with a Strep-Tactin resin, as well as un-induced cells expressing only CD63. The supernatants **(FT)** were then collected and the resins washed **(W)** followed by elution of any bound proteins from the resins **(E).** Molecular weight markers **(M)** revealed CD63 migrating at an expected ~ 25 kDa and STRA6 migrating at an expected ~ 74 kDa as expected. STRA6 is present in the elution. CD63 is present in the FT, indicating no interaction occurred. 5 µl of the HEK293T lysate expressing only CD63 was used as a positive control **(pos control).**

4.3.6.5 STRA6 Binding Capacity of OCIAD2 with Washing

As in 4.3.6.3, however PDZK1-IP1 was replaced with OCIAD2. STRA6 was present in the eluted fraction for the induced sample and OCIAD2 was present in the supernatant indicating that the two did not interact, illustrated in Figure 4.11.

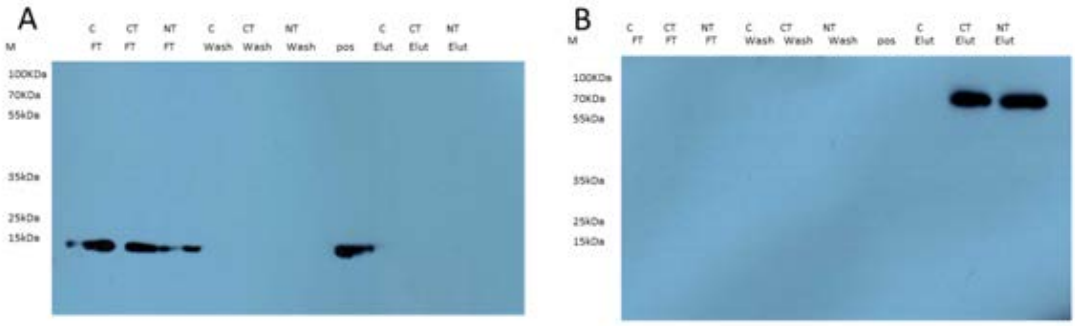

Figure 4.11: STRA6 and OCIAD2 Binding Assay

Representative Western blot showing lack of STRA6 binding capacity for OCIAD2, as detected by *α*-Myc **(A),** *α*-HA **(B)** and *α*-mouse-HRP antibodies. 5 µl loaded per well. STRA6 contains either an N- **(NT)** or C- **(CT)** terminal HA/StrepII epitope tag. Un-induced cells **(C)** were used as a control. The soluble fraction of the cleared HEK293T lysates expressing both STRA6 and OCIAD2 were incubated with a Strep-Tactin resin, as well as un-induced cells expressing only OCIAD2. The supernatants **(FT)** were then collected and the resins washed **(Wash)** followed by elution of any bound proteins from the resins **(Elut).** Molecular weight markers **(M)** revealed OCIAD2 migrating at an expected ~ 17 kDa and STRA6 migrating at an expected ~ 74 kDa as expected. STRA6 is present in the elution. OCIAD2 is present in the FT, indicating no interaction occurred. 5 µl of the HEK293T lysate expressing only OCIAD2 was used as a positive control **(pos).**

4.3.6.6 STRA6 Binding Capacity of Osteopontin with Washing

As in 4.3.6.3, however PDZK1-IP1 was replaced with osteopontin, STRA6 was present in the eluted fraction for the induced sample and osteopontin was present in the supernatant indicating that the two did not interact, illustrated in Figure 4.12.

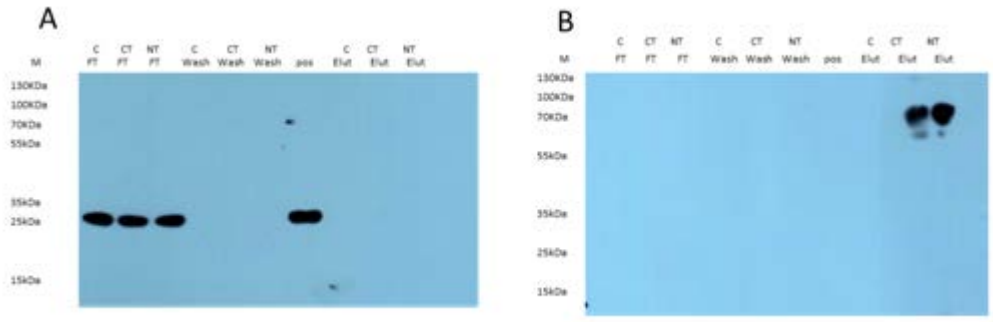

Figure 4.12: STRA6 and Osteopontin Binding Assay

Representative Western blot showing lack of STRA6 binding capacity for osteopontin, as detected by α-Myc **(A),** α-HA **(B)** and α-mouse-HRP antibodies. 5 µl loaded per well. STRA6 contains either an N- **(NT)** or C- **(CT)** terminal HA/StrepII epitope tag. Un-induced cells **(C)** were used as a control. The soluble fraction of the cleared HEK293T lysates expressing both STRA6 and osteopontin were incubated with a Strep-Tactin resin, as well as un-induced cells expressing only osteopontin. The supernatants **(FT)** were then collected and the resins washed **(Wash)** followed by elution of any bound proteins from the resins **(Elut).** Molecular weight markers **(M)** revealed osteopontin migrating at an expected ~ 32 kDa and STRA6 migrating at an expected ~ 74 kDa as expected. STRA6 is present in the elution. Osteopontin is present in the FT, indicating no interaction occurred. 5 µl of the HEK293T lysate expressing only osteopontin was used as a positive control **(pos).**

4.3.6.7 STRA6 Binding Capacity of Coexpressed MYTH Hits without Washing

Stable HEK293T cells with inducible STRA6 were transfected with PDZK1-IPI, CD63, OCIAD2 or osteopontin and STRA6 expression induced (un-induced cells were used as a control). Cells were harvested and lysed. The cleared lysates were incubated with a Strep-Tactin resin, ~ 10 µg of protein. Any nonspecifically bound proteins were removed by the rapid centrifugation through oil, a 3:2 dibutyl phthalate: dinonyl phthalate preparation. This circumvents the wash step of traditional pull-down protocols, allowing even low affinity interactions to be detected. Each fraction was analysed by SDS-PAGE and Western blotting to determine if a specific interaction had occurred. Previously, the binding assay was performed at 4 °C to prevent aggregation of proteins and using a wash step to remove nonspecifically bound proteins. However, this did not result in any detectable interactions. Performing the binding assay at 4 °C may inhibit STRA6 binding. Therefore, the second binding assay, eliminating the wash step, was performed at room temperature. STRA6 was eluted from the resin alone, PDZK1-IPI, CD63, OCIAD2 and osteopontin were present in the aqueous phase indicating that an interaction did not occur.

4.4 Discussion

Using the MYTH, 11 novel protein interactions for STRA6 were detected. These potential interactions need to be verified independently of the MYTH. The MYTH can give a number of false positives; hits which do not interact with the bait *in vivo*. The estimated reliability of the high-throughput MYTH has been suggested to be approximately fifty percent (Sprinzak et al., 2003). There are a number of reasons for a high level of false positives; proteins that bind and activate the reporter gene directly, "sticky" or incorrectly folded proteins that nonspecifically bind many baits, plasmid rearrangements or copy number changes that generate auto activators or alternations at one of the reporter genes that results in constitutive expression. Therefore, validation of all interacting proteins is needed before the interaction can be deemed biologically relevant (Stynen et al., 2012).

The 11 novel protein interactions for STRA6 were to be verified using *in vitro* pull-down assays. Recombinant STRA6, with a strepII epitope tag, was immobilised on a strep-tactin resin and the MYTH hits added individually. Nonspecifically bound proteins were removed with either a wash or the rapid centrifugation through an oil preparation designed to maintain low affinity interactions (Sivaprasadarao and Findlay, 1988b). The binding assays were performed at 4 °C and room temperature (20 -22 °C) to ensure all possible chances of capturing an interaction. The STRA6 construct contained a HA and StrepII tag on either the N- or C-terminus of STRA6. These epitope tags are necessary for the purification and detection of STRA6. Both constructs were used for pull-down assays to reduce the risk of the epitope tags preventing STRA6 interacting with the MYTH hits.

The MYTH hits, bar PLP2, were all detected in the kidney library screen. STRA6 is expressed in its native form in HEK293T cells and thus represents an ideal mammalian expression system for overexpression of the recombinant receptor and the MYTH hits. A number of MYTH hits (PDZK1-IP1, CD63, OCIAD2 and osteopontin) were prioritised due to their cellular location (Kocher et al., 1998), the fact osteopontin is induced by RA (Park et al., 1997, Sodek et al., 2002, Harada et al., 1995) and as OCIAD2 was previously detected in an assay to identify any protein(s) that copurify with STRA6 (unpublished data). These proteins were

expressed with STRA6 in HEK293T cells to ensure that if any intermediate protein or *in vivo* post-translational modification (PTM) was involved, the interaction would be captured.

Despite considerable efforts, the hits obtained in all three screens could not be verified using pull-down experiments. These hits may be false positives or form transient interactions with STRA6, which cannot be captured using pull-down experiments. Interestingly, binding of RBP with its receptor also proved hard to isolate, despite the interaction between STRA6 and RBP being captured in the 1980s (Sivaprasadarao and Findlay, 1988a), it wasn't until 2008 that STRA6 was isolated and identified as the RBP receptor (Kawaguchi et al., 2007). A more specialised approach may be necessary to detect protein interactions for STRA6, aimed at capturing weak or transient interactions. STRA6 was subject to a second assay to identify potential interacting proteins whereby recombinant STRA6 was purified and any bound proteins were identified using mass spectrometer (unpublished data). OCIAD2 was the only MYTH hit detected using both assays. It is not clear why recombinant OCIAD2 did not pull-down with STRA6. The OCIAD2 construct contains a HA epitope tag on its C-terminus but as a small epitope tag (9 amino acids), this is unlikely to prevent the protein interacting with STRA6. Data presented in this thesis would imply that OCIAD2 does not interact with STRA6 despite several attempts and a range of different conditions.

The detection of interacting proteins may require the presence of STRA6 in complex with holo-RBP and CRBP (Berry et al., 2012b). CRBP was not detected in the MYTH, even in the presence of RBP-ROH. Expression of CRBP in HEK293T cells has not been detected previously but CRBP has been shown to be expressed in kidney cells (Kato et al., 1984). Up to 90 % of known interactions were previously shown not to be detected using the traditional yeast two hybrid assay (Causier, 2004), this may explain why CRBP was not detected, or this interacting may be too weak to detect using the MYTH.

CHAPTER 5

THIRD INTRACELLULAR LOOP OF STRA6

5.1 Introduction

STRA6 binds extracellular holo-RBP, facilitates the dissociation of the protein-ligand complex and transfers retinol from the RBP to CRBP. STRA6 thus possesses a transport mechanism that is distinct from that of other transporters of small lipids (Redondo et al., 2008). Furthermore, the function of the protein is more complex than simply delivering retinol to extrahepatic tissues; STRA6 has been implicated in regulating biological activities such as insulin signalling and lipid metabolism (Berry et al., 2012b). STRA6 catalyses not only retinol influx but also efflux and exchange dependent on the presence of RBP and CRBP (Sivaprasadarao and Findlay, 1988b), (Kawaguchi et al., 2012). These observations raise important questions relating to the structural bases that underlie STRA6's functions.

Resolution of the 3-dimensional structure of the receptor will help elucidate the conformational switches that accompany retinol exchange between RBP and CRBP and shed light on the mechanisms by which transfer of retinol through the transporter triggers STRA6 signalling but as yet, this has not been accomplished. Characterisation of membrane proteins is challenging due to the protein's hydrophobic surfaces, flexibility and lack of stability, leading to challenges at all levels, including expression, solubilisation, purification, crystallisation, data collection and structure solution. Currently, there are over 50,000 entries in the PDB repository of protein structures, but less than 1 % of these entries represent membrane proteins (Carpenter et al., 2008). Alternative ways in which to gain structural, and thereby functional, insight are, therefore, often necessary. To date, only the transmembrane topology of STRA6 is known (illustrated in Figure 5.1).

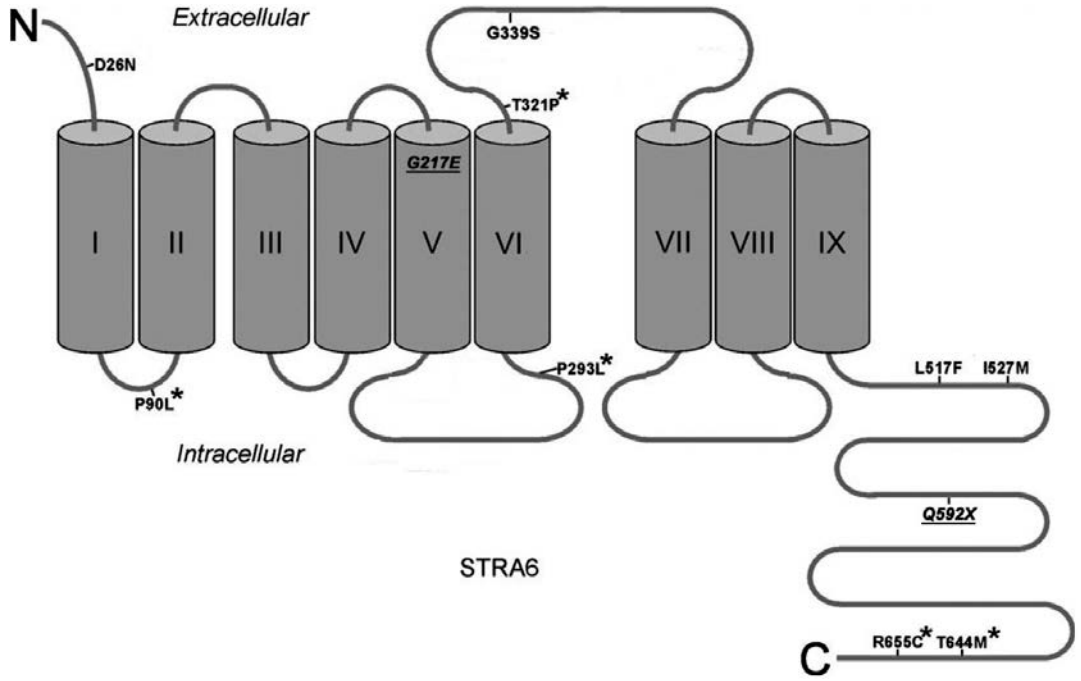

Figure 5.1: Transmembrane Topology Model of STRA6. Taken from (White et al., 2008)

STRA6's transmembrane topology (Kawaguchi et al., 2008b) with naturally occurring STRA6 mutations highlighted. Underlined sequence variants were recently identified (White et al., 2008). The nonsense sequence variant at amino acid 592 causes a premature stop codon on the COOH-terminus end of the STRA6 protein. Previously discovered sequence variants marked with asterisks are involved in human disease (Pasutto et al., 2007). Other sequence variants are missense mutations annotated in the GenBank database, and are not currently known to be associated with human disease (White et al., 2008).

Although computer programs predict 11 transmembrane domains for STRA6, its topology has been studied experimentally to suggest 9 transmembrane segments. This was achieved by inserting an epitope tag into all potential extracellular and intracellular domains of STRA6. The accessibility of each tag on the surface of live cells, the accessibility of each tag in permeabilized cells, and the effect of each tag on RBP binding and STRA6-mediated retinol uptake from the retinol-RBP complex was assessed. In addition, a new lysine accessibility technique combining cell-surface biotinylation and tandem-affinity purification to study a region of the protein not revealed by the epitope tagging method was used. These studies not only revealed STRA6's extracellular, transmembrane, and intracellular domains but also implicated extracellular regions of STRA6 in RBP binding (Kawaguchi et al., 2008b).

The identification of a putative RBP-binding domain in the third extracellular loop region of STRA6 (V^{319} through L^{362}), by mutation of residues Y^{335}, G^{339} and G^{341} (Kawaguchi et al., 2008a), was the first observation made regarding experimentally determined structure-function relationships of the RBP receptor. More recently, the predicted large third intracellular loop (ICL3) of STRA6 has been suggested to be involved in binding CRBP (Berry et al., 2012b) and due to its large size, is a potential candidate for interactions within the receptor itself as well as with other proteins. As illustrated in Figure 5.2, STRA6-ICL3 is highly conserved. The importance of STRA6-ICL3 has been further enhanced by the discovery of human polymorphism P293L, associated with severe multisystem birth defects (Pasutto et al., 2007). STRA6-ICL3 was extracted from the full length protein and characterised in the hope of gaining insights into STRA6's architecture and function, with particular attention to the binding of CRBP and the C-terminus of STRA6.

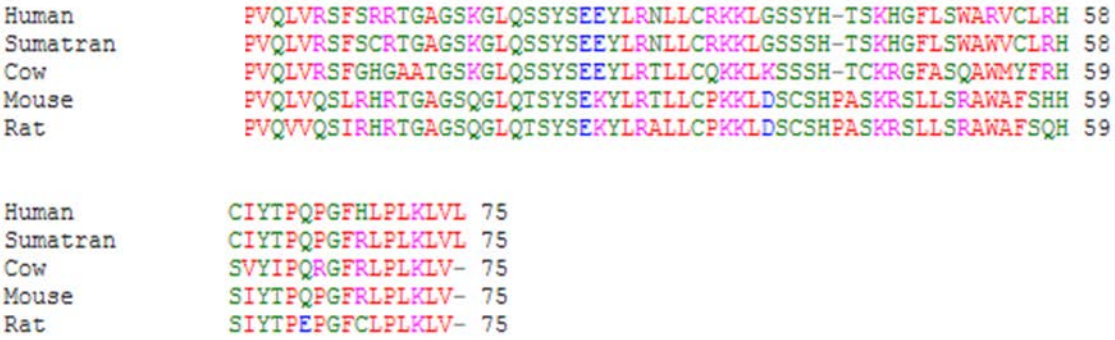

Figure 5.2: Conserved Sequence of STRA6-ICL3

Multiple sequence alignment using CLUSTAL 2.1 (Goujon et al., 2010). STRA6-ICL3 (amino acids 224-298) sequence aligned for human, sumatran orangutang, cow, mouse and rat (Uniport Q9BX79, Q5R7B4, Q0V8E7, O70491, Q4QR83 respectively). As illustrated, STRA6-ICL3 is highly conserved.

Characterisation of STRA6-ICL3 was achieved using a number of techniques; size-exclusion chromatography (SEC) and SDS-PAGE to determine oligomeric size and circular dichroism (CD) in combination with the secondary structure prediction server Jpred to elucidate secondary structure. Functionality was explored using pull-down assays to determine if STRA6-ICL3 does in fact bind CRBP. The binding activity for the C-terminus of STRA6 (L^{535}-P^{667}) was also determined. Finally, crystallisation of STRA6-ICL3 was attempted.

Proteins often self-associate to oligomers for specific purposes. For newly identified proteins, such as STRA6, it is often unknown whether the protein exists in solution as a monomer, dimer, or other oligomer. Therefore, determining the molecular weight of a protein is an important step in understanding how it functions. Empirical techniques such as SEC and SDS-PAGE have been employed for protein molecular weight determination. SEC is a simple, fast and robust method for estimating the molecular weight of a protein in its native form, based on its elution position, and for monitoring protein oligomerization (Hong et al., 2012). The elucidation of the oligomeric size of STRA6-ICL3 may shed light on the oligomeric status of the full-length protein and on the location of any putative oligomerization site(s).

The protein's secondary structure was explored using CD and Jpred. CD is a convenient and widely used spectroscopic technique that can be used to determine the secondary structural content of proteins and can give an indication as to whether the protein is folded. This is because the electronic transitions of polypeptide backbone peptide bonds in different conformations produce differential absorption spectra for left- and right-handed circularly polarized light in the far UV and vacuum UV wavelength ranges, which are both distinct and linearly independent. The information contained in CD spectra can be treated as a sum of the characteristic individual spectra arising from each type of secondary structure present in a protein sample. Empirical analysis methods usually utilize a reference database comprised of spectra of proteins whose crystal structures (and therefore their secondary structures) are known. Using singular value deconvolutions, principal component analyses, variable selection procedures or neural networks, the fraction that each component structure contributes to the net experimental spectrum can be determined (Whitmore

and Wallace, 2004). Jpred, a secondary structure prediction server that is a well-used and accurate source of predicted secondary structure was also used (Cole et al., 2008).

Proteins function through interactions with other proteins in a highly specific manner and therefore, knowledge of how they interact is fundamental for any understanding of their function. Owing to evidence thus far that STRA6 may in fact also be a receptor for the intracellular RBP homologue, CRBP (Redondo et al., 2008), it is reasonable to suppose that STRA6-ICL3 may exhibit some interaction with CRBP. This possible interaction was explored using pull-down assays. The intracellular cytoplasmic tail of STRA6 is unusually large; lending plausibility to interaction within the protein itself. For this reason, the C-terminus of STRA6 (STRA6-CT) was expressed and the STRA6-CT binding activity of STRA6-ICL3 explored.

X-ray crystallography is the method of choice for determining high-resolution structures of proteins. Structures of membrane proteins determined using X-ray crystallography highlight all the atomic details of the protein and also show any bound water, lipid and detergent molecules. However, despite protein crystallography being a well-established method, solving the structures of membrane proteins remains very challenging. Crystallisation of water-soluble domains which may fold independently, such as STRA6-ICL3, therefore, represents a realistic approach to generating structural and functional insights into the full length protein (Lacapère et al., 2007).

Aims and Objectives

The aim was to characterise STRA6-ICL3. This region was expressed, purified and characterised as a chimera with a stabilising protein, the *E.coli* colicin E7 immunity protein (Im7, also known as IMME7). Im7 is a 87-residue (Hosse et al., 2006), monomeric (Dennis et al., 1998), scaffold protein. The protein is composed of four anti-parallel α-helices wrapped around a central hydrophobic core, as illustrated in Figure 5.3, which stabilises folding of the soluble protein. There are exposed connecting loops which, from other studies, can be derivatised without affecting the overall fold. Im7 is an ideal protein scaffold due to its small size, robust helical structure, tolerance to extensive loop substitutions and ease of expression, active and in large amount using E.coli systems.

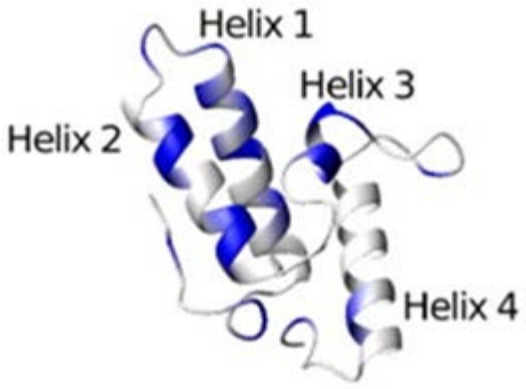

Figure 5.3: Structure of Im7. Taken from (Whittaker et al., 2007)

Structure of Im7 (PDB code 1AYI). The coding sequence for STRA6-ICL3 (P224 – L298) was grafted onto Im7 between helices I and II (Val^{27} through Asp^{32}) (Whittaker et al., 2007).

It has been demonstrated that Im7 is tolerant to loop exchange between helices I and II (Val^{27} through Asp^{32}) (Juraja et al., 2006). Therefore, the coding sequence for STRA6-ICL3 (P224 – L298) was grafted into Im7 between these two helices to aid folding, solubility and stability of the expressed protein and to anchor the domain as it might be in its native state. Chimeric loop STRA6-ICL3, in the *E. coli* expression vector pETd9, was a kind gift from Dr. Conor Breen and was designed to incorporate an N-terminal 6xHis tag; purification of the domain was therefore reliant upon affinity chromatography using Ni-NTA agarose.

This chapter describes the characterisation of STRA6-ICL3 using a number of techniques including, SEC and SDS-PAGE to determine oligomeric size, CD to elucidate secondary structure and pull-down assays to determine if STRA6-ICL3 does in fact bind CRBP and/or STRA6-CT. Crystallisation of STRA6-ICL3 is also being attempted.

5.2 Materials and Methods

5.2.1 Expression of STRA6-ICL3

5.2.1.1 Construct Design

The third intracellular loop of STRA6 (P224 – L298) was grafted onto Im7 between helices I and II (Val^{27} through Asp^{32}) and inserted into *E.coli* expression vector pET9d. The construct was a kind gift from Dr. Conor Breen. Im7, in the *E.coli* expression vector pTRC99a with restriction sites but not STRA6-ICL3, was a kind gift from Dr. Werner Vos

5.2.1.2 Selection of Growth Medium for STRA6-ICL3 Expression

BL21(DES) cells previously transformed with the STRA6-ICL3 construct were streaked onto a LB agar plate containing 50 µg/mL kanamycin and incubated overnight at 37 °C. Single colonies were used to inoculate 10 mL terrific broth (TB) medium (12 g/L tryptone, 24 g/L yeast extract, 4 ml/L glycerol, 12.5 g/L potassium diphosphate, 2.3 g/L potassium phosphate, pH 7.0), 10 mL LB medium or 10 ml super LB broth (SB) medium (32 g/L peptone, 20 g/L yeast extract, 5 g/L NaCl, pH 7.0) and incubated overnight at 37 °C, with shaking (225-250 rpm).

Following overnight growth, each culture (LB, TB or SB) was split into two cultures (1:50 dilution in fresh medium) and grown overnight at room temperature (20-22 °C) and 37 °C, with shaking (225-250 rpm).

The cultures were centrifuged (4,000 g for 15 minutes at 4 °C), the supernatants discarded and the pellets resuspended in cold wash buffer (300 mM Na_2HPO_4, 300 mM NaCl). Centrifugation was repeated and again the supernatants discarded. Cell pellets weight was noted and used to assess the most favourable medium and temperature for the growth of STRA6-ICL3.

5.2.1.3 Un-induced and IPTG-Induced Expression of STRA6-ICL3 in *E.coli*

BL21(DES) cells expressing STRA6-ICL3 were streaked on an LB agar plate containing 50 µg/mL kanamycin and a single colony used to inoculate 10 mL TB medium and incubated overnight at 37 °C with shaking (225-250 rpm).

Following overnight growth, the culture was divided in two (diluted 1:100 into fresh medium) and grown to an OD_{600} of 0.6 to 0.8 at room temperature (20-22 °C). Protein expression was subsequently induced by the addition of 0.1 mM IPTG in one culture and left un-induced in the second culture. Growth continued overnight at room temperature (20-22 °C), with shaking (225-250 rpm).

The cultures were centrifuged (4,000 g for 15 minutes at 4 °C), the supernatants discarded and the pellets resuspended in cold wash buffer (300 mM Na_2HPO_4, 300 mM NaCl). Centrifugation was repeated and again the supernatants discarded. Cell pellets were resuspended in 3-5 ml of lysis buffer (300mM Na_2HPO_4, 300 mM NaCl, 1x EDTA-free protease inhibitor cocktail, 1 mM TCEP, 1 mM PMSF, 10 mM β-mercaptoethanol 1 % Triton X-100, 1 mg/ml lysozyme) per gram of wet cell pellet. Resuspension and lysis of the cells was facilitated by passing the resuspended pellet through an 18-gauge needle fitted to a 20 ml syringe. Once resuspended, the cells were incubated at 4 °C for 1 hour with constant agitation. The sample was then sonicated at 15 % power for 1 minute. The sonication was repeated three times with 1 minute breaks. Following sonication, the samples were passed through a 25-gauge needle fitted to a 20 ml syringe until no longer viscous. The samples were then centrifuged (12,000 g for 20 minutes at 4 °C), the supernatants harvested, the volume of the supernatants noted and the pellets discarded. Protein expression for both the induced and un-induced culture was determined by SDS-PAGE and Western blotting.

5.2.1.4 Buffer Selection for the Lysis of STRA6-ICL3 Expressing Cells

BL21(DES) cells expressing STRA6-ICL3 were streaked onto an LB agar plate containing 50 µg/mL kanamycin and a single colony used to inoculate 10 mL TB medium and incubated overnight at 37 °C with shaking (225-250 rpm).

Following overnight growth, the culture was diluted (1:100) into fresh medium and grown at room temperature (20-22 °C) with shaking (225-250 rpm) overnight, to an OD_{600} of ~ 2.8. The culture was centrifuged (4,000 g for 15 minutes at 4 °C), the supernatant discarded and the pellet resuspended in cold wash buffer. Centrifugation was repeated and again the supernatant discarded. The cell pellet was divided and resuspended in a range of different lysis buffers (3 ml/ g pellet), with varying pH, detergent type, salt type and salt concentration. Resuspension and lysis of the cells was facilitated by passing the resuspended pellets through an 18-gauge needle fitted to a 20 ml syringe. Once resuspended, the cells were incubated at 4 °C for 1 hour with constant agitation. The samples were then sonicated at 15 % power for 1 minute. The sonication was repeated three times with 1 minute breaks. Following sonication, the samples were passed through a 25-gauge needle fitted to a 20 ml syringe until no longer viscous. The samples were then centrifuged (12,000 g for 20 minutes at 4 °C) and the soluble fractions isolated. Protein solubility was determined by SDS-PAGE and Western blotting. 200 µl of the supernatants were also added to a 96 well plate and stored at room temperature for 5 days. The 96 well plate was incubated at 37 °C for a following 4 days. The OD_{600} was read at a number of time points and the lysis buffer with the least aggregation determined.

5.2.1.5 Expression and Purification of STRA6-ICL3

BL21(DES) cells expressing STRA6-ICL3 were streaked onto an LB agar plate containing 50 µg/mL kanamycin and a single colony used to inoculate 10 mL TB medium and incubated overnight at 37 °C, with shaking (225-250 rpm).

Following overnight growth, the culture was diluted (1:100) into fresh medium and grown at room temperature (20-22 °C) with shaking (225-250 rpm) overnight, to an

OD_{600} of ~ 2.8. The culture was centrifuged (4,000 g for 15 minutes at 4 °C), the supernatant discarded and the pellet resuspended in cold wash buffer. Centrifugation was repeated and again the supernatant discarded. The cell pellet was stored at -80 °C or continued onto lysis and purification.

The cell pellet was resuspended in 3-5 ml of lysis buffer A (100 mM Tris, 50 mM NaCl, pH 8.5, 1 % N,N-Dimethyldodecylamine N-oxide (LDAO), 20 % glycerol, 1x EDTA-free protease inhibitor cocktail, 1 mM TCEP, 1 mM PMSF, 10 mM β-mercaptoethanol, 1 mg/ml lysozyme) per gram of wet cell pellet. Resuspension and lysis of the cells was facilitated by passing the resuspended pellet through an 18-gauge needle fitted to a 20 ml syringe. Once resuspended, the cells were incubated at 4 °C for 1 hour with constant agitation. The sample was then sonicated at 15 % power for 1 minute. The sonication was repeated three times with 1 minute breaks. Following sonication, the sample was passed through a 25-gauge needle fitted to a 20 ml syringe until no longer viscous. The sample was then centrifuged (12,000 g for 20 minutes at 4 °C). Following centrifugation, the supernatant was harvested, the volume of the supernatant noted and the pellet discarded.

1.0 ml Ni-NTA agarose was pre-equilibrated in column binding buffer (100 mM Tris, 50 mM NaCl, pH 8.5, 0.5 % LDAO, 2.7 g/L imidazole, 20 % glycerol) before being added to the solubilised pellet and incubated for 90 minutes at 4 °C under gentle agitation by rotation. The mixture was added to a 5 ml column at 4 °C. The resin was allowed to settle and the flow-through was collected. The column was washed by the addition of wash buffer 1 (100 mM Tris, 1 M NaCl, pH 8.5, 0.5 % LDAO, 2.7 g/L imidazole, 20 % glycerol) and wash buffer 2 (100 mM Tris, 50 mM NaCl, pH 8.5, 0.5 % LDAO, 4 g/L imidazole, 20 % glycerol) (5 mL per 1 mL bed volume). The protein was eluted from the resin by the addition of 5 ml of elution buffer (100 mM Tris, 50 mM NaCl, pH 8.5, 0.5 % LDAO, 17 g/L imidazole, 20 % glycerol) to the column. Protein was dialysed against dialysis buffer (100 mM Tris, 50 mM NaCl, pH 8.5, 0.5 % LDAO, 20 % glycerol) overnight at 4 °C to remove imidazole and the protein concentrated. Protein expression, solubility and purity were analysed by Coomassie Brilliant Blue staining of SDS-PAGE gels and Western blotting.

5.2.2 Expression and Purification of Im7

BL21(DES) cells expressing Im7 were streaked onto an LB agar plate containing 50 µg/mL ampicillin and a single colony used to inoculate 10 mL TB medium and incubated overnight at 37 °C, with shaking (225-250 rpm).

Following overnight growth, the culture was diluted 1:100 into fresh medium and grown to an OD_{600} of 0.6 to 0.8 at room temperature (20-22 °C) with shaking (225-250 rpm). Expression was induced using 0.1 mM IPTG. Growth continued overnight, to an OD_{600} of ~ 2.8, at room temperature (20-22 °C), with shaking (225-250 rpm). The culture was centrifuged (4,000 g for 15 minutes at 4 °C), the supernatant discarded and the pellet resuspended in cold wash buffer. Centrifugation was repeated and again the supernatant discarded. The cell pellet was stored at -80 °C or continued into lysis and purification.

The cell pellet was resuspended in 3-5 ml of lysis buffer A per gram of wet cell pellet. Resuspension and lysis of the cells was facilitated by passing the resuspended pellet through an 18-gauge needle fitted to a 20 ml syringe. Once resuspended, the cells were incubated at 4 °C for 1 hour with constant agitation. The sample was then sonicated at 15 % power for 1 minute. The sonication was repeated three times with 1 minute breaks. Following sonication, the sample was passed through a 25-gauge needle fitted to a 20 ml syringe until no longer viscous. The sample was then centrifuged (12,000 g for 20 minutes at 4 °C). Following centrifugation, the supernatant was harvested, the volume of the supernatant noted and the pellet discarded.

1.0 ml Ni-NTA agarose was pre-equilibrated in column binding buffer before being added to the solubilised pellet and incubated for 90 minutes at 4 °C under gentle agitation by rotation. The mixture was added to a 5 ml column at 4 °C. The resin was allowed to settle and the flow-through was collected. The column was washed by the addition of wash buffer 1 and wash buffer 2 (5 mL per 1 mL bed volume). The protein was eluted from the resin by the addition of 5 ml of elution buffer to the

column. Protein was dialysed against dialysis buffer overnight at 4 °C to remove imidazole and the protein concentrated. Protein expression, solubility and purity were analysed by Coomassie Brilliant Blue staining of SDS-PAGE gels and Western blotting.

5.2.3 Expression, Purification and Cleavage of CRBP

5.2.3.1 Expression and Purification of CRBP

CRBP (UniProt entry P09455) in the GST gene fusion expression vector, pGEX-4T-3 was a kind gift from Dr. Lyndsey Brown

BL21(DES) cells expressing CRBP were streaked onto an LB agar plate containing 50 µg/mL kanamycin and incubated overnight at 37 °C. A single colony was used to inoculate 100 mL LB medium and incubated overnight at 37 °C, with shaking (225-250 rpm). Following overnight growth, the cultures was diluted (1:100) into fresh medium and grown to an OD_{600} of 0.6 to 0.8. Protein expression was subsequently induced by the addition of 0.1 mM IPTG and growth continued for 4 hours at room temperature (20-22 °C), with shaking (225-250 rpm). The culture was centrifuged (4,000 g for 15 minutes at 4 °C), the supernatant was discarded and the pellet resuspended in cold wash buffer. Centrifugation was repeated and again the supernatant discarded. The cell pellet was stored at -80 °C or continued into lysis and purification.

The cell pellet was resuspended in 3-5 ml of lysis buffer I (1x PBS, 1 % Triton X-100, 1x EDTA-free protease inhibitor cocktail, 1 mM TCEP, 1 mM PMSF, 10 mM *β*-mercaptoethanol, 1 mg/ml lysozyme) per gram of wet cell pellet. Resuspension and lysis of the cells was facilitated by passing the resuspended pellet through an 18-gauge needle fitted to a 20 ml syringe. Once resuspended, the cells were incubated at 4 °C for 1 hour with constant agitation. The sample was then sonicated at 15 % power for 1 minute. The sonication was repeated three times with 1 minute breaks. Following sonication, the sample was passed through a 25-gauge needle fitted to a 20 ml syringe until no longer viscous. The sample was then centrifuged (12,000 g

for 20 minutes at 4 °C). Following centrifugation, the supernatant was harvested, the volume of the supernatant noted and the pellet discarded. The soluble fraction was incubated overnight at 4 °C with Glutathione Sepharose™ 4 Fast Flow under gentle agitation by rotation. Following this incubation period, the cell lysate slurry mix was packed into a 5 mL disposable column and the flow-through collected. The sedimented Sepharose was then washed by the addition of ice-cold PBS (5 mL per 1 mL bed volume). Protein was either eluted from the resin using 5 ml elution buffer B (3 g/L glutathione, 6 g/L Tris-HCl, pH 8.0) or kept on the resin for cleavage. Samples were taken for subsequent analysis by Coomassie Brilliant Blue staining of SDS-PAGE gels and Western blotting.

5.2.3.2 Cleavage of CRBP

Following column packing as described previously, the Sepharose with bound fusion protein was washed in ten bed volumes of ice-cold PBS. A thrombin mix (80 U/mL of starting bed volume in PBS) was then loaded directly onto the column, prior to incubation at room temperature (20-22 °C) overnight. The cleaved protein was subsequently eluted from the resin with three bed volumes of ice-cold PBS. The flow-through containing CRBP and thrombin was then applied to Benzamidine Sepharose™ 6B slurry, prepared according to the manufacturer's instructions and incubated for a minimum of one hour at 4 °C, under gentle agitation by rotation, in order to remove the protease. The flow-through, containing the fusion protein only, was then reapplied to pre-washed 50 % slurry of Glutathione Sepharose™ 4 Fast Flow in order to remove any residual GST.

5.2.4 Expression and Purification of STRA6-CT

The coding sequence of the C-terminal region of STRA6 (L^{535}-P^{667}), in the GST gene fusion expression vector pGEX-4T-3 along with a C-terminus 6xHis epitope tag was a kind gift from Dr. Lyndsey Brown

For expression and purification details refer to 5.2.3.1.

5.2.5 CRBP Binding Activity of STRA6-ICL3

5.2.5.1 CRBP Binding Activity of STRA6-ICL3 with Washing

STRA6-ICL3 was expressed in BL21(DES) cells as described in 5.2.1.5. The soluble bacterial lysate, ~ 5 µg of protein, was immobilised on a Ni-NTA agarose under gentle agitation by rotation, for 90 minutes at room temperature (20-22 °C). Ni-NTA agarose with no protein bound was used as a negative control. The resins were washed twice with 200µl wash buffer (100 mM Tris, 50 mM NaCl, 0.5 % LDAO, 20 % glycerol, pH 8.5), centrifuged (700 g for 3 minutes) and the washes collected. Cleaved CRBP, ~ 5 µg of protein, +/- 0.5 µM retinol was incubated with the resins for 30 minutes at room temperature (20-22 °C). The resins were centrifuged (700 g for 5 minutes) and any nonspecifically bound proteins collected. The resins were incubated with elution buffer (100 mM Tris, 50 mM NaCl, 0.5 % LDAO, 17 g/L imidazole, 20 % glycerol, pH 8.5) for 5 minutes, the resins centrifuged (700 g for 3 minutes) and the eluates collected. Samples were analysed by SDS-PAGE and Western blotting to ascertain the presence of any bound CRBP.

5.2.5.2 CRBP Binding Activity of STRA6-ICL3 without Washing

Protein: protein interactions were probed using a pull-down assay adapted to accommodate the low affinity binding of STRA6-ICL3 to CRBP. A 3:2 dibutyl phthalate: dinonyl phthalate preparation has a combined density of ~ 1.09 g/mL, whereas Ni-NTA agarose is of higher density and free CRBP of lower density than the oil mix, resulting in separation of CRBP in solution from CRBP bound to STRA6-ICL3 immobilised using Ni-NTA agarose.

STRA6-ICL3 was expressed in BL21(DES) cells as described in 5.2.1.5. The soluble bacterial lysates, ~ 5 µg of protein, was immobilised on Ni-NTA agarose under gentle agitation by rotation, for 90 minutes at room temperature (20-22 °C). Ni-NTA agarose with no protein bound was used as a negative control. The resins were

washed twice with 200µl wash buffer. The resins were centrifuged (700 g for 3 minutes) and the washes collected. Cleaved CRBP, ~ 5 µg of protein, +/- 0.5 µM retinol was incubated with the resins for 30 minutes at room temperature (20-22 °C). Following incubation, reactions were carefully resuspended prior to rapid centrifugation (6,800 g for 5 minutes) through an oil layer to separate the aqueous, oil and agarose layers. The pellets were incubated with 2x SDS sample buffer for 10 minutes at 70 °C. Samples were analysed by SDS-PAGE and Western blotting to ascertain the presence of any bound CRBP.

5.2.6 STRA6-CT Binding Activity of STRA6-ICL3

5.2.6.1 STRA6-CT Binding Activity of STRA6-ICL3 with Washing

STRA6-CT was expressed in BL21(DES) cells as described in 5.2.4. The soluble bacterial lysate, ~ 5 µg of protein, was immobilised on Glutathione Sepharose™ 4 Fast Flow resin under gentle agitation by rotation, for 90 minutes at room temperature (20-22 °C). Glutathione Sepharose™ 4 Fast Flow resin with no protein bound was used as a negative control. The resins were washed twice with 200µl PBS, centrifuged (700 g for 3 minutes) and the washes collected. STRA6-ICL3, ~ 5 µg of protein, was incubated with the resins for 30 minutes at room temperature (20-22 °C). The resins were centrifuged (700 g for 5 minutes) and any nonspecifically bound proteins collected. The resins were incubated with elution buffer for 5 minutes, the resins centrifuged (700 g for 3 minutes) and the eluates collected. Samples were analysed by SDS-PAGE and Western blotting to ascertain the presence of any bound STRA6-ICL3. The binding assay was repeated in the presence of 0.5 µM retinol.

5.2.6.2 STRA6-CT Binding Activity of STRA6-ICL3 without Washing

Protein: protein interactions were probed using a pull-down assay adapted to accommodate the low affinity binding of STRA6-ICL3 to STRA6-CT. A 3:2 dibutyl

phthalate: dinonyl phthalate preparation has a combined density of ~ 1.09 g/mL, whereas Glutathione Sepharose™ 4 Fast Flow is of higher density and free STRA6-ICL3 of lower density than the oil mix, resulting in separation of STRA6-ICL3 in solution from STRA6-ICL3 bound to STRA6-CT immobilised using Glutathione Sepharose™ 4 Fast Flow.

STRA6-CT was expressed in BL21(DES) cells as described in 5.2.4. The soluble bacterial lysate, ~ 5 µg of protein, was immobilised on Glutathione Sepharose™ 4 Fast Flow resin under gentle agitation by rotation, for 90 minutes at room temperature (20-22 °C). Glutathione Sepharose™ 4 Fast Flow resin with no protein bound was used as a negative control. The resins were washed twice with 200µl PBS, centrifuged (700 g for 3 minutes) and the washes collected. STRA6-ICL3, ~ 5 µg of protein, was incubated with the resins for 30 minutes at room temperature (20-22 °C). Following incubation, reactions were carefully resuspended prior to rapid centrifugation (6,800 g for 5 minutes) through an oil layer to separate the aqueous, oil and agarose layers. The pellets were incubated with 2x SDS sample buffer for 10 minutes at 70 °C. Samples were analysed by SDS-PAGE and Western blotting to ascertain the presence of any bound STRA6-ICL3. The binding assay was repeated in the presence of 0.5 µM retinol.

5.2.7 Size-Exclusion Chromatography

5.2.7.1 STRA6-ICL3 Subjected to Size-Exclusion Chromatography

STRA6-ICL3 was expressed and purified as in 5.2.1.5. Purified STRA6-ICL3 was concentrated (to approximately 10 mg/ml) and centrifuged to remove any precipitation (12,000 g for 20 minutes at 4 °C) and subsequently chromatographed on gel filtration medium Superdex 200 (GE healthcare). The column was first equilibrated with several column volumes of dialysis buffer before the addition of 0.5 ml STRA6-ICL3. The flow rate of the column was 0.3 ml/min. Fractions (0.5 ml) were collected and analysed by SDS-PAGE and Western blotting. β-amylase, alcohol dehydrogenase, BSA and carbonic anhydrase were chromatographed on the

same column under identical conditions to serve as molecular weight markers. The UV absorbance was measured at 280, 254 and 215 nm.

5.2.7.2 Im7 Subjected to Size-Exclusion Chromatography

Im7 was expressed and purified as in 5.2.2. Purified Im7 was concentrated (to approximately 10 mg/ml), centrifuged to remove any precipitation (12,000 g for 20 minutes at 4 °C) and subsequently chromatographed on gel filtration medium Superdex 200. The column was first equilibrated with several column volumes of dialysis buffer before the addition of 0.5 ml Im7. The flow rate of the column was 0.3 ml/min. Fractions (0.5 ml) were collected and analysed by SDS-PAGE and Western blotting. The UV absorbance was measured at 280, 254 and 215 nm.

5.2.8 Circular Dichroism

5.2.8.1 Circular Dichroism Spectra of STRA6-ICL3

STRA6-ICL3 was expressed, purified and subjected to size-exclusion chromatography previous to the recording of the CD spectra. The 14 ml fraction from size-exclusion chromatography was used; the concentration adjusted to 0.2 mg/ml and centrifuged to remove any precipitation (12,000 g for 20 minutes at 4 °C). The far-UV CD spectra were recorded at room temperature (20-22 °C) using a JASCO J715 spectrapolarimeter over the wavelength range 180–280 nm. Spectra were recorded in duplicate and averaged. The percentage of secondary structure was calculated by deconvoluting the CD spectra using the program K2d from the DichroWeb CD secondary structure server [http://dichroweb.cryst.bbk.ac.uk/html/home.shtml (Andrade et al., 1993)]. Recording of the CD spectra was carried out in Leeds University with the help of G. Nasir Khan.

5.2.8.2 Circular Dichroism Spectra of Im7

As in 5.2.8.1, using the 18 ml fraction from size-exclusion chromatography.

5.2.9 Crosslinking of STRA6-ICL3

STRA6-ICL3 was expressed and purified as described in 5.2.1.5. For crosslinking studies, STRA6-ICL3 was dialysed against PBS. STRA6-ICL3 was treated with dimethyl 3, 3′ -dithiobispropionimidate (DTBP). STRA6-ICL3, ~ 5 µg, was incubated with the cross-linking agent, at a 50-fold molar excess in PBS, at room temperature (20-22 °C) for 30 minutes. Reactions were stopped with the addition of 50 mM Tris. The reaction mixture was resolved on an SDS–PAGE gel under reducing conditions using 5x loading buffer and non-reducing conditions, using 5x non-reducing loading buffer [250 mM Tris-HCl, pH 6.8, 50 % (v/v) glycerol, 10 % (w/v) SDS, 0.5 % bromophenol blue] and subsequent analysed by Western blotting.

5.2.10 Crystallisation of STRA6-ICL3

STRA6-ICL3 was expressed, purified and subjected to size-exclusion chromatography. The 14 ml fraction was subsequently used and the concentration adjusted to 10 mg/ml prior to crystallization trials. The sample was centrifuged (12,000 g for 20 min) to remove initial precipitate and was crystallized in a hanging-drop vapour diffusion set-up in 96 well-agar plates. Crystallization was carried out in Leeds University, with the help of Dr. Chi Trinh.

5.2.11 Detection of Protein Expression

In the detection of STRA6-ICL3, Im7 and STRA6-CT; α-His-HRP antibody was used. In the detection of CRBP; α–CRBP and α-mouse-HRP antibodies were used.

5.3 Results

5.3.1 Expression of STRA6-ICL3

5.3.1.1 Selection of Growth Medium for STRA6-ICL3 Expression in *E. coli*

STRA6-ICL3 (P224 – L298) was grafted onto Im7 between helices I and II (Val^{27} through Asp^{32}) and inserted into *E.coli* expression vector pET9d. BL21(DES) cells, transformed with the construct, were used to inoculate TB medium, LB medium or SB medium and cultures grown at room temperature (20-22 °C) or 37 °C. The culture with the largest pellet weight was deemed the most favourable medium and temperature for growth of STRA6-ICL3, TB medium at room temperature (20-22 °C), and was therefore used for future expression.

5.3.1.2 Un-induced and IPTG-Induced Expression of STRA6-ICL3 in *E. coli*

STRA6-ICL3 expression in the presence and absence of IPTG was examined. Appropriate media were inoculated with cells expressing STRA6-ICL3. At an OD_{600} of 0.6 one culture was induced, the other was not. Growth of both cultures continued overnight. Samples of the soluble fractions were taken for subsequent analysis by SDS-PAGE and Western blotting.

STRA6-ICL3 had leaky expression and was detected in the presence and absence of IPTG. However more soluble protein was produced in the absence of IPTG than with 0.1 mM IPTG, as illustrated in Figure 5.4. This may be due to the fact that the induced culture grew slower; cells had an OD_{600} of 1.9 after overnight induction versus an OD_{600} of 2.8 with un-induced expression. After overnight incubation, IPTG-induced cells had a pellet weight of 1.72 g/400 ml versus 5.45 g/400 ml with un-induced expression. Further expression of STRA6-ICL3 was carried out without the use of IPTG.

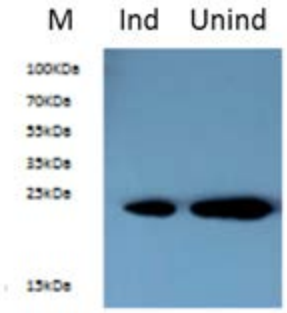

Figure 5.4: IPTG-Induced and Un-induced Expression of STRA6-ICL3

Representative Western blot showing the soluble bacterial lysates (5 µl). STRA6-ICL3 was expressed both in the presence **(Ind)** and absence **(Unind)** of IPTG, cells were lysed and the soluble fractions isolated. Protein was quantified using BCA and 5 µg of protein loaded in each lane. STRA6-ICL3, ~ 19.5 kDa, as detected by α-his-HRP antibody, is present for both induced and un-induced fractions however the un-induced fraction has a higher yield of soluble protein.

5.3.1.3 Buffer Selection for the Lysis of STRA6-ICL3 Expressing Cells

STRA6-ICL3 was expressed in BL21(DES) cells. Once the culture reached an OD_{600} of 2.8, the cell pellet was harvested and resuspended in a range of different lysis buffers with varying pH, detergent type, salt type and salt concentrations. In all, 36 buffers were screened. After lysis, the soluble fractions were isolated and analysed using SDS-PAGE and Western blotting.

The soluble fractions were also added to a 96 well plate and stored at room temperature (20-22 °C) for 5 days and subsequently incubated at 37 °C for a following 4 days. The OD_{600} was read at a number of time points, illustrated in Figure 5.5. The STRA6-ICL3 bacterial lysate contained the least amount of aggregates using lysis buffer A and was therefore used for all further experiments.

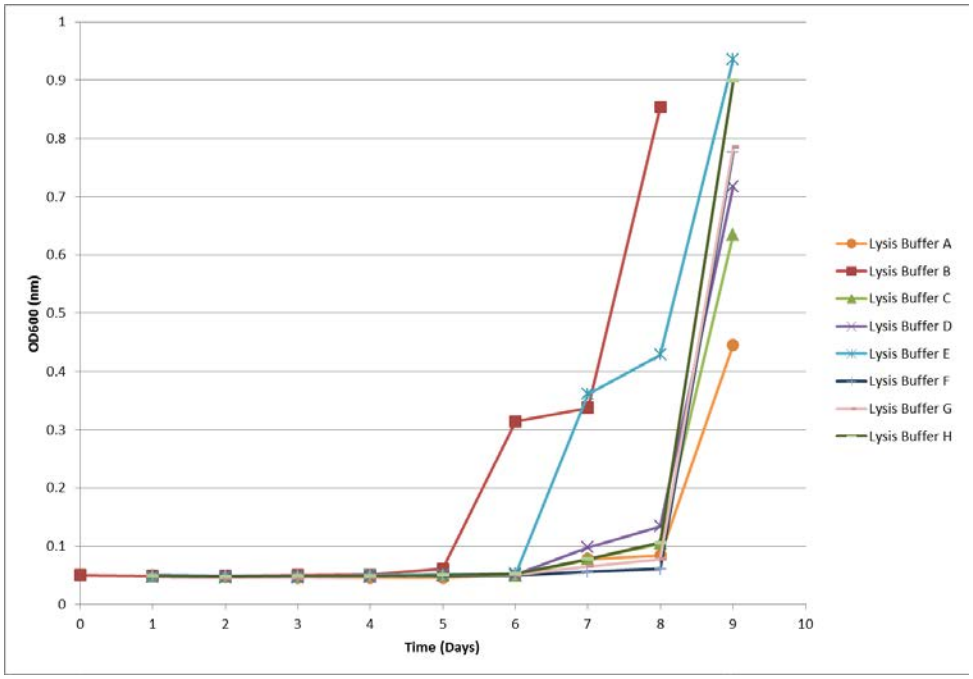

Figure 5.5: Lysis of STRA6-ICL3 and Detection of Aggregation

STRA6-ICL3 expressing bacterial cells were lysed with 36 different buffers and the soluble fractions incubated in a 96 well plate for 5 days at room temperature, followed by 4 day at 37 °C. The OD_{600} was then read. Illustrated here are the OD_{600} readings for 8 different buffers **(Lysis buffers A-H)**. Lysis buffer A (100 mM Tris, 50 mM NaCl, pH 8.5, 1 % LDAO, 20 % glycerol, 1x EDTA-free protease inhibitor cocktail, 1 mM TCEP, 1 mM PMSF and 10 mM β-mercaptoethanol) was found to have the least aggregation. Lysis buffers B-E substituted the 100 mM Tris for 20 mM, 40 mM, 60 mM and 80 mM Tris respectively. Lysis buffers F-H substituted 50 mM NaCl for 75 mM, 100 mM and 125 mM NaCl respectively.

5.3.1.4 Purification of STRA6-ICL3

The large, third intracellular loop of STRA6 was purified via its 6xHis tag using Ni-NTA agarose. Samples were taken for subsequent analysis by Coomassie Brilliant Blue staining of SDS-PAGE gels and Western blotting, illustrated in Figure 5.6. Although a significant amount of the protein of interest bound to the Ni-NTA agarose and was subsequently eluted from the resin in a 5 mL fraction, a small quantity was lost in the second wash. The protein preparation contained some contaminants but the protein of interest was of sufficient purity for downstream application.

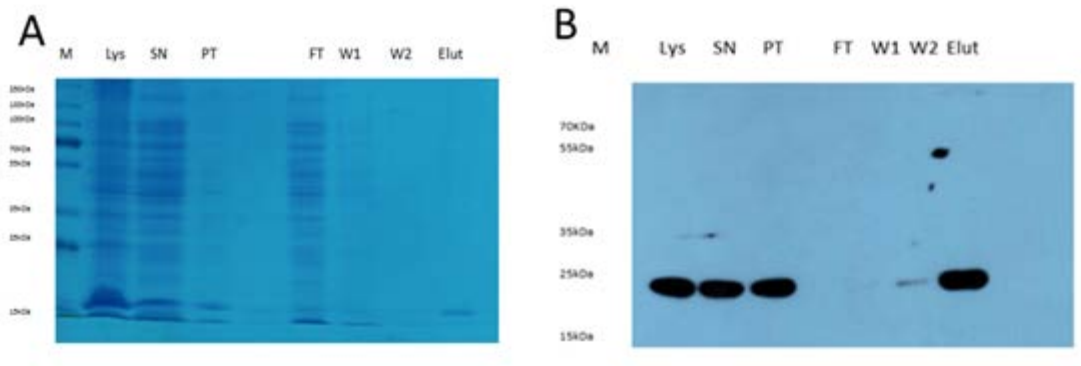

Figure 5.6: Purification of STRA6-ICL3

(A) Coomassie Brilliant Blue stained (12%) SDS-PAGE gel showing the purification of STRA6-ICL3, ~ 19.5 kDa, using Ni-NTA agarose. 5 µl loaded for each fraction. Lysed cells **(LYS)**, soluble fraction after centrifugation **(SN)** and insoluble fraction after centrifugation **(PT)** are shown. The soluble fraction of the cleared bacterial lysate was incubated with Ni-NTA to allow binding of the protein of interest. The flow-through **(FT)** was then collected and the resin washed with wash buffer 1 and 2 **(W1, W2)**, prior to elution from the resin with 0.25 M imidazole **(Elut)**. **(B)** Representative Western blot showing the purification of STRA6-ICL3 using Ni-NTA agarose, as detected by α-his-HRP antibody. STRA6-ICL3 is present in the lysed cells, soluble and insoluble fraction. After purification, STRA6-ICL3 is predominantly present in the eluate, with a small amount of STRA6-ICL3 present in the second wash.

5.3.2 Expression and Purification of Im7

Im7 was expressed in *E.coli*, following induction with IPTG. Im7 was purified via its 6xHis tag by affinity chromatography, using Ni-NTA agarose, as illustrated in Figure 5.7.

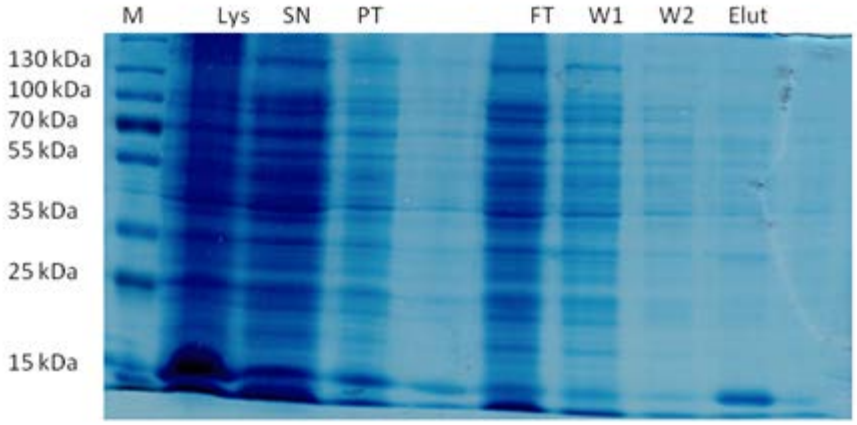

Figure 5.7: Purification of Im7

Coomassie Brilliant Blue stained (12%) SDS-PAGE gel showing the purification of Im7, ~ 10 kDa, using Ni-NTA agarose. 5 µl loaded for each fraction. Lysed cells **(LYS)**, soluble fraction after centrifugation **(SN)** and insoluble fraction after centrifugation **(PT)** are shown. The soluble fraction of the cleared bacterial lysate was incubated with Ni-NTA to allow binding of the protein of interest. The flow-through **(FT)** was then collected and the resin washed with wash buffer 1 and 2 **(W1, W2)**, prior to elution from the resin with 0.25 M imidazole **(Elut)**. After purification, Im7 is predominantly present in the eluate, with little contaminants.

5.3.3 Expression, Purification and Cleavage of CRBP

5.3.3.1 Expression and Purification of CRBP

CRBP was strongly expressed as a fusion protein in pGEX-4T-3, following induction with IPTG. CRBP was purified via its amino-terminal GST-tag using Glutathione Sepharose™ 4 Fast Flow.

5.3.3.2 Cleavage of CRBP

As CRBP was required in its native, untagged form in downstream functional assays, on-column enzymatic cleavage of the GST-tag was necessary. The on-column method was chosen as it allows for removal of contaminants and ultimately, a higher purity end-product.

On column thrombin cleavage of CRBP were analysed by Coomassie Brilliant Blue staining of SDS-PAGE gels and Western blotting. Majority of protein was found to be successfully cleaved.

5.3.4 Expression and Purification of STRA6-CT

STRA6-CT was strongly expressed as a fusion protein in pGEX-4T-3, following induction with IPTG. STRA6-CT was purified via its N-terminus GST epitope tag.

5.3.5 CRBP Binding Activity of STRA6-ICL3

The CRBP binding activity of STRA6-ICL3 was investigated using a traditional wash step or the rapid centrifugation through an oil preparation.

STRA6-ICL3 was immobilised on Ni-NTA agarose and CRBP added in the presence and absence of retinol. After an appropriate incubation, any nonspecifically bound proteins were removed by washing the resin and any bound material eluted from the resin. Alternatively, nonspecifically bound proteins were removed by the rapid centrifugation through oil, a 3:2 dibutyl phthalate: dinonyl phthalate preparation.

This circumvents the wash step of traditional pull-down protocols, allowing even low affinity interactions to be detected.

Each fraction was analysed by SDS-PAGE gels and Western blotting to determine if a specific interaction had occurred, illustrated in Figure 5.8. In both binding assays STRA6-ICL3 was eluted from the resin alone, CRBP was present in the supernatant, indicating that an interaction did not occur. The CRBP binding activity of STRA6-ICL3 in the presence of retinol was also explored. Again, in both binding assays STRA6-ICL3 was eluted from the resin alone, CRBP was present in the supernatant, indicating that an interaction did not occur.

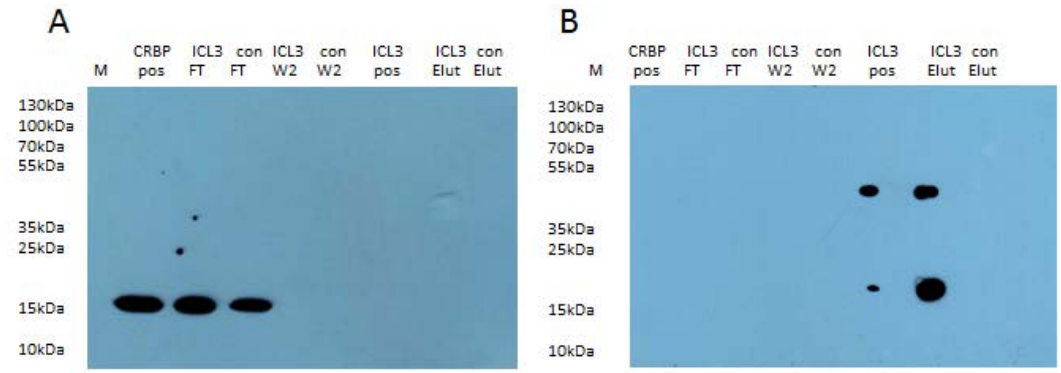

Figure 5.8: CRBP Binding Activity of STRA6-ICL3

STRA6-ICL3, ~ 19.5 kDa, was expressed in *E.coli* and the soluble fraction of the cleared bacterial lysate was incubated with Ni-NTA agarose to allow binding of the protein of interest. CRBP, ~ 17 kDa, was then added to the resin and again incubated. The supernatants **(FT)** were then collected and the resins washed twice **(W2)**, prior to elution **(Elut)**. Empty resin was used as a control **(con)**. Positive controls for both CRBP **(CRBP pos)** and STRA6-ICL3 **(ICL3 pos)** were also run on the gel. 5 µl loaded for each fraction. **(A)** Western blots as detected by α-CRBP and α-mouse-HRP antibodies. CRBP is present in the supernatants indicating an interaction does not occur **(B)** Western blots as detected by α-his-HRP antibody, STRA6-ICL3 is present in the elution. There is the presence of a second higher band, ~ 40 kDa, which may be the dimer form of STRA6-ICL3 which was not fully reduced.

5.3.6 STRA6-CT Binding Activity of STRA6-ICL3

The STRA6-CT binding activity of STRA6-ICL3 was investigated.

STRA6-CT was immobilised on a Glutathione Sepharose™ 4 Fast Flow resin and STRA6-ICL3 added in the presence and absence of retinol. After an appropriate incubation, any nonspecifically bound proteins were removed by washing the resin and any bound material eluted from the resin. Alternatively, any nonspecifically bound proteins were removed by the rapid centrifugation through oil, a 3:2 dibutyl phthalate: dinonyl phthalate preparation. Each fraction was analysed by SDS-PAGE gels and Western blotting to determine if a specific interaction had occurred, illustrated in Figure 5.9. In both binding assays STRA6-CT was eluted from the resin alone, STRA6-ICL3 was present in the supernatant, indicating that an interaction did not occur. The STRA6-CT binding activity of STRA6-ICL3 in the presence of retinol was also explored. Again, in both binding assays STRA6-ICL3 was present in the supernatant, indicating that an interaction did not occur.

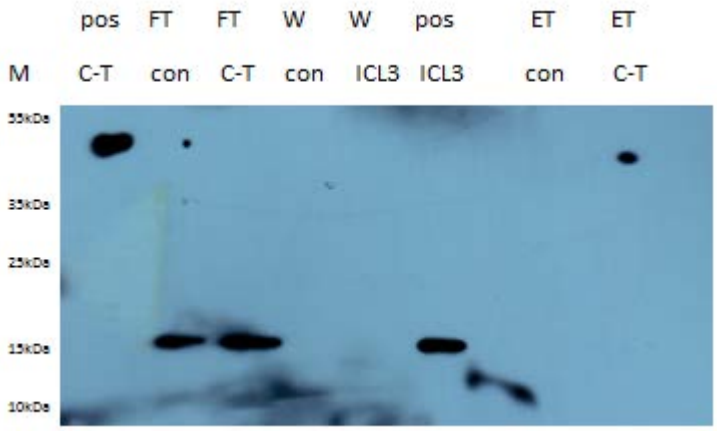

Figure 5.9: STRA6-CT Binding Activity of STRA6-ICL3

STRA6-CT, ~ 42 kDa, was expressed in *E.coli* and immobilised using a Glutathione Sepharose™ 4 Fast Flow resin. Glutathione Sepharose™ 4 Fast Flow resin with no protein bound was used as a negative control **(con)**. STRA6-ICL3 was incubated with the resins. The supernatants **(FT)** were then collected and the resins washed **(W)**, prior to elution **(ET)**. Positive controls for both STRA6-CT **(pos C-T)** and STRA6-ICL3 **(pos ICL3)** were also run on the gel. 5 µl loaded for each fraction. Western blots as detected by α-his-HRP antibody, STRA6-ICL3, ~ 19.5 kDa, is present in the FT whereas STRA6-CT is present in the ET, indicating an interaction does not occur.

5.3.7 Size-Exclusion Chromatography

5.3.7.1 STRA6-ICL3 Subjected to Size-Exclusion Chromatography

STRA6-ICL3 was subjected to size-exclusion chromatography on a Superdex 200 10/300 GL resin, which separates globular proteins with MWs that range from approximately 10 to 600 kD, by fast protein liquid chromatography using an AKTA purifier (GE Healthcare). SEC was carried out at room temperature (20-22 °C) at a flow rate of 0.3 mL/min. The total column volume is approximately 24 mL.

Results of size-exclusion chromatography are illustrated in Figure 5.11. The elution profile of BSA, β-amylase, alcohol dehydrogenase and carbonic anhydrase are illustrated in Figure 5.10. The protein elutes near BSA (molecular weight of 68,000). Analysis by SDS-PAGE and Western blotting of all the fractions resulted in a band for STRA6-ICL3 at 13 ml and 14 ml, indicating that the domain is running as a tetramer (~ 60 kDa).

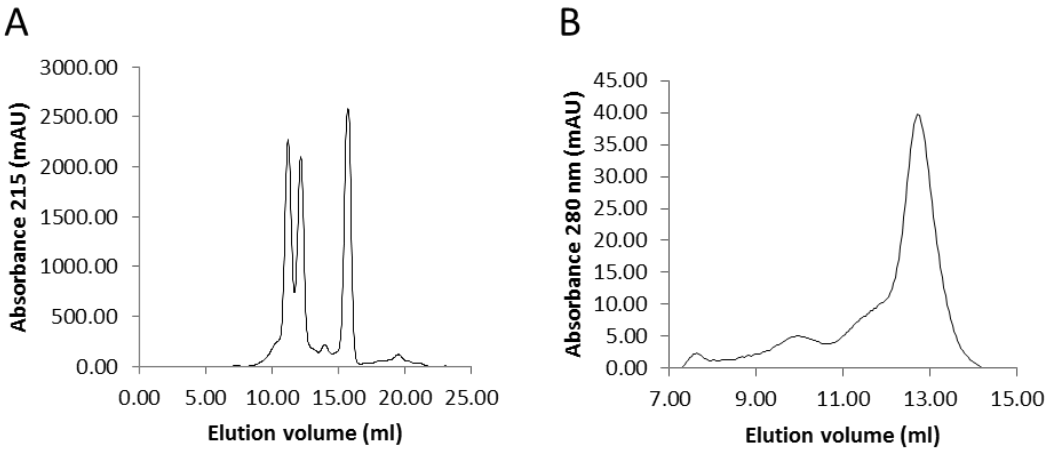

Figure 5.10: Size-Exclusion Chromatography Elution Profile of Calibrants

Elution profile of calibrants. **(A)** Size-exclusion chromatography elution profile of β-amylase, alcohol dehydrogenase and carbonic anhydrase shows three major peaks at ~ 11 ml, ~ 12 ml and ~ 16 ml. These peaks are believed to be β-amylase (200 kDa), alcohol dehydrogenase (150 kDa), and carbonic anhydrase (29 kDa) respectively. **(B)** Size-exclusion chromatography of BSA shows a major peak at ~ 13 ml (68 kDa).

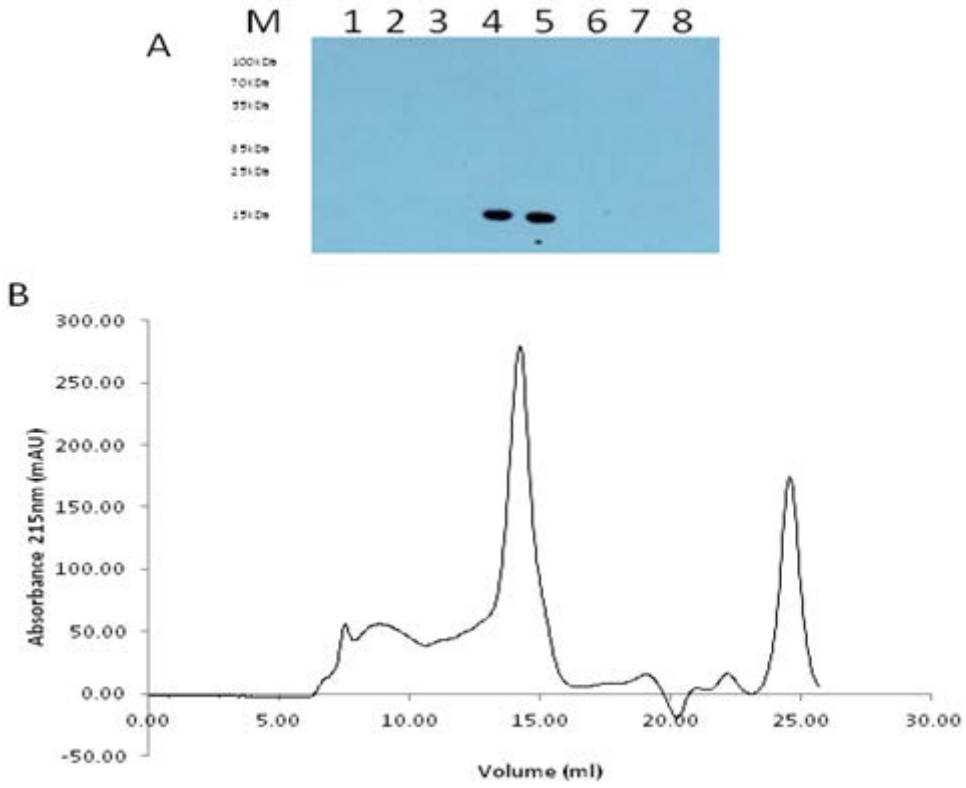

Figure 5.11: Size-Exclusion Chromatography Elution Profile of STRA6-ICL3

Size-exclusion chromatography elution profile of STRA6-ICL3. **(A)** Representative Western blot with eluted fractions (20 µl). Each fraction (0.5 ml) was collected and fractions 10 ml to 17 ml **(1-8)** are shown here. STRA6-ICL3, ~ 19.5 kDa, as detected by α-his-HRP antibody, is present in the 13 ml and 14 ml fraction **(B)** Elution profile of STRA6-ICL3 shows one major peak at ~14 ml (MW of ~ 60 kDa).

5.3.7.2 Im7 Subjected to Size-Exclusion Chromatography

Im7 itself was subjected to size-exclusion chromatography on a Superdex 200 10/300 GL resin by fast protein liquid chromatography using an AKTA purifier.

Results of size-exclusion chromatography of Im7 are given in Figure 5.12. The protein elutes near carbonic anhydrase (molecular weight of 29,000), ~ 16 ml. Analysis by SDS-PAGE and Western blotting of all the fractions resulted in a band for Im7 at 18 ml indicating that the protein is running as a monomer (~ 10 kDa).

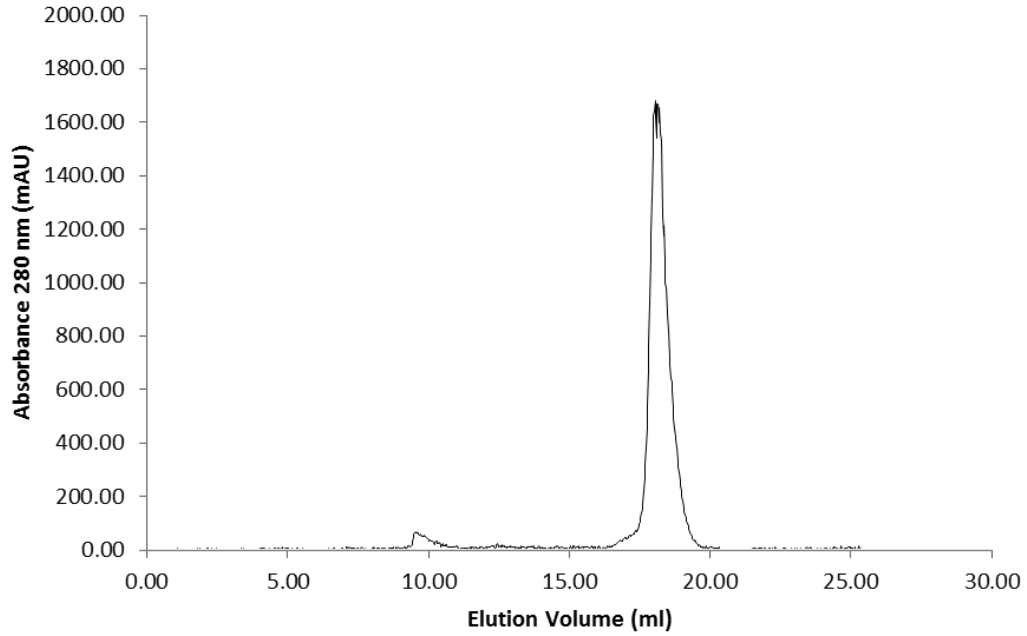

Figure 5.12: Size-Exclusion Chromatography Elution Profile of Im7

Size-exclusion chromatography elution profile of Im7 shows one major peak at ~18ml (MW of ~ 10 kDa)

5.3.8 Circular Dichroism

The structures of some thousands of proteins have been completely resolved by analysing the X-ray diffraction patterns of the crystallized molecule. However, crystallization of a protein is a difficult and not always feasible task. Therefore, techniques for prediction of secondary structure from more readily measurable protein characteristics have been developed. CD is a spectroscopic technique that can be used to determine the secondary structural content of proteins. CD is used also to confirm that expressed proteins are likely to be folded.

The far-UV CD spectra of STRA6-ICL3 and Im7 are shown in Figure 5.12. The percentage of secondary structure was calculated by deconvoluting the CD spectra using the program K2d from the DichroWeb CD secondary structure server (http://dichroweb.cryst.bbk.ac.uk/html/home.shtml (Andrade et al., 1993)). Im7 was found to be composed of 68 % α-helical, 4 % β-sheet and 28 % coil. STRA6-ICL3 was found to be composed of 53 % α-helical, 9 % β-sheet and 38 % coil. STRA6-IC3 decreased the α-helical content when inserted into Im7, thereby implying it is largely composed of β-sheet or random coil.

Jpred (http://www.compbio.dundee.ac.uk/jpred) is a secondary structure prediction server powered by the Jnet algorithm. The recently updated Jnet algorithm provides a three-state (alpha-helix, beta-strand and coil) prediction of secondary structure at an accuracy of 81.5% (Cole et al., 2008). Interestingly, Jpred gave similar findings, with a 14.2 % reduction in the α-helical content when STRA6-ICL3 was inserted into Im7.

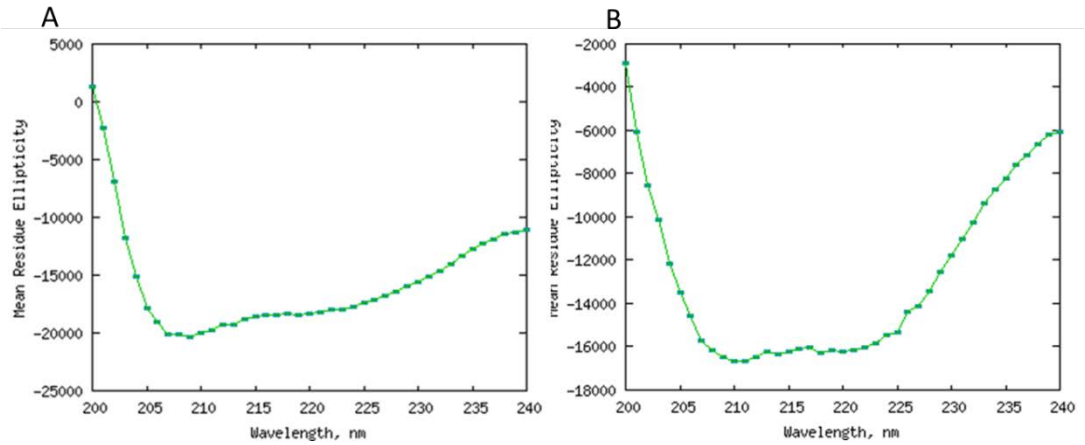

Figure 5.13: CD spectra of Im7 and STRA6-ICL3

The far-UV CD spectra of **(A)** Im7 and **(B)** STRA6-ICL3.

5.3.9 Crosslinking of STRA6-ICL3

Chemical crosslinking is a technique involving the formation of covalent bonds between two proteins by using bifunctional reagents containing reactive end groups that react with functional groups-such as primary amines and sulfhydryls-of amino acid residues. If two proteins physically interact with each other, they can be covalently cross-linked. Crosslinking has been used for determination of the quaternary structure of homo-oligomeric proteins (Carpenter and Harrington, 1972).

STRA6-ICL3 was treated with a cross-linking reagent DTBP. DTBP is a cleavable, amine to amine crosslinker. The reaction mixture was resolved on a SDS–PAGE gel under reducing and non-reducing conditions. STRA6-ICL3 ran as a monomer and dimer under reducing conditions but mostly as a dimer and tetramer under non-reducing conditions, as illustrated in Figure 5.14. This experiment validates the information obtained using size-exclusion chromatography and ensures that the elution profile of STRA6-ICL3 is not due to the protein aggregating but rather STRA6-ICL3 running as a tetramer.

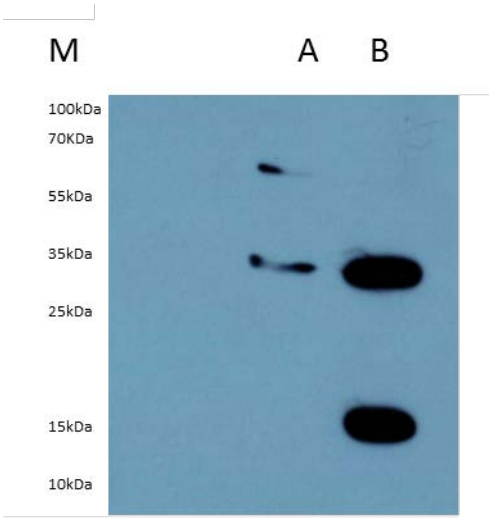

Figure 5.14: Crosslinking of STRA6-ICL3

Western blot with the crosslinking of STRA6-ICL3 in the **(A)** absence and **(B)** presence of a reducing agent. 5 µl loaded per well. STRA6-ICL3 as detected by α-his-HRP antibody. Molecular weight markers **(M)** revealed STRA6-ICL3 migrating at an expected ~ 19.5 kDa in reducing conditions, as well as a ~ 35 kDa species, which was not fully reduced. In the absence of a reducing agent, STRA6-ICL3 migrated at ~ 35 kDa and ~60 kDa.

5.3.10 Crystallisation of STRA6-ICL3

For X-ray crystallization, STRA6-ICL3 was concentrated to 10 mg/ml. The sample was centrifuged (12,000 g for 20 min) to remove initial precipitate, and was crystallized in a hanging-drop vapour diffusion set-up in 96 well-agar plates. Crystallization trials were carried out in Leeds University, with the help of Dr. Chi Trinh. As yet, a STRA6-ICL3 crystal is eagerly awaited. Early indications show small thin needle shaped crystals (and several wells with salt crystals).

5.4 Discussion

STRA6-ICL3 was expressed in *E.coli* as a chimera with the stabilising protein Im7 and purified via its 6xHis tag by affinity chromatography using Ni-NTA agarose. Considerable effort was invested in identifying the optimum buffer for the lysis and storage of STRA6-ICL3 to ensure the protein did not aggregate at room temperature and could, therefore, be used for downstream experiments. Concentrated STRA6-ICL3 was applied to a size-exclusion Superdex 200 resin. The elution profile of STRA6-ICL3 had one major peak for STRA6-ICL3 at ~ 14 ml, near BSA (molecular weight of 68,000 which elutes at ~ 13 ml), implying that STRA6-ICL3 runs as a tetramer. Cross-linking data also showed STRA6-ICL3 forms higher molecular weight species. A dimer and tetramer could be detected using the cross-linking reagent DTBP. These data suggest that native STRA6 is likely to occur as a tetramer and that at least some of the oligomerization sites are located on this large intracellular loop. This raises the possibility of a structural organisation not unlike the K^+-channel (Miller, 2000), with the RBP molecule (one per tetramer) and potentially also CRBP sitting on top of a vestibule into the transport channel. Clearly, the stoichiometry of RBP binding with respect to the putative STRA6 tetramer should be established. Future work includes finer refinement of the interaction site(s) by mutagenesis.

The structure of STRA6-ICL3 was explored. CD spectroscopy and Jpred both showed that STRA6-ICL3 reduced the percentage of α-helix content of Im7 alone (by ~ 15 %), thereby suggesting STRA6-ICL3 is composed of β-sheet and random coil. Many proteins function as dimers or higher oligomers that are held together in part by the formation of a β-sheet. For example, a number of cytokines form β-sheet dimers or higher oligomers such as interleukin 8 (Il-8). β-sheet formation is critical in forming cell-cell junctions and clustering of ion channels and receptors. β-sheet formation between proteins constitutes an important form of molecular recognition between amide groups and represents one general mode of PPIs. For example, the X-ray crystallographic structure of the complex between c-Raf1 and Ras-related protein

Rap-1A shows that the main-chains of the two proteins form an antiparallel β-sheet and their side-chains form a rich array of polar contacts (Maitra, 2000).

Crystallization of STRA6-ICL3 was attempted by the hanging-drop, vapour-diffusion method. Early indications show small thin needle shaped crystals (and several wells with salt crystals). The crystal structure of STRA6-ICL3 is eagerly awaited to further confirm the hypothesis proposed here.

Due to its large size, the third intracellular loop of STRA6 is predicted to be of critical importance for binding within the receptor and other components. The binding capacity of STRA6-ICL3 for both STRA6-CT and CRBP was assessed. The protein was previously subjected to size-exclusion chromatography and cross-linking to ensure the protein had not aggregated and was shown to form a tetramer. STRA6-ICL3 was pulled down using Ni-NTA agarose in the presence of both holo- and apo-CRBP. CRBP was detected in the unbound fraction indicating that no interaction occurs. The binding of activity of STRA6-ICL3 for STRA6-CT was also explored. STRA6-ICL3 was found not to interact with STRA6-CT. The third intracellular loop of STRA6, expressed as a chimera with Im7, may not be sufficient to bind to CRBP as this interaction may require the full length protein. The presence of Im7 may also inhibit the interaction between STRA6-ICL3 and CRBP/STRA6-CT.

Chapter 6

Summarising Discussion

Membrane proteins are essential for many biological processes, particularly signalling and transport. A thorough understanding of protein-protein interactions is vital for understanding the role of the protein, furthermore, given that protein-protein interactions regulate nearly every living processes, it is also essential for the understanding of diseases and for drug discovery (Suter et al., 2008). The objective of the work undertaken in this thesis is aimed at a greater understanding of the RBP receptor, STRA6, with specific interest in the identification of interacting proteins. This approach utilises the MYTH, a type of yeast two hybrid which allows interactions between integral membrane proteins, membrane-associated proteins and cytoplasmic proteins to be detected (Snider et al., 2010a). This system maintains eukaryotic proteins in an environment close to their physiological norm and allows post-translational modifications to occur, allowing the expression of correctly folded and functional proteins (Causier, 2004).

Three libraries were screened using STRA6 as the bait; a human kidney, and a human brain library and a human kidney library in the presence of holo-RBP. This resulted in 11 potential protein interactions for STRA6. From, the human kidney library CD63, PDZK1-IP1 and SERP1 were identified. The human brain library generated CD63, PDZK1-IP1, SERP1 and PLP2 and the human kidney library, in the presence of RBP-ROH, generated CD63, PDZK1-IP1 and SERP1 as potential STRA6 interactors as well as previously undetected proteins; MCP-1, CCL2, CXCL14, IFITM1, IFITM3, MIF, OCIAD2, and osteopontin. Attempts were made to verify these MYTH hits independently of the MYTH. Despite considerable efforts, the hits obtained in all three screens could not be validated using pull-down experiments. This technology often results in a relatively large number of false-positives for a number of reasons; the MYTH involves the overexpression of the protein of interest and prey, thus modifying the relative concentrations of potential interaction partners from the in vivo state. Furthermore, the use of heterologous systems can eliminate competing activities that exist in the native system and can also introduce novel competitors (Lalonde et al., 2008). The “hits” produced here appear not to interact with STRA6 and may simple be false positives. Alternatively,

these proteins may only form weak, transient interactions with STRA6 which are difficult to capture.

Membrane proteins represent approximately one-third of the proteins encoded in the genome, yet fewer than 1% of them are of known structure. A deeper understanding of structure–function relationships of membrane proteins requires high-resolution structural information. A few decades ago, it was believed to be hardly possible to determine crystal structures for integral membrane proteins. However it is now known that determining 3-D structures for integral membrane proteins is possible though still very difficult. The majority of membrane proteins, with the exception of bacterial membrane proteins, are found naturally in very small quantities, and therefore not in sufficient quantities for crystallisation. Expression, particularly of eukaryotic membrane proteins using prokaryotic systems, is often problematic. Once synthesis of a membrane protein begins, the secretory machinery is engaged, and that protein must be targeted to and inserted into the membrane. For many cells, the bulk of the proteins synthesized are intracellular; such cells are not equipped to handle heavy traffic in newly synthesized membrane proteins. Hence, high-level expression of a membrane protein can saturate the secretory pathway, leading either to the build-up of toxic intermediates or to inclusion body formation. In addition, many membrane proteins are relatively unstable once solubilised in detergent. Therefore, purification procedures need to be fast and gentle to prevent significant deterioration of the protein during purification. (Loll, 2003).

For these reasons, producing large quantities of soluble cytoplasmic fragments of membrane proteins in *E. co*li can be used in the quest for structural insights, for example, in the determination of the structures of the cytoplasmic N-terminal portion of transient receptor potential (TRP) channels (Moiseenkova-Bell and Wensel, 2009).

The predicted large third intracellular loop of STRA6 has been suggested to be involved in binding CRBP (Berry et al., 2012b) and due to its large size, is a potential candidate for interactions within the receptor itself as well as with other proteins. The importance of STRA6-ICL3 has been further enhanced by the

discovery of human polymorphism P293L, associated with severe multisystem birth defects (Pasutto et al., 2007). STRA6-ICL3 was extracted from the full length protein and characterised in the hope of gaining insights into STRA6's architecture and function, with particular attention to the binding of CRBP and the C-terminus of STRA6. This region was expressed, purified and characterised as a chimera with a stabilising protein, Im7, to aid folding, solubility and stability of the expressed protein and to anchor the domain as it might be in its native state. Characterisation of STRA6-ICL3 was achieved using a number of techniques such as SEC and SDS-PAGE to determine oligomeric size, CD to elucidate secondary structure (also to provide some evidence for it being folded) and pull-down assays to determine if STRA6-ICL3 does in fact bind CRBP and/or STRA6-CT. Crystallisation of STRA6-ICL3 was also attempted.

SEC and SDS-PAGE revealed that STRA6-ICL3 eluted at approximately 14 ml, (molecular weight of ~ 60,000) implying the protein migrates with a molecular mass which approximates that of a tetramer. Crosslinking was also used for determination of the oligomeric size. The crosslinking reagent DTBP, in combination with SDS-PAGE, revealed that STRA6-ICL3 runs as a dimer and tetramer under non-reducing conditions and as a monomer and dimer in the presence of a reducing agent. These data both imply that STRA6-ICL3 forms a tetramer and that the SEC data is not simply due to unfolded STRA6-ICL3 but rather reflects the functional form of the protein. The work presented here infers that native STRA6 is likely also to occur as a tetramer and that at least some of the oligomerization sites are located on this large intracellular loop.

CD data revealed that incorporation of STRA6-ICL3 into Im7 reduced the percentage of α-helix in comparison to Im7 alone, implying that STRA6-ICL3 is mostly composed of β-sheet or random coil since the proportion of the latter forms increased significantly. Jpred, a secondary structure prediction server powered by the Jnet algorithm, gave similar results. Interestingly, many proteins function as dimers or higher oligomers held together in part by the formation of a β-sheet, such as Il-8 (Maitra, 2000).

Crystallization of STRA6-ICL3 was attempted by the hanging-drop, vapour-diffusion method. Early indications show small thin needle shaped crystals (and

several wells with salt crystals). The crystal structure of STRA6-ICL3 is eagerly awaited.

Due to its large size, the third intracellular loop of STRA6 is likely to be of critical importance for binding within the receptor and/or with other components. The binding capacity of STRA6-ICL3 for both STRA6-CT and CRBP was assessed. However neither interaction could be detected using pull-down assays despite several attempts in the presence and absence of retinol as well as using a traditional wash step and the rapid centrifugation through an oil preparation to remove unbound material. The third intracellular loop of STRA6, expressed as a chimera with Im7, may not be sufficient to bind to CRBP as this interaction may require the full length protein or post translational modification within the cell. The presence of Im7 may also inhibit the interaction between STRA6-ICL3 and CRBP/STRA6-CT.

The work presented here provides compelling evidence that STRA6 functions as a tetramer. Further work is needed for finer refinement of the interaction site(s) by mutagenesis. However, it is clear that at least some of the oligomerization sites are located on the third intracellular loop of STRA6. Currently, there is no published data in relation to the secondary or tertiary structure of STRA6. The CD spectra of STRA6-ICL3, in comparison to the CD spectra for Im7 alone, implies the loop is composed of mainly β-sheet or random coil. STRA6-ICL3 did not interact with CRBP or STRA6-CT in pull-down experiments. This is unsurprising considering the full length protein did not identify CRBP as a potential interactor in the MYTH. Presumably these proteins form a weak or transient interaction which is difficult to capture and may require the presence of other proteins such as holo-RBP and functionally generated modifications.

Bibliography

ALBALAT, R. 2009. The retinoic acid machinery in invertebrates: ancestral elements and vertebrate innovations. *Mol Cell Endocrinol,* 313**,** 23-35.

ALBERTI, K. G. & ZIMMET, P. Z. 1998. Definition, diagnosis and classification of diabetes mellitus and its complications. Part 1: diagnosis and classification of diabetes mellitus provisional report of a WHO consultation. *Diabet Med,* 15**,** 539-53.

AMENGUAL, J., GOLCZAK, M., PALCZEWSKI, K. & VON LINTIG, J. 2012. Lecithin:retinol acyl transferase is critical for cellular uptake of vitamin A from serum retinol binding protein. *J Biol Chem*.

ANDO, Y. & JONO, H. 2008. [Pathogenesis and therapy for transthyretin related amyloidosis]. *Rinsho Byori,* 56**,** 114-20.

ANDRADE, M. A., CHACÓN, P., MERELO, J. J. & MORÁN, F. 1993. Evaluation of secondary structure of proteins from UV circular dichroism spectra using an unsupervised learning neural network. *Protein Eng,* 6**,** 383-90.

ARINAMINPATHY, Y., KHURANA, E., ENGELMAN, D. M. & GERSTEIN, M. B. 2009. Computational analysis of membrane proteins: the largest class of drug targets. *Drug Discov Today,* 14**,** 1130-5.

AUERBACH, D., THAMINY, S., HOTTIGER, M. O. & STAGLJAR, I. 2002. The post-genomic era of interactive proteomics: facts and perspectives. *Proteomics,* 2**,** 611-23.

AZAÏS-BRAESCO, V. & PASCAL, G. 2000. Vitamin A in pregnancy: requirements and safety limits. *Am J Clin Nutr,* 71**,** 1325S-33S.

BATTEN, M. L., IMANISHI, Y., MAEDA, T., TU, D. C., MOISE, A. R., BRONSON, D., POSSIN, D., VAN GELDER, R. N., BAEHR, W. & PALCZEWSKI, K. 2004. Lecithin-retinol acyltransferase is essential for accumulation of all-trans-retinyl esters in the eye and in the liver. *J Biol Chem,* 279**,** 10422-32.

BERRY, D. C., CRONIGER, C. M., GHYSELINCK, N. B. & NOY, N. 2012a. Transthyretin blocks retinol uptake and cell signalling by the holo-retinol-binding protein receptor STRA6. *Mol Cell Biol*, 32:3851-9

BERRY, D. C., JIN, H., MAJUMDAR, A. & NOY, N. 2011. Signaling by vitamin A and retinol-binding protein regulates gene expression to inhibit insulin responses. *Proc Natl Acad Sci U S A,* 108**,** 4340-5.

BERRY, D. C. & NOY, N. 2012. Signaling by vitamin A and retinol-binding protein in regulation of insulin responses and lipid homeostasis. *Biochim Biophys Acta,* 1821**,** 168-76.

BERRY, D. C., O'BYRNE, S. M., VREELAND, A. C., BLANER, W. S. & NOY, N. 2012b. Cross-talk between signalling and vitamin A transport by the retinol-binding protein receptor STRA6. *Mol Cell Biol*, 32: 3164–3175

BIESALSKI, H. K. 2003. The significance of vitamin A for the development and function of the lung. *Forum Nutr,* 56**,** 37-40.

BIESALSKI, H. K., FRANK, J., BECK, S. C., HEINRICH, F., ILLEK, B., REIFEN, R., GOLLNICK, H., SEELIGER, M. W., WISSINGER, B. & ZRENNER, E. 1999. Biochemical but not clinical vitamin A deficiency results from mutations in the gene for retinol binding protein. *Am J Clin Nutr,* 69**,** 931-6.

BLAKELEY, L. R., CHEN, C., CHEN, C. K., CHEN, J., CROUCH, R. K., TRAVIS, G. H. & KOUTALOS, Y. 2011. Rod outer segment retinol formation is independent of Abca4, arrestin, rhodopsin kinase, and rhodopsin palmitylation. *Invest Ophthalmol Vis Sci,* 52**,** 3483-91.

BLANER, W. S. 2007. STRA6, a cell-surface receptor for retinol-binding protein: the plot thickens. *Cell Metab,* 5**,** 164-6.

BLOMHOFF, R. & BLOMHOFF, H. K. 2006. Overview of retinoid metabolism and function. *J Neurobiol,* 66**,** 606-30.

BOUILLET, P., SAPIN, V., CHAZAUD, C., MESSADDEQ, N., DÉCIMO, D., DOLLÉ, P. & CHAMBON, P. 1997. Developmental expression pattern of Stra6, a retinoic acid-responsive gene encoding a new type of membrane protein. *Mech Dev,* 63**,** 173-86.

BRAY, G. A. 2004. Medical consequences of obesity. *J Clin Endocrinol Metab,* 89**,** 2583-9.

BUGGE, T. H., POHL, J., LONNOY, O. & STUNNENBERG, H. G. 1992. RXR alpha, a promiscuous partner of retinoic acid and thyroid hormone receptors. *EMBO J,* 11**,** 1409-18.

BUSHUE, N. & WAN, Y. J. 2010. Retinoid pathway and cancer therapeutics. *Adv Drug Deliv Rev,* 62**,** 1285-98.

CALANDRA, T. & ROGER, T. 2003. Macrophage migration inhibitory factor: a regulator of innate immunity. *Nat Rev Immunol,* 3**,** 791-800.

CARPENTER, E. P., BEIS, K., CAMERON, A. D. & IWATA, S. 2008. Overcoming the challenges of membrane protein crystallography. *Curr Opin Struct Biol,* 18**,** 581-6.

CARPENTER, F. H. & HARRINGTON, K. T. 1972. Intermolecular cross-linking of monomeric proteins and cross-linking of oligomeric proteins as a probe of quaternary structure. Application to leucine aminopeptidase (bovine lens). *J Biol Chem,* 247**,** 5580-6.

CAUSIER, B. 2004. Studying the interactome with the yeast two-hybrid system and mass spectrometry. *Mass Spectrom Rev,* 23**,** 350-67.

CHEN, C. C. & HELLER, J. 1977. Uptake of retinol and retinoic acid from serum retinol-binding protein by retinal pigment epithelial cells. *J Biol Chem,* 252**,** 5216-21.

CHEN, C. H., HSIEH, T. J., LIN, K. D., LIN, H. Y., LEE, M. Y., HUNG, W. W., HSIAO, P. J. & SHIN, S. J. 2012. Increased unbound retinol-binding protein 4 concentration induces apoptosis through receptor-mediated signaling. *J Biol Chem,* 287**,** 9694-707.

CHRISTIAN, P., WEST, K. P., KHATRY, S. K., KATZ, J., SHRESTHA, S. R., PRADHAN, E. K., LECLERQ, S. C. & POKHREL, R. P. 1998. Night blindness of pregnancy in rural Nepal--nutritional and health risks. *Int J Epidemiol,* 27**,** 231-7.

COLE, C., BARBER, J. D. & BARTON, G. J. 2008. The Jpred 3 secondary structure prediction server. *Nucleic Acids Res,* 36**,** W197-201.

CUSI, K., MAEZONO, K., OSMAN, A., PENDERGRASS, M., PATTI, M. E., PRATIPANAWATR, T., DEFRONZO, R. A., KAHN, C. R. & MANDARINO, L. J. 2000. Insulin resistance differentially affects the PI 3-kinase- and MAP kinase-mediated signaling in human muscle. *J Clin Invest,* 105**,** 311-20.

D'AMBROSIO, D. N., CLUGSTON, R. D. & BLANER, W. S. 2011. Vitamin A metabolism: an update. *Nutrients,* 3**,** 63-103.

DANDONA, P., ALJADA, A. & BANDYOPADHYAY, A. 2004. Inflammation: the link between insulin resistance, obesity and diabetes. *Trends Immunol,* 25**,** 4-7.

DENHARDT, D. T. & NODA, M. 1998. Osteopontin expression and function: role in bone remodeling. *J Cell Biochem Suppl,* 30-31**,** 92-102.

DENNIS, C. A., VIDELER, H., PAUPTIT, R. A., WALLIS, R., JAMES, R., MOORE, G. R. & KLEANTHOUS, C. 1998. A structural comparison of the colicin immunity proteins Im7 and Im9 gives new insights into the molecular determinants of immunity-protein specificity. *Biochem J,* 333 (Pt 1)**,** 183-91.

DESHMANE, S. L., KREMLEV, S., AMINI, S. & SAWAYA, B. E. 2009. Monocyte chemoattractant protein-1 (MCP-1): an overview. *J Interferon Cytokine Res,* 29**,** 313-26.

DESVERGNE, B. 2007. Retinaldehyde: more than meets the eye. *Nat Med,* 13**,** 671-673.

DINIZ, A. A. S. & SANTOS, L. M. 2000. [Vitamin A deficiency and xerophtalmia]. *J Pediatr (Rio J),* 76 Suppl 3**,** S311-22.

DITTRICH, A. M., MEYER, H. A. & HAMELMANN, E. 2013. The role of lipocalins in airway disease. *Clin Exp Allergy,* 43**,** 503-11.

DUERBECK, N. B. & DOWLING, D. D. 2012. Vitamin A: too much of a good thing? *Obstet Gynecol Surv,* 67**,** 122-8.

DUESTER, G. 2008. Retinoic acid synthesis and signaling during early organogenesis. *Cell,* 134**,** 921-31.

EGAÑA, L. A., CUEVAS, R. A., BAUST, T. B., PARRA, L. A., LEAK, R. K., HOCHENDONER, S., PEÑA, K., QUIROZ, M., HONG, W. C., DOROSTKAR, M. M., JANZ, R., SITTE, H. H. & TORRES, G. E. 2009. Physical and functional interaction between the dopamine transporter and the synaptic vesicle protein synaptogyrin-3. *J Neurosci,* 29**,** 4592-604.

FARJO, K. M., FARJO, R. A., HALSEY, S., MOISEYEV, G. & MA, J. X. 2012. Retinol-binding protein 4 induces inflammation in human endothelial cells by an NADPH oxidase-

and nuclear factor kappa B-dependent and retinol-independent mechanism. *Mol Cell Biol,* 32**,** 5103-15.

FELKL, M. & LEUBE, R. E. 2008. Interaction assays in yeast and cultured cells confirm known and identify novel partners of the synaptic vesicle protein synaptophysin. *Neuroscience,* 156**,** 344-52.

FERNÁNDEZ, I., DARIAS, M., ANDREE, K. B., MAZURAIS, D., ZAMBONINO-INFANTE, J. L. & GISBERT, E. 2011. Coordinated gene expression during gilthead sea bream skeletogenesis and its disruption by nutritional hypervitaminosis A. *BMC Dev Biol,* 11**,** 7.

FLOWER, D. R. 1996. The lipocalin protein family: structure and function. *Biochem J,* 318 (Pt 1)**,** 1-14.

FRANZONI, L., CAVAZZINI, D., ROSSI, G. L. & LÜCKE, C. 2010. New insights on the protein-ligand interaction differences between the two primary cellular retinol carriers. *J Lipid Res,* 51**,** 1332-43.

FREY, S. K. & VOGEL, S. 2011. Vitamin a metabolism and adipose tissue biology. *Nutrients,* 3**,** 27-39.

GEELEN, J. A. 1979. Hypervitaminosis A induced teratogenesis. *CRC Crit Rev Toxicol,* 6**,** 351-75.

GHYSELINCK, N. B., BÅVIK, C., SAPIN, V., MARK, M., BONNIER, D., HINDELANG, C., DIERICH, A., NILSSON, C. B., HÅKANSSON, H., SAUVANT, P., AZAÏS-BRAESCO, V., FRASSON, M., PICAUD, S. & CHAMBON, P. 1999. Cellular retinol-binding protein I is essential for vitamin A homeostasis. *EMBO J,* 18**,** 4903-14.

GOLZIO, C., MARTINOVIC-BOURIEL, J., THOMAS, S., MOUGOU-ZRELLI, S., GRATTAGLIANO-BESSIERES, B., BONNIERE, M., DELAHAYE, S., MUNNICH, A., ENCHA-RAZAVI, F., LYONNET, S., VEKEMANS, M., ATTIE-BITACH, T. & ETCHEVERS, H. C. 2007. Matthew-Wood syndrome is caused by truncating mutations in the retinol-binding protein receptor gene STRA6. *Am J Hum Genet,* 80**,** 1179-87.

GONCALVES, A. M., PEDRO, A. Q., MAIA, C., SOUSA, F., QUEIROZ, J. A. & PASSARINHA, L. A. 2013. Pichia pastoris: A Recombinant Microfactory for Antibodies and Human Membrane Proteins. *J Microbiol Biotechnol,* 23**,** 587-601.

GOUJON, M., MCWILLIAM, H., LI, W., VALENTIN, F., SQUIZZATO, S., PAERN, J. & LOPEZ, R. 2010. A new bioinformatics analysis tools framework at EMBL-EBI. *Nucleic Acids Res,* 38**,** W695-9.

GRAHAM, T. E., YANG, Q., BLÜHER, M., HAMMARSTEDT, A., CIARALDI, T. P., HENRY, R. R., WASON, C. J., OBERBACH, A., JANSSON, P. A., SMITH, U. & KAHN, B. B. 2006. Retinol-binding protein 4 and insulin resistance in lean, obese, and diabetic subjects. *N Engl J Med,* 354**,** 2552-63.

GREENBERG, A. S. & OBIN, M. S. 2006. Obesity and the role of adipose tissue in inflammation and metabolism. *Am J Clin Nutr,* 83**,** 461S-465S.

GRZYB, J., LATOWSKI, D. & STRZAŁKA, K. 2006. Lipocalins - a family portrait. *J Plant Physiol,* 163**,** 895-915.

GUDAS, L. J. & WAGNER, J. A. 2011. Retinoids regulate stem cell differentiation. *J Cell Physiol,* 226**,** 322-30.

HARADA, H., MIKI, R., MASUSHIGE, S. & KATO, S. 1995. Gene expression of retinoic acid receptors, retinoid-X receptors, and cellular retinol-binding protein I in bone and its regulation by vitamin A. *Endocrinology,* 136**,** 5329-35.

HAYASHI, K., CHENG, H. M., XIONG, J., XIONG, H. & KENYON, K. R. 1989. Metabolic changes in the cornea of vitamin A-deficient rats. *Invest Ophthalmol Vis Sci,* 30**,** 769-72.

HEDFALK, K. 2013. Further advances in the production of membrane proteins in Pichia pastoris. *Bioengineered,* 4:363-7

HELLER, J. 1975. Interactions of plasma retinol-binding protein with its receptor. Specific binding of bovine and human retinol-binding protein to pigment epithelium cells from bovine eyes. *J Biol Chem,* 250**,** 3613-9.

HEMLER, M. E. 2001. Specific tetraspanin functions. *J Cell Biol,* 155**,** 1103-7.

HIROSUMI, J., TUNCMAN, G., CHANG, L., GÖRGÜN, C. Z., UYSAL, K. T., MAEDA, K., KARIN, M. & HOTAMISLIGIL, G. S. 2002. A central role for JNK in obesity and insulin resistance. *Nature,* 420**,** 333-6.

HONG, P., KOZA, S. & BOUVIER, E. S. 2012. Size-Exclusion Chromatography for the Analysis of Protein Biotherapeutics and their Aggregates. *J Liq Chromatogr Relat Technol,* 35**,** 2923-2950.

HOOKER, B. S., BIGELOW, D. J. & LIN, C. T. 2007. Methods for mapping of interaction networks involving membrane proteins. *Biochem Biophys Res Commun,* 363**,** 457-61.

HOSSE, R. J., ROTHE, A. & POWER, B. E. 2006. A new generation of protein display scaffolds for molecular recognition. *Protein Sci,* 15**,** 14-27.

HUANG, W., CARLSEN, B., RUDKIN, G., BERRY, M., ISHIDA, K., YAMAGUCHI, D. T. & MILLER, T. A. 2004. Osteopontin is a negative regulator of proliferation and differentiation in MC3T3-E1 pre-osteoblastic cells. *Bone,* 34**,** 799-808.

ISHIYAMA, T., KANO, J., ANAMI, Y., ONUKI, T., IIJIMA, T., MORISITA, Y., YOKOTA, J. & NOGUCHI, M. 2007. OCIA domain containing 2 is highly expressed in adenocarcinoma mixed subtype with bronchioloalveolar carcinoma component and is associated with better prognosis. *Cancer Sci,* 98**,** 50-7.

JIN, M., YUAN, Q., LI, S. & TRAVIS, G. H. 2007. Role of LRAT on the retinoid isomerase activity and membrane association of Rpe65. *J Biol Chem,* 282**,** 20915-24.

JOHNSSON, N. & VARSHAVSKY, A. 1994. Split ubiquitin as a sensor of protein interactions in vivo. *Proc Natl Acad Sci U S A,* 91**,** 10340-4.

JURAJA, S. M., MULHERN, T. D., HUDSON, P. J., HATTARKI, M. K., CARMICHAEL, J. A. & NUTTALL, S. D. 2006. Engineering of the Escherichia coli Im7 immunity protein as a loop display scaffold. *Protein Eng Des Sel,* 19**,** 231-44.

KANAI, M., RAZ, A. & GOODMAN, D. S. 1968. Retinol-binding protein: the transport protein for vitamin A in human plasma. *J Clin Invest,* 47**,** 2025-44.

KATO, M., KATO, K. & GOODMAN, D. S. 1984. Immunocytochemical studies on the localization of plasma and of cellular retinol-binding proteins and of transthyretin (prealbumin) in rat liver and kidney. *J Cell Biol,* 98**,** 1696-704.

KAWAGUCHI, R., YU, J., HONDA, J., HU, J., WHITELEGGE, J., PING, P., WIITA, P., BOK, D. & SUN, H. 2007. A membrane receptor for retinol binding protein mediates cellular uptake of vitamin A. *Science,* 315**,** 820-5.

KAWAGUCHI, R., YU, J., TER-STEPANIAN, M., ZHONG, M., CHENG, G., YUAN, Q., JIN, M., TRAVIS, G. H., ONG, D. & SUN, H. 2011. Receptor-mediated cellular uptake mechanism that couples to intracellular storage. *ACS Chem Biol,* 6**,** 1041-51.

KAWAGUCHI, R., YU, J., WIITA, P., HONDA, J. & SUN, H. 2008a. An essential ligand-binding domain in the membrane receptor for retinol-binding protein revealed by large-scale mutagenesis and a human polymorphism. *J Biol Chem,* 283**,** 15160-8.

KAWAGUCHI, R., YU, J., WIITA, P., TER-STEPANIAN, M. & SUN, H. 2008b. Mapping the membrane topology and extracellular ligand binding domains of the retinol binding protein receptor. *Biochemistry,* 47**,** 5387-95.

KAWAGUCHI, R., ZHONG, M., KASSAI, M., TER-STEPANIAN, M. & SUN, H. 2012. STRA6-Catalyzed Vitamin A Influx, Efflux, and Exchange. *J Membr Biol*.

KLEIN, M. & HUSSEY, G. D. 1990. Vitamin A reduces morbidity and mortality in measles. *S Afr Med J,* 78**,** 56-8.

KLÖTING, N., GRAHAM, T. E., BERNDT, J., KRALISCH, S., KOVACS, P., WASON, C. J., FASSHAUER, M., SCHÖN, M. R., STUMVOLL, M., BLÜHER, M. & KAHN, B. B. 2007. Serum retinol-binding protein is more highly expressed in visceral than in subcutaneous adipose tissue and is a marker of intra-abdominal fat mass. *Cell Metab,* 6**,** 79-87.

KOCHER, O., COMELLA, N., TOGNAZZI, K. & BROWN, L. F. 1998. Identification and partial characterization of PDZK1: a novel protein containing PDZ interaction domains. *Lab Invest,* 78**,** 117-25.

KUMANYIKA, S., JEFFERY, R. W., MORABIA, A., RITENBAUGH, C., ANTIPATIS, V. J. & (IOTF), P. H. A. T. T. P. O. O. P. W. G. O. T. I. O. T. F. 2002. Obesity prevention: the case for action. *Int J Obes Relat Metab Disord,* 26**,** 425-36.

LACAPÈRE, J. J., PEBAY-PEYROULA, E., NEUMANN, J. M. & ETCHEBEST, C. 2007. Determining membrane protein structures: still a challenge! *Trends Biochem Sci,* 32**,** 259-70.

LALONDE, S., EHRHARDT, D. W., LOQUÉ, D., CHEN, J., RHEE, S. Y. & FROMMER, W. B. 2008. Molecular and cellular approaches for the detection of protein-protein interactions: latest techniques and current limitations. *Plant J,* 53**,** 610-35.

LATYSHEVA, N., MURATOV, G., RAJESH, S., PADGETT, M., HOTCHIN, N. A., OVERDUIN, M. & BERDITCHEVSKI, F. 2006. Syntenin-1 is a new component of tetraspanin-enriched microdomains: mechanisms and consequences of the interaction of syntenin-1 with CD63. *Mol Cell Biol,* 26**,** 7707-18.

LEE, L. M., LEUNG, C. Y., TANG, W. W., CHOI, H. L., LEUNG, Y. C., MCCAFFERY, P. J., WANG, C. C., WOOLF, A. S. & SHUM, A. S. 2012. A paradoxical teratogenic mechanism for retinoic acid. *Proc Natl Acad Sci U S A,* 109**,** 13668-73.

LEE, S. M., SHIN, H., JANG, S. W., SHIM, J. J., SONG, I. S., SON, K. N., HWANG, J., SHIN, Y. H., KIM, H. H., LEE, C. K., KO, J., NA, D. S., KWON, B. S. & KIM, J. 2004. PLP2/A4 interacts with CCR1 and stimulates migration of CCR1-expressing HOS cells. *Biochem Biophys Res Commun,* 324**,** 768-72.

LETO, D. & SALTIEL, A. R. 2012. Regulation of glucose transport by insulin: traffic control of GLUT4. *Nat Rev Mol Cell Biol,* 13**,** 383-96.

LOBO, G. P., AMENGUAL, J., BAUS, D., SHIVDASANI, R. A., TAYLOR, D. & VON LINTIG, J. 2013. Genetics and Diet Regulate Vitamin A Production via the Homeobox Transcription Factor ISX. *J Biol Chem,* 288**,** 9017-27.

LOLL, P. J. 2003. Membrane protein structural biology: the high throughput challenge. *J Struct Biol,* 142**,** 144-53.

MAECKER, H. T., TODD, S. C. & LEVY, S. 1997. The tetraspanin superfamily: molecular facilitators. *FASEB J,* 11**,** 428-42.

MAITRA, S. A. J. S. N. 2000. John Wiley & Sons, New York.

MARCEAU, G., GALLOT, D., BOREL, V., LÉMERY, D., DASTUGUE, B., DECHELOTTE, P. & SAPIN, V. 2006. Molecular and metabolic retinoid pathways in human amniotic membranes. *Biochem Biophys Res Commun,* 346**,** 1207-16.

MATA-GRANADOS, J. M., CUENCA-ACEVEDO, J. R., LUQUE DE CASTRO, M. D., HOLICK, M. F. & QUESADA-GÓMEZ, J. M. 2013. Vitamin D insufficiency together with high serum levels of vitamin A increases the risk for osteoporosis in postmenopausal women. *Arch Osteoporos,* 8**,** 124.

MCKENNA, N. J. 2012. EMBO Retinoids 2011: mechanisms, biology and pathology of signaling by retinoic acid and retinoic acid receptors. *Nucl Recept Signal,* 10**,** e003.

MELHUS, H., MICHAËLSSON, K., KINDMARK, A., BERGSTRÖM, R., HOLMBERG, L., MALLMIN, H., WOLK, A. & LJUNGHALL, S. 1998. Excessive dietary intake of vitamin A is associated with reduced bone mineral density and increased risk for hip fracture. *Ann Intern Med,* 129**,** 770-8.

MILLER, C. 2000. An overview of the potassium channel family. *Genome Biol,* 1**,** REVIEWS0004.

MOISEENKOVA-BELL, V. Y. & WENSEL, T. G. 2009. Hot on the trail of TRP channel structure. *J Gen Physiol,* 133**,** 239-44.

MORA, J. R., IWATA, M. & VON ANDRIAN, U. H. 2008. Vitamin effects on the immune system: vitamins A and D take centre stage. *Nat Rev Immunol,* 8**,** 685-98.

NAYLOR, H. M. & NEWCOMER, M. E. 1999. The structure of human retinol-binding protein (RBP) with its carrier protein transthyretin reveals an interaction with the carboxy terminus of RBP. *Biochemistry,* 38**,** 2647-53.

NEWCOMER, M. E., JONES, T. A., AQVIST, J., SUNDELIN, J., ERIKSSON, U., RASK, L. & PETERSON, P. A. 1984. The three-dimensional structure of retinol-binding protein. *EMBO J,* 3**,** 1451-4.

NORSEEN, J., HOSOOKA, T., HAMMARSTEDT, A., YORE, M. M., KANT, S., ARYAL, P., KIERNAN, U. A., PHILLIPS, D. A., MARUYAMA, H., KRAUS, B. J., USHEVA, A., DAVIS, R. J., SMITH, U. & KAHN, B. B. 2012. Retinol-binding protein 4 inhibits insulin signaling in adipocytes by inducing proinflammatory cytokines in macrophages through a c-Jun N-terminal kinase- and toll-like receptor 4-dependent and retinol-independent mechanism. *Mol Cell Biol,* 32**,** 2010-9.

NOY, N. 2000. Retinoid-binding proteins: mediators of retinoid action. *Biochem J,* 348 Pt 3**,** 481-95.

ONG, D. E. 1994. Cellular transport and metabolism of vitamin A: roles of the cellular retinoid-binding proteins. *Nutr Rev,* 52**,** S24-31.

PARK, C. K., ISHIMI, Y., OHMURA, M., YAMAGUCHI, M. & IKEGAMI, S. 1997. Vitamin A and carotenoids stimulate differentiation of mouse osteoblastic cells. *J Nutr Sci Vitaminol (Tokyo),* 43**,** 281-96.

PASUTTO, F., STICHT, H., HAMMERSEN, G., GILLESSEN-KAESBACH, G., FITZPATRICK, D. R., NÜRNBERG, G., BRASCH, F., SCHIRMER-ZIMMERMANN, H., TOLMIE, J. L., CHITAYAT, D., HOUGE, G., FERNÁNDEZ-MARTÍNEZ, L., KEATING, S., MORTIER, G., HENNEKAM, R. C., VON DER WENSE, A., SLAVOTINEK, A., MEINECKE, P., BITOUN, P., BECKER, C., NÜRNBERG, P., REIS, A. & RAUCH, A. 2007. Mutations in STRA6 cause a broad spectrum of malformations including anophthalmia, congenital heart defects, diaphragmatic hernia, alveolar capillary dysplasia, lung hypoplasia, and mental retardation. *Am J Hum Genet,* 80**,** 550-60.

PAUMI, C. M., CHUK, M., CHEVELEV, I., STAGLJAR, I. & MICHAELIS, S. 2008. Negative regulation of the yeast ABC transporter Ycf1p by phosphorylation within its N-terminal extension. *J Biol Chem,* 283**,** 27079-88.

PERVAIZ, S. & BREW, K. 1987. Homology and structure-function correlations between alpha 1-acid glycoprotein and serum retinol-binding protein and its relatives. *FASEB J,* 1**,** 209-14.

POPE, S. N. & LEE, I. R. 2005. Yeast two-hybrid identification of prostatic proteins interacting with human sex hormone-binding globulin. *J Steroid Biochem Mol Biol,* 94**,** 203-8.

PRAPUNPOJ, P. & LEELAWATWATTANA, L. 2009. Evolutionary changes to transthyretin: structure-function relationships. *FEBS J,* 276**,** 5330-41.

QUADRO, L., BLANER, W. S., HAMBERGER, L., VAN GELDER, R. N., VOGEL, S., PIANTEDOSI, R., GOURAS, P., COLANTUONI, V. & GOTTESMAN, M. E. 2002. Muscle expression of human retinol-binding protein (RBP). Suppression of the visual defect of RBP knockout mice. *J Biol Chem,* 277**,** 30191-7.

QUADRO, L., BLANER, W. S., SALCHOW, D. J., VOGEL, S., PIANTEDOSI, R., GOURAS, P., FREEMAN, S., COSMA, M. P., COLANTUONI, V. & GOTTESMAN, M. E. 1999. Impaired retinal function and vitamin A availability in mice lacking retinol-binding protein. *EMBO J,* 18**,** 4633-44.

QUADRO, L., HAMBERGER, L., GOTTESMAN, M. E., WANG, F., COLANTUONI, V., BLANER, W. S. & MENDELSOHN, C. L. 2005. Pathways of vitamin A delivery to the embryo: insights from a new tunable model of embryonic vitamin A deficiency. *Endocrinology,* 146**,** 4479-90.

RADHIKA, M. S., BHASKARAM, P., BALAKRISHNA, N., RAMALAKSHMI, B. A., DEVI, S. & KUMAR, B. S. 2002. Effects of vitamin A deficiency during pregnancy on maternal and child health. *BJOG,* 109**,** 689-93.

RAMANA, J. & GUPTA, D. 2009. LipocalinPred: a SVM-based method for prediction of lipocalins. *BMC Bioinformatics,* 10**,** 445.

REDONDO, C., BURKE, B. J. & FINDLAY, J. B. 2006. The retinol-binding protein system: a potential paradigm for steroid-binding globulins? *Horm Metab Res,* 38**,** 269-78.

REDONDO, C., VOUROPOULOU, M., EVANS, J. & FINDLAY, J. B. 2008. Identification of the retinol-binding protein (RBP) interaction site and functional state of RBPs for the membrane receptor. *FASEB J,* 22**,** 1043-54.

ROTHMAN, K. J., MOORE, L. L., SINGER, M. R., NGUYEN, U. S., MANNINO, S. & MILUNSKY, A. 1995. Teratogenicity of high vitamin A intake. *N Engl J Med,* 333**,** 1369-73.

SALTIEL, A. R. & KAHN, C. R. 2001. Insulin signalling and the regulation of glucose and lipid metabolism. *Nature,* 414**,** 799-806.

SCHWIKOWSKI, B., UETZ, P. & FIELDS, S. 2000. A network of protein-protein interactions in yeast. *Nat Biotechnol,* 18**,** 1257-61.

SEMBA, R. D. 1998. The role of vitamin A and related retinoids in immune function. *Nutr Rev,* 56**,** S38-48.

SHI, H., KOKOEVA, M. V., INOUYE, K., TZAMELI, I., YIN, H. & FLIER, J. S. 2006. TLR4 links innate immunity and fatty acid-induced insulin resistance. *J Clin Invest,* 116**,** 3015-25.

SHIRAKAMI, Y., LEE, S. A., CLUGSTON, R. D. & BLANER, W. S. 2012. Hepatic metabolism of retinoids and disease associations. *Biochim Biophys Acta,* 1821**,** 124-36.

SILVER, D. L., WANG, N. & VOGEL, S. 2003. Identification of small PDZK1-associated protein, DD96/MAP17, as a regulator of PDZK1 and plasma high density lipoprotein levels. *J Biol Chem,* 278**,** 28528-32.

SIVAPRASADARAO, A., BOUDJELAL, M. & FINDLAY, J. B. 1994. Solubilization and purification of the retinol-binding protein receptor from human placental membranes. *Biochem J,* 302 (Pt 1)**,** 245-51.

SIVAPRASADARAO, A. & FINDLAY, J. B. 1988a. The interaction of retinol-binding protein with its plasma-membrane receptor. *Biochem J,* 255**,** 561-9.

SIVAPRASADARAO, A. & FINDLAY, J. B. 1988b. The mechanism of uptake of retinol by plasma-membrane vesicles. *Biochem J,* 255**,** 571-9.

SIVAPRASADARAO, A. & FINDLAY, J. B. 1994. Structure-function studies on human retinol-binding protein using site-directed mutagenesis. *Biochem J,* 300 (Pt 2)**,** 437-42.

SIVAPRASADARAO, A., SUNDARAM, M. & FINDLAY, J. B. 1998. Interactions of retinol-binding protein with transthyretin and its receptor. *Methods Mol Biol,* 89**,** 155-63.

SMITH, F. R., GOODMAN, D. S., ZAKLAMA, M. S., GABR, M. K., EL-MARAGHY, S. & PATWARDHAN, V. N. 1973. Serum vitamin A, retinol-binding protein, and prealbumin concentrations in protein-calorie malnutrition. I. A functional defect in hepatic retinol release. *Am J Clin Nutr,* 26**,** 973-81.

SNIDER, J., KITTANAKOM, S., CURAK, J. & STAGLJAR, I. 2010a. Split-ubiquitin based membrane yeast two-hybrid (MYTH) system: a powerful tool for identifying protein-protein interactions. *J Vis Exp*.

SNIDER, J., KITTANAKOM, S., DAMJANOVIC, D., CURAK, J., WONG, V. & STAGLJAR, I. 2010b. Detecting interactions with membrane proteins using a membrane two-hybrid assay in yeast. *Nat Protoc,* 5**,** 1281-93.

SODEK, J., ZHU, B., HUYNH, M. H., BROWN, T. J. & RINGUETTE, M. 2002. Novel functions of the matricellular proteins osteopontin and osteonectin/SPARC. *Connect Tissue Res,* 43**,** 308-19.

SOMMER, A. 1996. Uses and misuses of vitamin A. *Curr Issues Public Health,* 2**,** 161-4.

SOMMER, A. 1997. 1997 Albert Lasker Award for Clinical Research. Clinical research and the human condition: moving from observation to practice. *Nat Med,* 3**,** 1061-3.

SPORN, M. B. & ROBERTS, A. B. 1983. Role of retinoids in differentiation and carcinogenesis. *Cancer Res,* 43**,** 3034-40.

SPRINZAK, E., SATTATH, S. & MARGALIT, H. 2003. How reliable are experimental protein-protein interaction data? *J Mol Biol,* 327**,** 919-23.

STAGLJAR, I. & FIELDS, S. 2002. Analysis of membrane protein interactions using yeast-based technologies. *Trends Biochem Sci,* 27**,** 559-63.

STAGLJAR, I., KOROSTENSKY, C., JOHNSSON, N. & TE HEESEN, S. 1998. A genetic system based on split-ubiquitin for the analysis of interactions between membrane proteins in vivo. *Proc Natl Acad Sci U S A,* 95**,** 5187-92.

STYNEN, B., TOURNU, H., TAVERNIER, J. & VAN DIJCK, P. 2012. Diversity in genetic in vivo methods for protein-protein interaction studies: from the yeast two-hybrid system to the mammalian split-luciferase system. *Microbiol Mol Biol Rev,* 76**,** 331-82.

SUNDARAM, M., SIVAPRASADARAO, A., DESOUSA, M. M. & FINDLAY, J. B. 1998. The transfer of retinol from serum retinol-binding protein to cellular retinol-binding protein is mediated by a membrane receptor. *J Biol Chem,* 273**,** 3336-42.

SUNDARAM, M., VAN AALTEN, D. M., FINDLAY, J. B. & SIVAPRASADARAO, A. 2002. The transfer of transthyretin and receptor-binding properties from the plasma retinol-binding protein to the epididymal retinoic acid-binding protein. *Biochem J,* 362**,** 265-71.

SUTER, B., KITTANAKOM, S. & STAGLJAR, I. 2008. Two-hybrid technologies in proteomics research. *Curr Opin Biotechnol,* 19**,** 316-23.

SZETO, W., JIANG, W., TICE, D. A., RUBINFELD, B., HOLLINGSHEAD, P. G., FONG, S. E., DUGGER, D. L., PHAM, T., YANSURA, D. G., WONG, T. A., GRIMALDI, J. C., CORPUZ, R. T., SINGH, J. S., FRANTZ, G. D., DEVAUX, B., CROWLEY, C. W., SCHWALL, R. H., EBERHARD, D. A., RASTELLI, L., POLAKIS, P. & PENNICA, D. 2001. Overexpression of the retinoic acid-responsive gene Stra6 in human cancers and its synergistic induction by Wnt-1 and retinoic acid. *Cancer Res,* 61**,** 4197-205.

TANAKA, S. S., YAMAGUCHI, Y. L., TSOI, B., LICKERT, H. & TAM, P. P. 2005. IFITM/Mil/fragilis family proteins IFITM1 and IFITM3 play distinct roles in mouse primordial germ cell homing and repulsion. *Dev Cell,* 9**,** 745-56.

TERSTAPPEN, G. C. & REGGIANI, A. 2001. In silico research in drug discovery. *Trends Pharmacol Sci,* 22**,** 23-6.

TICE, D. A., SZETO, W., SOLOVIEV, I., RUBINFELD, B., FONG, S. E., DUGGER, D. L., WINER, J., WILLIAMS, P. M., WIEAND, D., SMITH, V., SCHWALL, R. H., PENNICA, D. & POLAKIS, P. 2002. Synergistic induction of tumor antigens by Wnt-1 signaling and retinoic acid revealed by gene expression profiling. *J Biol Chem,* 277**,** 14329-35.

TOIT, E. F. D. & DONNER, D. G. 2012. *Myocardial Insulin Resistance: An Overview of Its Causes, Effects, and Potential Therapy*.

TUGUES, S., HONJO, S., KONIG, C., PADHAN, N., KROON, J., GUALANDI, L., LI, X., BARKEFORS, I., THIJSSEN, V. L., GRIFFIOEN, A. W. & CLAESSON-WELSH, L. 2013. Tetraspanin CD63 promotes VEGF receptor-2 / b1 integrin complex formation, thereby regulating activation and downstream signaling in endothelial cells in vitro and in vivo. *J Biol Chem*.

TURNER, N. 2013. *Mitochondrial Metabolism and Insulin Action*.

VALERA, A., PUJOL, A., PELEGRIN, M. & BOSCH, F. 1994. Transgenic mice overexpressing phosphoenolpyruvate carboxykinase develop non-insulin-dependent diabetes mellitus. *Proc Natl Acad Sci U S A,* 91**,** 9151-4.

VAN BENNEKUM AM, WEI, S., GAMBLE, M. V., VOGEL, S., PIANTEDOSI, R., GOTTESMAN, M., EPISKOPOU, V. & BLANER, W. S. 2001. Biochemical basis for depressed serum retinol levels in transthyretin-deficient mice. *J Biol Chem,* 276**,** 1107-13.

VAN HOEK, M., DEHGHAN, A., ZILLIKENS, M. C., HOFMAN, A., WITTEMAN, J. C. & SIJBRANDS, E. J. 2008. An RBP4 promoter polymorphism increases risk of type 2 diabetes. *Diabetologia,* 51**,** 1423-8.

WENTE, M. N., MAYER, C., GAIDA, M. M., MICHALSKI, C. W., GIESE, T., BERGMANN, F., GIESE, N. A., BÜCHLER, M. W. & FRIESS, H. 2008. CXCL14 expression and potential function in pancreatic cancer. *Cancer Lett,* 259**,** 209-17.

WHITE, T., LU, T., METLAPALLY, R., KATOWITZ, J., KHERANI, F., WANG, T. Y., TRAN-VIET, K. N. & YOUNG, T. L. 2008. Identification of STRA6 and SKI sequence variants in patients with anophthalmia/microphthalmia. *Mol Vis,* 14**,** 2458-65.

WHITMORE, L. & WALLACE, B. A. 2004. DICHROWEB, an online server for protein secondary structure analyses from circular dichroism spectroscopic data. *Nucleic Acids Res,* 32**,** W668-73.

WHITTAKER, S. B., SPENCE, G. R., GÜNTER GROSSMANN, J., RADFORD, S. E. & MOORE, G. R. 2007. NMR analysis of the conformational properties of the trapped on-pathway folding intermediate of the bacterial immunity protein Im7. *J Mol Biol,* 366**,** 1001-15.

WOZNIAK, S. E., GEE, L. L., WACHTEL, M. S. & FREZZA, E. E. 2009. Adipose tissue: the new endocrine organ? A review article. *Dig Dis Sci,* 54**,** 1847-56.

WURTZ, J. M., BOURGUET, W., RENAUD, J. P., VIVAT, V., CHAMBON, P., MORAS, D. & GRONEMEYER, H. 1996. A canonical structure for the ligand-binding domain of nuclear receptors. *Nat Struct Biol,* 3**,** 206.

WYSOCKA-KAPCINSKA, M., CAMPOS-SANDOVAL, J. A., PAL, A. & FINDLAY, J. B. 2010. Expression and characterization of recombinant human retinol-binding protein in Pichia pastoris. *Protein Expr Purif,* 71**,** 28-32.

XENARIOS, I., FERNANDEZ, E., SALWINSKI, L., DUAN, X. J., THOMPSON, M. J., MARCOTTE, E. M. & EISENBERG, D. 2001. DIP: The Database of Interacting Proteins: 2001 update. *Nucleic Acids Res,* 29**,** 239-41.

YADAV, A., KATARIA, M. A. & SAINI, V. 2012. Role of leptin and adiponectin in insulin resistance. *Clin Chim Acta*.

YAMAGUCHI, A., HORI, O., STERN, D. M., HARTMANN, E., OGAWA, S. & TOHYAMA, M. 1999. Stress-associated endoplasmic reticulum protein 1 (SERP1)/Ribosome-associated membrane protein 4 (RAMP4) stabilizes membrane proteins during stress and facilitates subsequent glycosylation. *J Cell Biol,* 147**,** 1195-204.

YANG, Q., GRAHAM, T. E., MODY, N., PREITNER, F., PERONI, O. D., ZABOLOTNY, J. M., KOTANI, K., QUADRO, L. & KAHN, B. B. 2005. Serum retinol binding protein 4 contributes to insulin resistance in obesity and type 2 diabetes. *Nature,* 436**,** 356-62.

YOUNT, J. S., KARSSEMEIJER, R. A. & HANG, H. C. 2012. S-palmitoylation and ubiquitination differentially regulate interferon-induced transmembrane protein 3 (IFITM3)-mediated resistance to influenza virus. *J Biol Chem,* 287**,** 19631-41.

ZHONG, M., KAWAGUCHI, R., KASSAI, M. & SUN, H. 2012. Retina, retinol, retinal and the natural history of vitamin a as a light sensor. *Nutrients,* 4**,** 2069-96.

ZILE, M. H. 2001. Function of vitamin A in vertebrate embryonic development. *J Nutr,* 131**,** 705-8.